José Francisco Rodrigues Malta

Licenciado em Ciências da Engenharia Química e Bioquímica

Joule-Heating Effect for Erasing Information in PDLCs Devices with Memory

Dissertação para obtenção do Grau de Mestre em
Engenharia Química e Bioquímica

Presidente: Mário Fernando José Eusébio, Professor Auxiliar, FCT-UNL

Orientador: João Carlos da Silva Barbosa Sotomayor, Professor Auxiliar, FCT-UNL

Arguente: Pedro Lúcio Maia Marques de Almeida, Professor Assistente, ISEL-IPL

FACULDADE DE CIÊNCIAS E TECNOLOGIA
UNIVERSIDADE NOVA DE LISBOA

Outubro, 2016

Joule-Heating Effect for Erasing Information in PDLCs Devices with Memory

"Study hard what interests you the most in the most undisciplined, irreverent and original manner possible."

- **Richard Feynman**

Agradecimentos

Ao Professor João Sotomayor por me ter aceite neste projeto, pela motivação e entusiamo transmitidos, por toda a sua disponibilidade sempre que ao longo do trabalho questões ou problemas surgiram, e por me ter dado a oportunidade de levar algum do trabalho desenvolvido através de um *poster* ao XII Encontro Nacional de Química-Física.

À Ana Mouquinho (Tri-Mamã), pelo apoio dado no laboratório, pelas conversas, pelos conselhos, pela ajuda no tratamento de gráficos do DSC e principalmente por me ter dado na cabeça sempre que precisei. Ao Diogo Costa por me ter dado "uma mãozinha" sempre que já não tinha mais mãos e pelos momentos divertidos nas nossas pausas.

À Professora Madalena Dionísio por ter disponibilizado o DSC para os testes neste trabalho. Ao Professor Jorge Caldeira por toda a ajuda dada na caracterização de superfícies através de AFM e à Daniela Gomes pela caracterização através de SEM. Ao Professor Mário Eusébio pelo desenvolvimento do programa de estudos eletro-óticos e ao Professor João Figueirinhas pela ajuda teórica dada.

Ao senhor Zé Luís pela sua disponibilidade e simpatia sempre que precisei de cortar alguns vidros. À Dona Idalina e Dona Conceição pela ajuda e amabilidade sempre que precisava de levar alguma coisa dum laboratório para o outro. À Dona Maria José pelas vezes que a chateei em pedir fita adesiva quando precisava de montar o sistema de medição de transmitâncias com a temperatura.

Aos meus colegas e amigos, Ana Rita Nabais, João Valentim, André Oliveira e Liliana Beatriz pela descontração nas horas de almoço e pela partilha de desabafos sobre os nossos obstáculos acompanhada pela cafeína. Ao Tomás Monteiro por ter salvado os computadores do laboratório sempre que resolviam não funcionar. Ao David Lopes pela companhia e partilha de conhecimentos ao longo deste trabalho.

Ao pessoal do Núcleo de Literatura um agradecimento pela amizade e momentos de descontração que me proporcionaram durante os clubes de leitura.

À minha família em especial à minha irmã por ter aturado as minhas conversas à hora de jantar e aos meus pais que sempre estiveram do meu lado acontecesse o que tivesse que acontecer.

Por último, há uma série de pessoas que me acolheram de braços abertos quando cheguei a este curso, gesto que, por mais anos que passem e por mais voltas que a vida dê, nunca irei esquecer. Um obrigado não chega para agradecer o modo como fui recebido e como sempre fui tratado por todos. Fiz grandes amizades para a vida e apesar de tudo essa foi a minha maior conquista. São muitos os nomes, contudo eles sabem bem quem são. Muito obrigado a todos! Sem vocês chegar aqui não teria sido possível!

Resumo

O principal objetivo deste trabalho é tentar encontrar a melhor maneira de apagar informação escrita em dispositivos PDLC com memória por efeito de joule, e como é que pode ser aplicado num sistema de janelas inteligentes. Para isso foi usado uma mistura composta por 70% cristal líquido E7 e 30% oligómero PEGDMA875 em várias células com características diferentes.

Primeiro de tudo, foram feitos estudos DSC para o E7, oligómero e mistura E7/oligómero para determinar as suas propriedades térmicas. Depois, foram testadas seis tipos de células num estudo eletro-ótico. Verificou-se que o Efeito de Memória Permanente (PME) está apenas presente em células cujos vidros tenham alinhamento planar.

Análises AFM e SEM foram feitas nos vidros com o fim de determinar como o alinhamento planar consegue influenciar o PME da mistura polímero/cristal líquido e, por conseguinte, o desempenho do PDLC. Em vidros com *rubbing* foram vistas algumas estrias onde a mistura segue a sua direção preferencialmente.

Para estas células, foram realizados estudos da capacitância com a temperatura com diferentes tipos de dielétricos no seu interior: sem dielétrico (vazia), com cristal líquido e com polímero. Mais tarde, o mesmo estudo foi efetuado para as células com PDLC mas desta vez com medição da transmitância ao longo da temperatura. As curvas de capacitância e transmitância conseguem dar informação sobre a temperatura de clarificação (Tc). Esta será a temperatura onde se consegue observar a transição opaco-transparente. Foi também verificado que depois de um estudo EO os valores de capacitância aumentam e quando a informação escrita é apagada estes voltam aos seus valores iniciais.

Depois de conhecida cada Tc, os dispositivos foram aquecidos por efeito de Joule com diferentes tipos de corrente, medindo a variação da capacitância. Este estudo foi feito primeiro para células antes do estudo EO (células sem informação escrita) para encontrar que intensidades de corrente conseguem chegar à Tc e depois para células depois do estudo EO (células com informação escrita). Apenas um certo grupo de intensidades de corrente consegue apagar completamente a informação escrita. Isto pode ser verificado quando, durante o aquecimento, a Tc é alcançada, e se os valores de capacitância no final do aquecimento são iguais aos valores antes do estudo EO.

Palavras-Chave: PDLC, Cristal Líquido, Efeito de Joule, Efeito de Memória Permanente, Capacitância

Abstract

The main objective of this work is trying to find the best way to erase written information in PDLC devices with memory by Joule-heating effect, and how this can be applied on a smart window system. Then, a mixture composed by 70% liquid crystal E7 by Merck and 30% oligomer PEGDMA875 was used in several cells with different properties.

First of all, DSC studies were done for E7, oligomer and mixture E7/oligomer to determine their thermal properties. Then, six different cells with different alignment types were tested in an electro-optical (EO) study. It was verified that the Permanent Memory Effect (PME) is only present in cells which glasses have planar alignment.

AFM and SEM analysis were done on glasses to determine how the planar alignment can affect the mixture polymer/liquid crystal and thus the PDLC performance. On rubbed glasses some stretch marks were detected where the mixture follows their preferred direction. For these cells, capacitance studies with temperature were done for three types of dielectrics inside: with no dielectric (empty), with liquid crystal, and with polymer. Afterwards, the same study was also done for cells with PDLC but this time with a transmittance measuring along the temperature. The capacitance and transmittance curves can give the information about the clarification temperature (Tc). This will be the temperature where the opaque-transparent transition can be observed. It was also verified that after EO study the capacitance values increases and when the written information is erased they return to previous values.

After known each Tc, the devices were heated by Joule-Heating Effect with different levels of current, measuring the capacitance variation. This study was done first for the cells before EO study (with no written information) to find which current intensities can reach the Tc and then for the cells after EO study (with written information). Only a group of current intensities can completely erase the written information. This can be verified when, during heating, the Tc is reached, and if the capacitances values in the end of the heating are equal to values before EO study.

Keywords: PDLC, Liquid Crystal, Joule Heating-Effect, Permanent Memory Effect, Capacitance

Symbols, Abbreviations and Acronyms

5CB	4-cyano-4'-n-pentyl-biphenyl
7CB	4-cyano -4'-n-heptyl-biphenyl
8OCB	4-cyano-4'-n-oxyoctyl -biphenyl
5CT	4-cyano-4"-n-pentyl-p-terphenyl
A	Area
AFM	Atomic Force Microscopy
AIBN	α,α-azobisisobutyronitrile
BOO	Bond Orientational Order
C	Capacitance
C⊥	Capacitance perpendicular to the director
C∥	Capacitance parallel to the director
c	Speed of light in vacuum
d	Thickness (Distance between plates)
DSC	Differential Scanning Calorimetry
E	Electric Field
E7	Mixture of four nematic liquid crystals by Merk
E90	Electric field for 90% of maximum transmittance
EO	Electro Optical

FP90	F90 Central Processor
H	Heat by Joule-Heating Effect
I	Current Intensity
ITO	Indium Thin Oxide
$\mathbf{k_d}$	Rate constant for the dissociation of the initiator
$\mathbf{k_i}$	Rate constant for the initiation step
$\mathbf{k_p}$	Rate constant for the propagation step
$\mathbf{k_t}$	Rate constant for the termination step by combination
LC	Liquid Crystal
LCR	Inductance Capacitance Resistance Bridge
$\vec{n}$	Director vector
$\mathbf{n_e}$	Extraordinary refractive index
$\mathbf{n_o}$	Ordinary refractive index
$\mathbf{n_p}$	Polymer refractive index
OO	Orientational order
PDLC	Polymer Dispersed Liquid Crystal
PEGDMA875	Poly(ethyleneglycol) dimethacrilate 875
PME	Permanent Memory Effect
POM	Polarized Optical Microscopy
PO	Positional Order
PS	Power Supply
Q	Electric charge
R	Resistance
SEM	Scan Electron Microscopy
T	Transmittance (%)
Tc	Clarification Temperature
$\mathbf{T_{NI}}$	Nematic Isotropic Transition Temperature
Tg	Glass Transition Temperature
$\mathbf{T_{OFF}}$	Transmittance before an applied field (Minimum Transmittance)

$\mathbf{T_{OFF'}}$	Transmittance after an applied field
$\mathbf{T_{ON}}$	Transmittance during an applied field (Maximum Transmittance)
V	Voltage
Vth	Threshold Voltage
v	Speed of Light
Δn	Optical Anisotropy (Birefringence)
Δε	Dielectric Anisotropy
ε	Dielectric Permittivity
ε⊥	Dielectric constant perpendicular to the director
ε∥	Dielectric constant parallel to the director
ε_p	Polymer dielectric constant
ε_0	Vacuum dielectric constant

Content

Figures Index

Chapter 1

Chapter 2

Chapter 3

Appendix A

Appendix B

Appendix C

Tables Index

Chapter 2

Chapter 3

1

Chapter 1 - Introduction

1.1. Liquid Crystals

Matter is divided into three principal states: solid, liquid and gas. However, with the progress of technology and the evolution of science, new kind of substances and materials were discovered with different properties, and some of them with mixed properties. Liquid Crystals are an example of that, they have properties that a liquid and a crystal can have.

Liquid Crystals (LC) are anisotropic materials, and some physical properties of the system vary with the molecular average alignment of the director vector $\vec{n}$. The director is the vector associated with a preferred axis where LC molecules align through. If the alignment is large, the material is very anisotropic. If the alignment is small, the material is almost isotropic.[1]

LC can be divided into two major groups. **Lyotropic liquid crystals** which can be obtained by solution concentrations and **Thermotropic Liquid Crystals** which can be obtained by temperature variations. [2] Figure 1.1 shows a typical phase transition on a thermotropic liquid crystal

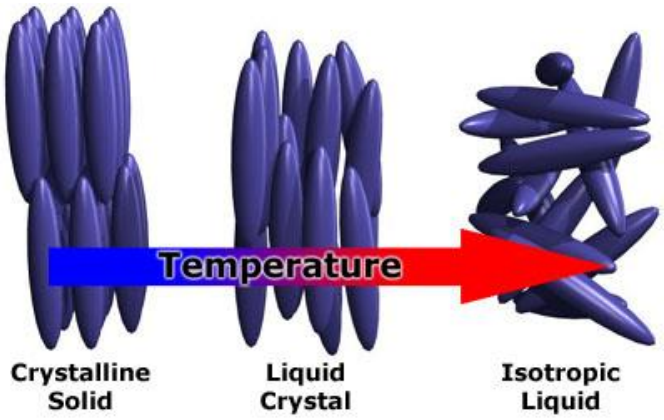

Figure 1. 1 - Thermotropic Liquid Crystal Transition[3]

1.1.1. Brief History of Liquid Crystals

The origin of Liquid Crystals was in 1888 when the Austrian chemist Friedrich Reinitzer, discovered a strange phenomenon when he was trying to precise the melting point of cholesterol. Everything was going well but when he tried to precisely determine the melting point he was struck by the fact that this substance seemed to have "two melting points". The solid crystal melted into a cloudy liquid which existed until a little higher temperature where the cloudiness suddenly disappeared, giving way to a clear transparent liquid.[4]

Reinitzer asked some help to the physicist Otto Lehmann, who was convinced that the cloudy liquid had only a kind of order. He realized that the cloudy liquid was a new state of matter and coined the name "liquid crystal," illustrating that it was something between a liquid and a solid, sharing important properties of both. In a normal liquid, the properties are isotropic, the same in all directions. In a liquid crystal, they are not; they strongly depend on direction even if the substance itself is fluid.[5]

This new idea was investigated and it grew years by years. Between 1910 and 1930 conclusive experiments and early theories supported the liquid crystal concept at the same time that new types of liquid crystalline states of the order were discovered. The twenty century 70's was a very important decade in liquid crystals experiments and their technologic applications evolution. Many scientists have started the study of liquid crystals and some of them were very successful. The greatest example was Pierre-Gilles de Gennes (Nobel Laureate in Physics, 1991) who had a great contribution to the liquid crystals and polymer-liquid crystals studies. De Gennes used the term *Soft Matter* to characterize them which means that liquid crystals are a kind of subfield of condensed matter comprising a variety of physical systems that are deformed or structurally altered by a thermal or mechanical stress of the magnitude of thermal fluctuations.[6]

Nowadays, liquid crystals are important in Digital and Electronic industry for developing new devices. Digital watches and screens, LCD (Liquid Crystal Display) systems and Smart Windows Displays (PDLCD's- Polymer Dispersed Liquid Crystals Displays), are some of the liquid crystals applications in the technology industry.[7]

1.1.2. Liquid crystals structural units

The structural units capable of forming liquid crystals are always molecules called mesogens. Mesogens are usually rather elongated organic ones that possess dissimilar local structural regions that can interact in an organized way with their neighbours. Over a certain range of temperatures, these attractive forces can lead to a degree of self-organization in which crystal-like order persists in some directions even though it is lost in other directions.[8]

The most common structures can be represented by:

-Two benzene rings which confer a degree of planarity on the molecule.

-The terminal group is often one that is somewhat polar, giving rise to intermolecular attractions along the long axis.

-The side chain is commonly a hydrocarbon chain that serves to elongate the molecule and give it some mobility. [7]

Figure 1.2. shows the structure of 5CB molecule, an example of mesogen molecule:

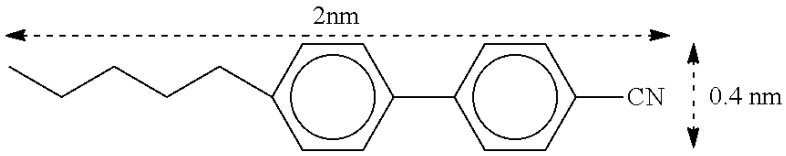

Figure 1. 2. - Example of a mesogen molecule (5CB)[9]

1.1.3. Mesophases

As the structural units, mesophases are different phases on thermotropic liquid crystals. These phases are between Crystalline Solid and Isotropic liquid states and the differences between them are essentially in the molecules order and position. Normally the order of molecules can be defined by two different kinds: orientational order (OO) and positional order (PO). In some cases, a very specific liquid crystals type have another kind of order called bond orientational order (BOO), an order which describes a line joining the centres of nearest-neighbour molecules.

PO and OO are temperature dependent. When the temperature increases the order decreases and therefore transitions in liquid crystal states can be observed.[10]

Crystalline Solid

In the crystalline solid state, the molecules are arranged in regular and fixed positions by intermolecular forces with a regularly repeating pattern in all directions. For these reasons, the molecules have OO and PO. As the temperature increases, molecules vibrate more vigorously. When these vibrations overcome the forces that hold the molecules in place, the molecules start to move. In the liquid state, this motion overcomes the intermolecular forces that maintain a crystalline state, and the molecules move into random positions, losing both OO and PO.[11]

Nematic phase

Nematic phase is the most common mesophase. It is characterized by long-range orientational order, the long axes of the molecules tend to align along a preferred direction.

There is no long-range order in the positions of the centres of mass of the molecules of a nematic, but a certain amount of short-range order may exist as in ordinary liquids. The molecules appear to be able to rotate about their long axes and also there seems to be no preferential arrangement of the two ends of the molecules if they differ. Hence the sign of the director is of no physical significance, n =−n. Optically a nematic behaves as a uniaxial material with a centre of symmetry.[12] Figure 1.3. shows an illustration and texture of Nematic Phase

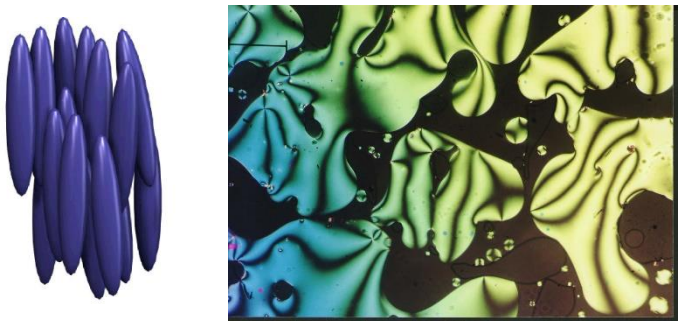

Figure 1. 3. - Nematic phase illustration and respective texture observed with a Polarized Optical Microscope with crossed polarizers[3] [13]

Cholesteric phase

Cholesteric phase is a nematic phase subtype, and is characterized by the rotation of director perpendicular to LC molecules longer axis. The rotation varies with layers and tends to be periodic in nature. This phase forms if the molecules which form the liquid crystal are either intrinsically chiral or if chiral dopants are added to a non-chiral nematic. This is a kind of phase with less order relatively to the custom nematic phase. Cholesteric liquid crystals have a helical structure and therefore they are chiral. Due the chirality some authors call them chiral nematic liquid crystals.[14] Figure 1.4. shows an illustration and texture of cholesteric phase.

Figure 1. 4 - Cholesteric phase illustration and respective texture observed with a Polarized Optical Microscope with crossed polarizers[3]

Smectic phase

Smectic phase has one more degree of order and tend to arrange themselves in layers. Their movement is restricted to within planes and separate planes will flow past each other. The smectics have PO along one direction. For instance, in the Smectic A phase, the molecules are oriented along the layer normal, while in the Smectic C phase they are tilted away from the layer normal. There are many different smectic phases, all characterized by different types and degrees of PO and OO.

Many compounds are observed to form more than one type of smectic phase. As many as 12 of these variations have been identified.[1] Figure 1.5. shows two smectic phases illustrations which different degrees of PO and OO can be observed

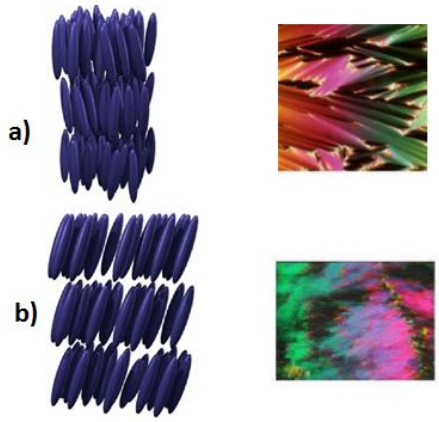

Figure 1. 5 – Illustration of Smectic phases A – a) and C b) and respective textures observed with a Polarized Optical Microscopy with crossed polarizers[3]

Isotropic Liquid

Isotropic Liquid is the phase where liquid crystal is in liquid state, and there is no OO and PO. If the LC molecules gain some OO or PO (namely with temperature decreasing), the LC turns to one of the mesophases described previously.

1.1.4. Liquid Crystals Properties

Liquid crystal phases are generally cloudy in appearance, which means that they scatter light in much the same way as colloids such as milk. This light scattering is a consequence of fluctuating regions of non-uniformity as small groups of molecules form and disperse. As special kind of materials, liquid crystals have some properties and advantages that make them very useful in many scientific, industrial and technologic applications.

Birefringence

Birefringence (or Optical Anisotropy) is an important property of LCs. In a nutshell, birefringence is the optical property of a material having a refractive index that depends on the polarization and propagation direction of light. The birefringence is often quantified as the maximum difference between refractive indices exhibited by the material. Crystals with asymmetric crystal structures are often birefringent, as are plastics under mechanical stress.[15] Figure 1. 6. shows how birefringence can be observed in a birefringent material:

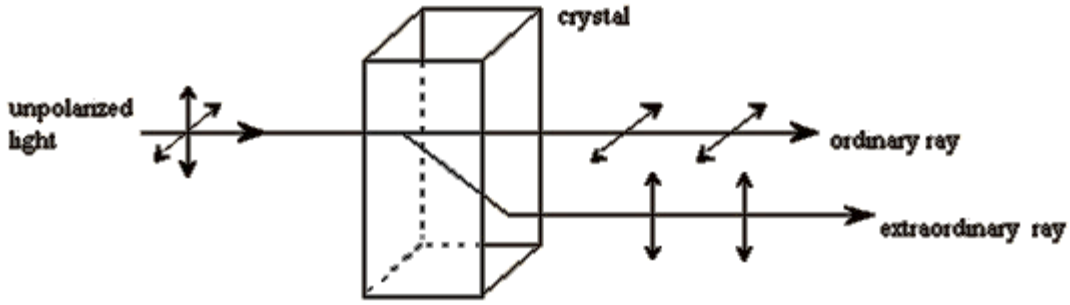

Figure 1. 6 - Illustrative scheme of light crossing a birefringent material[16]

Birefringence makes use of the refractive indices, n, of a material, as defined as the ratio between light speed in vacuum, c, and light speed in the sample, v.

$$n = \frac{c}{v} = \frac{speed\ of\ light\ in\ vacuum}{speed\ of\ light\ in\ sample}$$

In birefringent materials there are two types of refractive indices: Ordinary index (n_o) and extraordinary index (n_e)

$$n_e = \frac{c}{v_{parallel}} \qquad n_o = \frac{c}{v_{perpendicular}}$$

Then the maximum value of birefringence is given by

$$\Delta n = n_e - n_o$$

When the temperature is higher than the T_{NI} (nematic-isotropic transition temperature) the liquid crystal melts into an isotropic liquid, loosing all the positional and orientational order and the two indexes become together into an unique value. Figure 1. 7. shows a graph with refractive indexes variations along temperature.

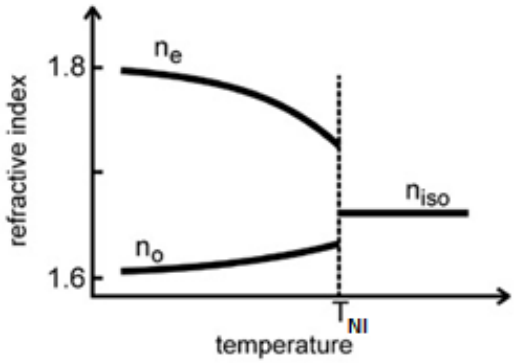

Figure 1. 7 - Birefringence on Nematic Liquid Crystals[17]

Dielectric Anisotropy

The Dielectric Permittivity is a physical quantity that describes how an electric field affects and is affected by a dielectric medium, and it is determined by the ability of a material to be polarized in response to an applied electric field, and therefore to cancel, partially, the field inside the material. Liquid crystals have restricted or even absent long-range positional order, but nevertheless there is a long-range orientational correlation between the molecules.

Due to LC molecules symmetry the fundamental components are reduced to two: ε∥ and ε⊥ are dielectric permittivity components along and perpendicular to the director, respectively. The dielectric anisotropy is given by

$$\Delta\varepsilon = \varepsilon\parallel - \varepsilon\perp.$$

Bellow the T_{NI} the parallel permittivity slope is sharper than the perpendicular one; the research presented in this work is based on the influence of temperature in positive dielectrc anisotropy. When the temperature exceeds the T_{NI} the LC transforms into an isotropic liquid and the LC permittivity turns constant.[18] This graph is represented by Figure 1.8, and it is very similar as the birefringence index graph changing with the temperature.

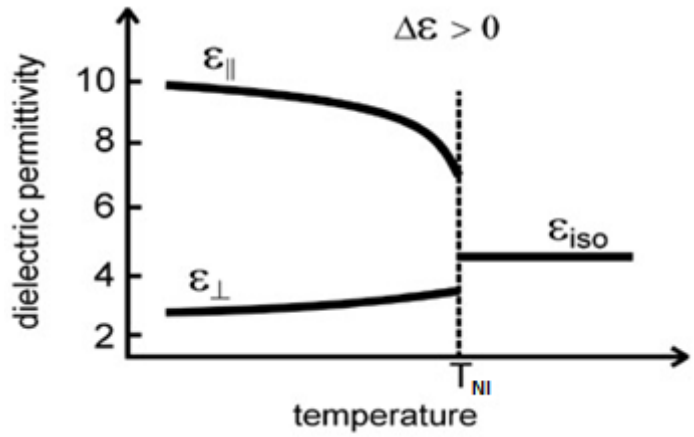

Figure 1. 8 - Dielectric Permittivity along Temperature for a liquid crystal with positive dielectric anisotropy [20]

Due to the anisotropy of the liquid crystals molecular structure, their response to an applied electric field may be different depending on the dielectric anisotropy of the liquid crystal.material.[19] The LC molecules can possess the permanent or induced dipole along or across the long molecular axis. If the dipole moment ($\vec{\mu}$) is parallel to the long molecular axis then $\Delta\varepsilon>0$ and the molecules tend to orient along the electric field direction. If the molecules carry

dipole moments that are more or less normal to the long molecular axis then $\Delta\varepsilon<0$ and molecules tend to orient perpendicular to the electric field direction [20] Figure 1.9. shows how an electric field acts on liquid crystal molecules.

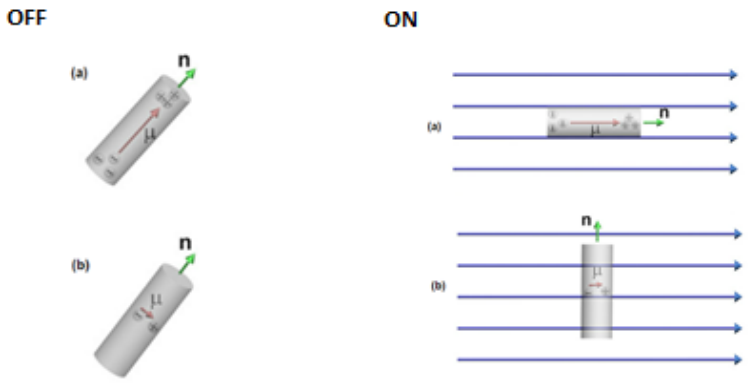

Figure 1. 9 - Orientation of Liquid crystal molecules with a) positive and b) negative dielectric anisotropy as a response to the applied electric field[20]

Therefore, it is possible to find the nematic-isotropic transition temperature of a liquid crystal if the refractive indexes or dielectric permittivity values were measured along temperature variation.

1.2. Polymer Dispersed Liquid Crystals

Polymer Dispersed Liquid Crystal (PDLC) are known to switch from opaque to transparent states, based on the ability of the liquid crystal (LC) micro-domains randomly oriented although inside each one molecules are aligned. In the absence of applied voltage, the director of each micro-domain is randomly oriented, allowing light scatter and the PDLC shows the characteristic opaque aspect. When an adequately high voltage is applied, the molecules align with the field, reducing the light dispersion passing through the PDLC, and it can show a transparent aspect. Figure 1.10. shows a scheme of how a PDLC device works:

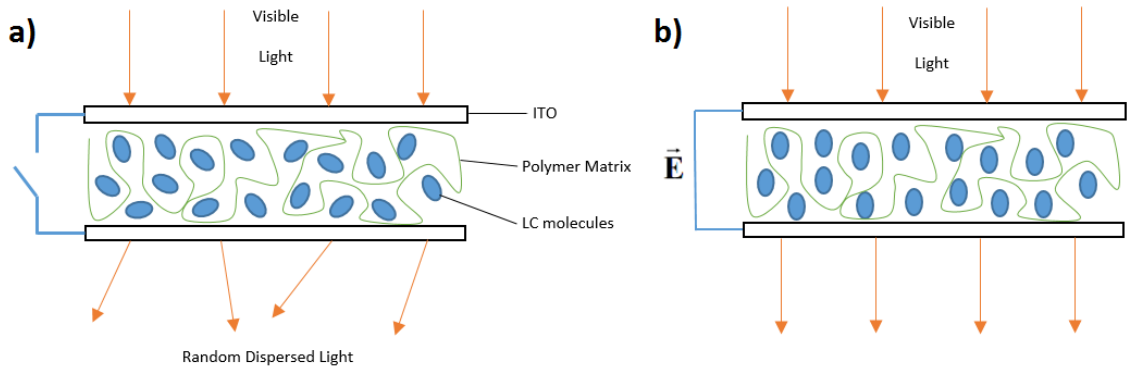

Figure 1. 10. - Illustration of a PDLC Device, (a) OFF State, (b) ON State

Although the polymer matrix optically has a single refractive index, the microdomains of LC have an ordinary and extraordinary refractive indexes (n_o and n_e). In an electrical off-condition, PDLC film is opaque because the refractive index mismatch between the LC droplets and the polymer matrix causes light scattering. In an electrical on-condition, PDLC film becomes transparent because the alignment of the LC is parallel to the applied electric field and the ordinary refractive index of the LC matches the refractive index of the polymer (n_p).

1.2.1. Brief History of PDLC's

The first polymer dispersed liquid crystal devices were demonstrated by James Fergason. In the course of experimentation in microencapsulating liquid crystals, Fergason noted that blending a nematic liquid crystal with a water-based solution of polyvinylalcohol enabled him to cast a turbid, flexible film. This electro-optical ''paint'' could be coated onto a plastic sheet itself coated with indium-tin oxide (ITO). Once dried, another sheet of ITO-based film could be laminated on the other side. Applying an AC voltage across the turbid film enabled it to clear, providing a means to a flexible, large area optical shutter. Fergason filed his first U.S. patent in this area in 1981, which was granted in 1984.[21]

Until the early, 1990's, the technology experienced substantial industrial progress, mainly in the US and Japan. In the mid-l990s, some companies were focused on the development of plastic PDLC for the architectural windows market. In the meantime, other small films and windows manufacturers have been continuing to produce PDLC film on a modest scale.[22]

The first material systems used for the fabrication of these systems were based on a single-phase solution of the liquid crystal and the polymer precursor that was induced to phase separate into a polymer network and liquid crystal domains. Photo-polymerisation of reactive monomers and oligomers was by far the most popular pathway, given the versatility of photo-polymerisation chemistry and ease of processing.[23]

PDLC devices exhibit several advantages in comparison to conventional displays and they are currently of high interest. They have promising new applications for light control and flexible electro-optic displays. Although the vast majority of groups working on liquid crystal dispersion displays used phase separation methods to form their devices, some forms are keeping used for developing these devices industrially.

1.2.2. Permanent Memory Effect

Normally, when an electric field is applied in a PDLC device, the liquid crystal molecules align through the director vector and there is a transition between opaque and transparent states.

When the electric field is turned off, the LC molecules return to their initial state and then the devices turns to the opaque state.

In some cases, the PDLC's transparent state remains even when the electric field is off. This is called the Permanent Memory Effect (PME).[24] PME occurs when after an applied electric field be applied the LC molecules can stand aligned trough the director or at least more aligned than before. With this, the device can stay on transparent state without a permanent electric field. The PME can be calculated through the following expression:

$$PME = \frac{T_{OFF'} - T_{OFF}}{T_{ON} - T_{OFF}} \times 100\%$$

where T_{OFF} is the transmittance when the electric field is not being applied, T_{ON} the maximum transmittance when the voltage is applied, and $T_{OFF'}$ when the electric field is switched off. When $T_{OFF'}$ is higher than T_{OFF} there is a case of PME.

The most common electro-optical response reported in the literature for PDLC is when the increasing voltage curve is coincident to the decreasing voltage curve as shown. It was observed that when the electric field is removed liquid crystal molecules relax back, so that the long shaped molecules which were oriented in the same direction in each droplet return to their original random orientation.[25] However, in some cases there is no total relaxation and the applied field increasing and decreasing curves are not the same. There are three different cases of transmittance variation when an electric field is applied:

With no hysteresis: when the increasing and decreasing applying field curves are coincident.

With hysteresis: when the increasing and decreasing applied field curves are different but the transmittance values at the beginning and ending cycle are coincident.

With Permanent Memory Effect: when the increasing and decreasing applied field curves are different and the transmittance at the ending is higher than beginning transmittance.

Figure 1. 11. shows the three different cases of transmittance variation when an electric field is applied:

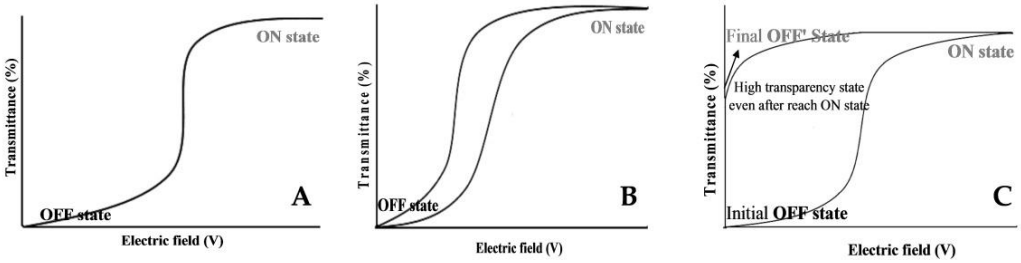

Figure 1. 11 - Transmittance variation when an electric field is applied (A- No Hysteresis, B-With Hysteresis, C-With PME)[25]

1.2.3. Factors that can influence PME

There are some factors that can influence the liquid crystal molecules disposition and then the PME on PDLC devices. The objective is that LC molecules stand aligned after an applied field. Afterwards, many studies have been done for finding which factors should be avoided to have great values of PME and how they can be avoided.

Anchoring Effect

On a PDLC device, the orientation of liquid crystal molecules is affected by the interaction between the polymeric matrix and the LC, called anchorage. There is a relationship between the size and the shape of the liquid crystal domains and the anchoring effect. When the shape and the size of liquid crystal domains increases the anchoring effect decrease. Strong anchoring forces hinder the alignment of liquid crystal molecules when an electric field is applied, which implies that the permanent memory effect decreases with the increase of anchoring effect. Figure 1. 12. shows how anchoring effect can influence the liquid crystal orientation and position before an applied electric field and during and applied threshold voltage (Vth).

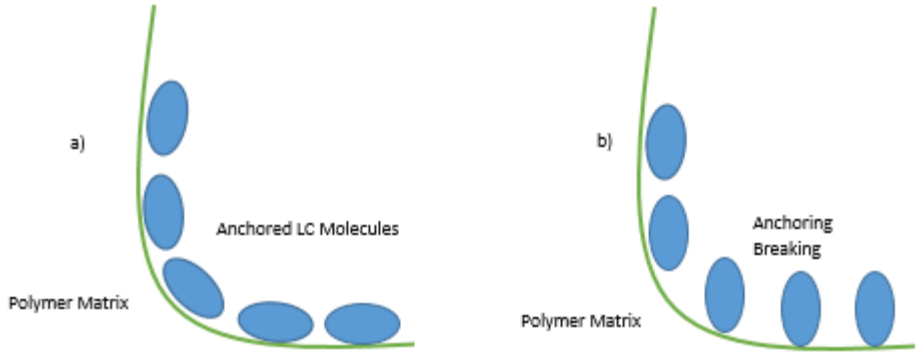

Figure 1. 12. - Anchoring Effect on Liquid Crystal Molecules a) when V=0; b) when V=Vth

PDLC morphology

After the polymerisation of a homogeneous solution of monomers and LC molecules, the polymer matrix can acquire a particular morphology with liquid crystal dispersed in its clusters. The polymerisation conditions, the chemical nature of the liquid crystal and the monomers determine the morphology of polymer matrix. Conventional PDLCs have two main morphologies: Swiss cheese or polymer ball types each one with different characteristics.[25] Figure 1.13. shows an image from SEM of two types of morphologies in PDLC mixtures.

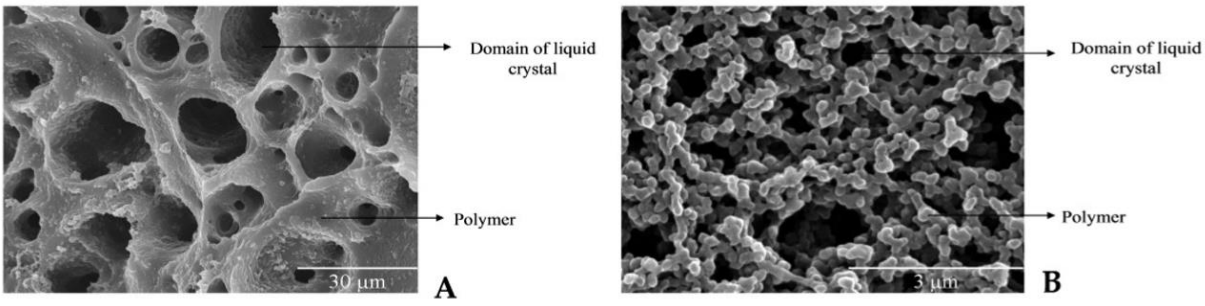

Figure 1. 13 -The two different type of morphologies in PDLC devices: a) Swiss Cheese; b) Polymer Ball[25]

In the swiss cheese morphology the memory effect is not found, but in the polymer ball morphology it is. This means that after voltage removal the liquid crystal alignment is maintained. Moreover, liquid crystal alignment induced by anchoring on the micro sized polymer balls surface appears to affect other liquid crystal molecules nearby, so they align collectively along the same direction. Since the liquid crystal is not isolated, this collective alignment may occur without increasing elastic energy. The memory effect depends strongly on the surface anchoring effects on the polymer balls surface. The PDLCs with a higher surface-volume ratio and complicated structure exhibit stronger memory effect.[25]

Polymer glass transition temperature

The polymer glass transition temperature (Tg) can also affect the PME in a PDLC. The mobility of molecules can be affected if the polymer used is glassy or plastic. Plastic polymers (polymers with low Tg) are mostly used because they change their configuration when an electric field is applied. This happens due the LC molecules orientation change, they can push the polymer chains. However, studies with different polymer types have been done to find which is the most suitable for higher values of PME on these devices.[26]

1.2.4. Clarification Temperature on PDLC

In a PDLC, the LC dispersed on polymer have a nematic-isotropic transition nearly at T_{NI}. However, due the different LC molecules disposition in each polymer microdomain, this temperature can be a little bit lower than T_{NI}. Therefore, it is called Clarification Temperature (Tc) for the Opaque-Transparent temperature transition. As was described in section 1.1.4., it is possible to find the nematic-isotropic temperature when there is a unique value for refractive index and also dielectric permittivity. When a PDLC device is being heated or cooled, it is possible to find Tc by two ways:

-Measuring Transmittance

Transmittance on PDLC devices can be measured along the temperature increasing and decreasing with a spectrophotometer. In the beginning of the heating, the device is in opaque state and transmittance has low values. When it reaches a temperature value where levels suddenly start to growth spontaneously, it means that occurred the opaque-transparent transition. This will be the temperature that matches the Tc. The same happens at same temperature during cooling but with high values of transmittance in the beginning and levels suddenly drop, but this time occurs the transparent-opaque transition

-Measuring Capacitance

As a PDLC device is composed by two conductive plates, it can be considered that these devices act as capacitors which mean that is possible to measure their capacitance.

A capacitor is a device that stores electric potential energy and electric charge. To make a capacitor, just insulate two conductors from each other with a certain area and distance between the two.[27] Capacitance is known to be the ability of a body to store an electrical charge. A capacitor can be expressed as a system with two conductive plates insulated from each other, usually sandwiching a dielectric material. Figure 1.14 shows an illustration of a capacitor:

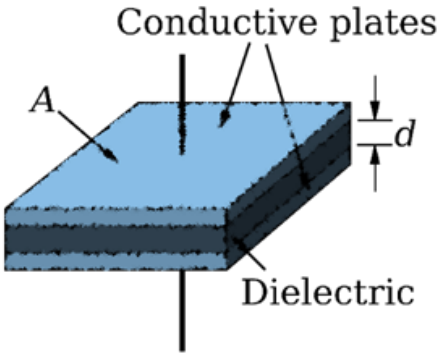

Figure 1. 14 - Illustrative scheme of a capacitor

Capacitance can be expressed by de charge divided by the voltage between both plates:

$$C = \frac{Q}{V}$$

The relation between distance and area can be deduced with the Gauss Law. This is a law that relates the distribution of electric charge to the resulting electric field.

$$\oint E \cdot dA = \frac{Q}{\varepsilon}$$

With the surface integration it can express the charge with the expression below:

$$C = \frac{\varepsilon A}{d}$$

where A is the plates area, d the distance between plates and ε the permittivity. The unities of charge and electric field are coulomb (C) and Volt per distance (V/μm), respectively. The unit of capacitance is Faraday (or Farad, F). In a parallel plate capacitor, the capacitance is directly proportional to the surface area of the conductor plates and inversely proportional to the separation distance between the plates.[28]

When the liquid crystal turns to isotropic, the permittivity values turns constant along temperature as is explained on figure 1.8. As the capacitance measuring is based on the distance between plates, the LC director vector is perpendicular to this distance. Therefore, the capacitance variation along temperature will be based on dielectric permittivity perpendicular to the director ($\varepsilon\perp$) variation and polymer dielectric permittivity (ε_p) variation. When the $\varepsilon\perp$ turns constant, a discontinuously point on capacitance curve must be viewed. This will be the Tc.

1.2.5. Transmittance and Capacitance values in a PDLC with PME

As is explain in figure 1. 11, in the case of PME the final transmittance is higher than initial. This is the principal parameter that can define if PDLC has or has not Permanent Memory Effect.

In terms of capacitance, it shall happen the same. When an electric field is turned on, the LC molecules orientation will change and by consequence the director will also change as was explained in figure 1.9. This will have contributions in capacitance values. Figure 1.15 shows how capacitance values can vary by an applied electric field in a LC device.[29]

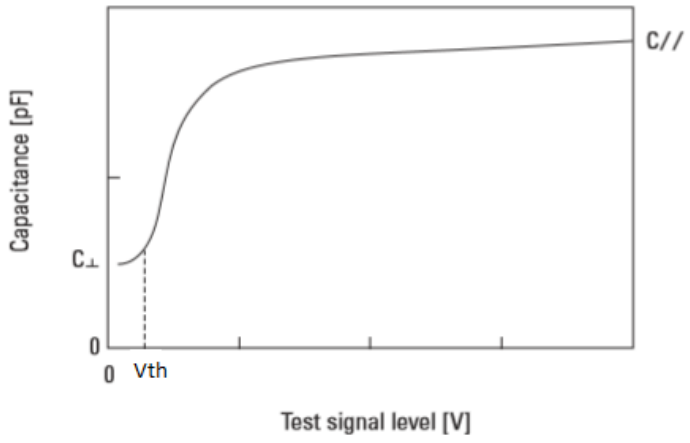

Figure 1. 15 - Capacitance variation when an electric field is applied on a LC device[29] **Adapted**

The capacitance varies with director orientation. In figure C∥ represent the capacitance value parallel to the director and C⊥ the capacitance perpendicular to the director. This happens because the ε∥ value is higher than ε⊥, which means that for capacitances will happen the same.

In a PDLC device with PME, when an electric field is applied, the director will turn parallel to the distance between plates and, by consequence, the capacitance values will increase.

1.2.6. Applications

PDLCs have a wide variety of applications due to their peculiar electro-optical and mechanical properties. Such properties allow the use of PDLC in situations where other devices cannot be used. The most popular application for PDLC are the smart windows. Smart windows are composed by two conductive glasses, between theses glasses is placed a PDLC. Initially, the device is opaque, but with the application of an electric field the window switch to a transparent state.

PDLC Film-enabled glass can provide easily-controllable and security for both exterior windows and for interior glazing such as conference rooms or patient consultation rooms.[30] Figure 1.16 shows a PDLC application from Polytronix Glass Co., a company that makes Switchable Glass Systems with PDLC films.

Figure 1. 16 - Example of PDLC application in a smart window: a) ON State b) OFF State[30] **Adapted**

1.2.7 Write, read and erase information on a PDLC device

PME can be cleared when heat is applied. When the temperature is nearly the opaque-transparent state, the molecules of liquid crystal turn off their order of disposition and the memory transmittance disappears.

Information is written with the application of voltage to each PDLC unit independently, read by the optical response for each unit (opaque or transparent), and the written information erased using either a heating source or a higher frequency electric field for a dual frequency liquid crystal. Opaque and transparent stable states can be the base of a digital binary language where opaque state matches to 0 and transparent state to 1. That means, we can:

Write information - by applying an electric field,

Read written information - by opaque/transparent differentiation by using a laser, and

Erase information - by heating the device until a temperature higher than Tc.

Figure 1. 17. shows a scheme of writing, reading and erasing in a PDLC on a set of 16 PDLC cells (2 bytes).

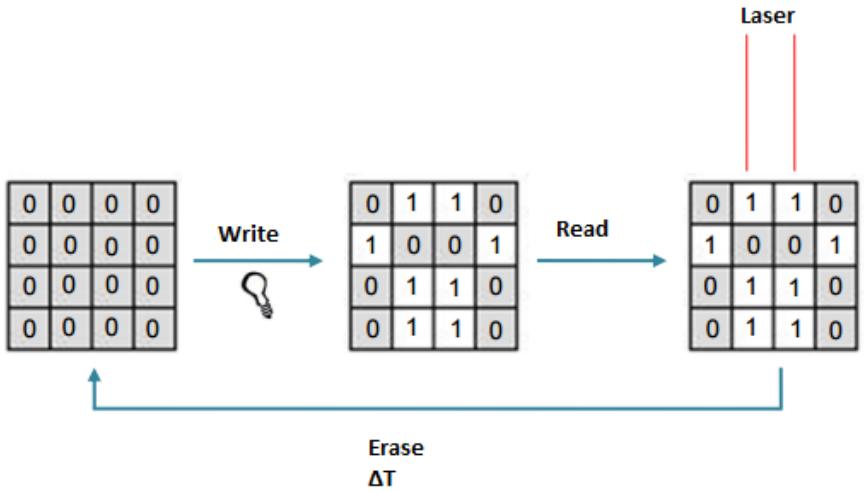

Figure 1. 17 - Write, read and erase information on a set of 16 PDLC cells device[31] **Adapted**

The written information can be erased if the device is heated by means Joule effect with an electric current for instance until the Tc is reached. If the Tc capacitance value is known, it is possible to measure the capacitance while the device is being heated. When the value is reached, the current can be turned off. The LC molecules return to their initial disposition and by consequence, the device returns to the opaque state.

This method can be very usefully on smart windows with PME displays. If a system can apply an electric field for turning the device transparent and heat the device with an electric current by joule-heating effect for returning to the opaque state, it can be very advantageous in terms of energetic waste.

The most advantageous way for controlling these parameters is by capacitance measuring. The capacitance variation along temperature can give more rigorous information than transmittance variation. In a smart window system it is more difficult controlling the transmittance than capacitance and, actually, transmittance curve can only show the jump between opaque and transparent states. Capacitance curve can also show this transition, has a trustworthy relationship with temperature variation and is easier to measure.

In this work, the method proposed for controlling the parameters in these systems consists in:

- Find the Tc by temperature variation, and which capacitance value matches it
- Write the information, this is, turn the device transparent with an electric field for a few seconds.
- Erase the written information, heating the device by Joule-effect and measuring the capacitance variation. If the heat is enough to reach the Tc capacitance value, the device will return to opaque state.

2

Chapter 2 - Materials and Methods

2.1. Materials

2.1.1. Liquid Crystal – E7

The E7 nematic liquid crystals mixture contains cyanobiphenyl and cyanoterphenol components made by Merck, at a specific composition, which possess relatively high birefringence and positive dielectric anisotropy. Due to these properties, it is widely used in polymer dispersed liquid crystals. The specific composition is critical to ensure physical properties and characteristic of the liquid crystal, such as T_{NI} higher than room temperature and a wide applicable temperature range. Even small changes can have pronounced effects on factors such as the nematic to isotropic transition (T_{NI}), and glass transition (Tg) temperatures.[32]

E7 is composted by four kinds of liquid crystals in different proportions that are described in table 2.1 [32]:

Table 2. 1 - E7 composition

Compound	Structure	Tempera-ture Range (Nematic - Isotropic)	Percentage (w/w)%
5CB 4-cyano-4'-n-pentyl-biphenyl	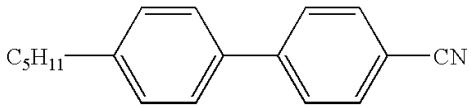	22-35ºC	51
7CB 4-cyano -4'-n-heptyl-biphenyl	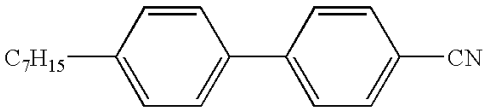	28-42ºC	25
8OCB 4-cyano-4'-n-oxyoctyl – biphenyl	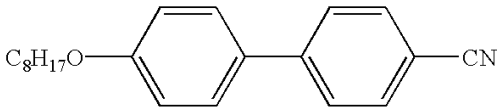	54-80ºC	16
5CT 4-cyano-4"-n-pentyl-p-terphenyl	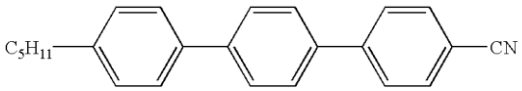	130-239ºC	8

E7 is composted by four kinds of liquid crystals in different proportions. These liquid crystal have different structures and therefore the temperature range of nematic-isotropic transition are not the same. It was necessary for the study cases the temperature be higher than room temperature. For those reasons, the E7 temperature of Nematic-Isotropic transition is about 58ºC.

E7 can be used in polymer dispersed liquid crystals, and it was used in all studies in this work, because it offers a wide range of operating temperatures in which it maintains anisotropic characteristics. The refractive indexes of E7 at T=20ºC are given as: no=1.5183, ne= 1.7378. The dielectric permittivity values of E7 at T=20ºC are given as: $\varepsilon\perp=18 \times 10^{-12}$ F m^{-1}, $\varepsilon\parallel=7.5\times10^{-12}$ F m^{-1}. It exhibits a nematic to isotropic transition at 58ºC and a nematic phase and no other transitions between 58 and -62ºC, where it shows a glass temperature transition. [33] Therefore, liquid crystalline properties are extended down to the glass transition. These features are possible due to the multicomponent nature of E7.

2.1.2. Oligomer and Initiator

Radical polymerisation was used in this work. This polymerisation consists in a reaction which a polymer forms by the successive addition of free radical building blocks, in this case the oligomer PEGDMA875. To make these reactions it was also needed an initiator that can discompose in free radicals and it will be the AIBN.

The oligomer PEGDMA875 (Polyethylene glycol dimethacrylate), from Aldrich has a molecular weight of 875g mol^{-1} and a density of 1.0135 g cm^{-3}. Figure 2.1. shows the Oligomer Molecule[34]:

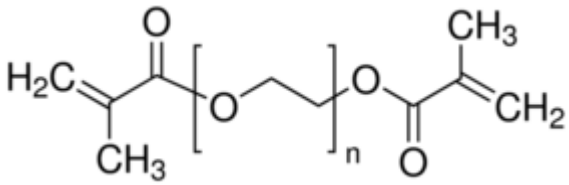

Figure 2. 1. – Oligomer PEGDMA875[34]

The polymerisation is initiated through the use of agents capable of forming free radicals, which are referred to polymerisation initiator. The initiator was a thermal initiator, α,α-azobisisobutyronitrile (AIBN), from Sigma Aldrich, and it has a molecular weight of 164.21 g mol^{-1}. When it heated, AIBN originates two free radicals and nitrogen (at T>64ºC). [35]. Figure 2.2. shows the AIBN molecule

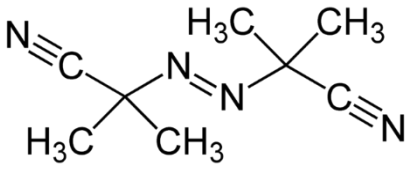

Figure 2. 2 – AIBN (α,α-Azobisisobutyronitrile) [35]

2.1.3 Radical Polymerisation

Steps of radical polymerisation.

There are three fundamental steps in radical polymerisation: initiation, propagation and termination. In the case of this polymerisation the initiator (I) will be the AIBN and the Monomer (M) will be the oligomer PEGDMA 875.

Initiation - Generation of free radicals (R·) by homolytic dissociation of the initiator (I). Chain polymerisation reactions are different because an initiation step is needed to start the polymer chain growth. Initiation can be achieved by adding a small amount of a chemical that decomposes easily to form free radicals.

$$I \xrightarrow{k_d} 2R\cdot$$

$$R\cdot + M \xrightarrow{k_i} RM\cdot$$

Propagation - Chain extension by successive addition of monomer molecules (M) to the monomer radical unities (Mn·) formed in the initiation step.

$$RM_n\cdot + M \xrightarrow{k_p} RM_{n+1}\cdot$$

Termination:

In the last step, radicals combine or disproportionate to terminate the chain growth and form polymer molecules. Termination can occur by the simple interaction between two active species and -Mn e Mm - termination by combination - or disproportionation, where one active centre is neutralized by transfer of a hydrogen atom of an active species to another. [36]

$$RM_n\cdot + RM_m\cdot \xrightarrow{k_t} \begin{cases} R_2M_{n+m} \\ RM_n + RM_m \end{cases}$$

2.1.4 PDLC preparation

The ratio liquid crystal/oligomer used was always 70/30 in all devices in this study. By the quantity of oligomer, a small quantity of initiator (1%) was dropped for inducing the polymerisation. All weights were measured in the analytical balance model AS 120/C/1 from RADWAG.

These mixtures were used directly in cells and it spreads completely their empty spaces by capillarity. The PDLC preparation was done slowly in a stove during night at 74ºC. This temperature ensures the formation of free radicals and then the polymerisation starting. Figure 2.3 shows the stove used for polymerisation.

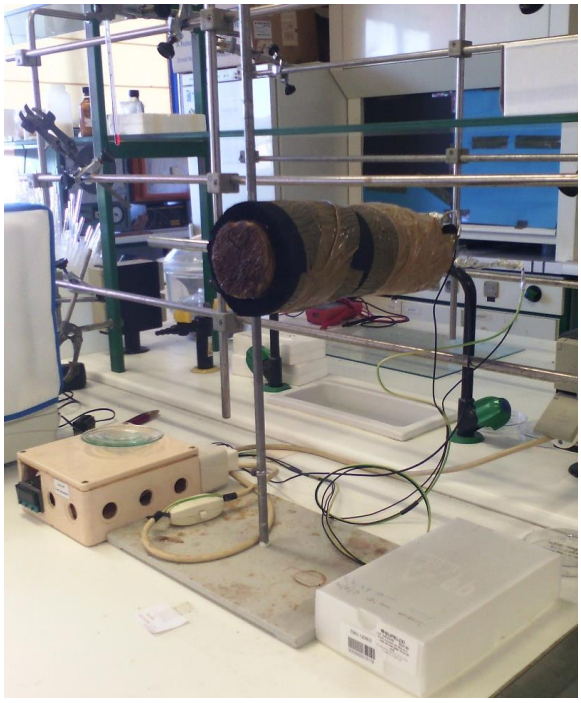

Figure 2. 3 – Stove used for polymerisation

2.2. Commercial and Handmade Cells

For this work two kinds of cells were used: LC2-20 commercial cells from Instec Co. and Handmade Cells made with conductive glasses made by Instec.

2.2.1. Alignment on Glass

Alignment layers are commonly used to align the liquid crystal molecules on substrates. In general, the LC alignment has to originate from symmetry breaking at the surface of the substrate. Asymmetries in either the macroscopic topographical or microscopic molecular structure of the substrate surface have been proposed for its origin. While a variety of methods can be used to determine the precise alignment direction of the LC molecules, even for monolayer films, it is more difficult to obtain detailed information regarding the molecular structure of the surface.[37]

Another important aspect of LC alignment is the origin of the so-called pretilt angle. The pretilt angle is of great technological importance in that it determines the gray scale contrast in LC displays.

The alignment can be divided into two major types: planar alignment, where LC molecules gain a parallel alignment and homeotropic alignment where LC molecules align perpendicularly to the substrate glass. Figure 2.4. shows how this two types of alignment can align the molecules on glass substrate.

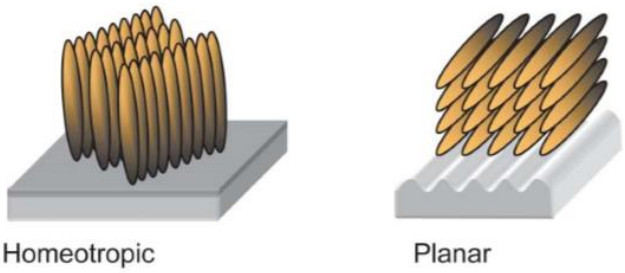

Figure 2. 4 - Illustrative scheme of Homeotropic and Planar Alignment[37]

The planar alignment can be combed in a preferential direction by a technique called rubbing. Rubbing consists in spread the substrate in one preferential direction for aligning the LC

molecules. On cells, rubbing can have three alignment types: parallel, where both glasses have rubbing in same direction and way, anti-parallel, where both glasses have rubbing in same direction but different ways and perpendicular where glasses have perpendicular directions. Figure 2.5. shows this three sub-types of planar rubbing:

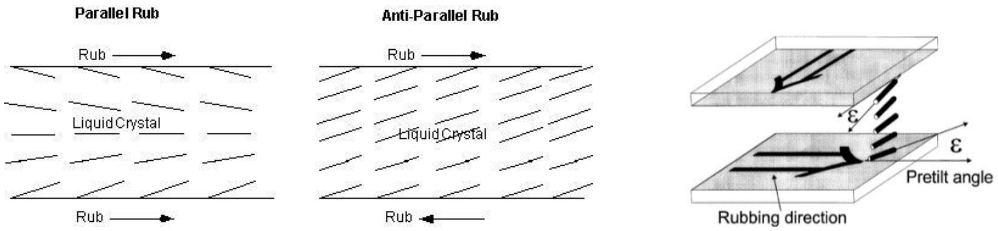

Figure 2. 5 - Illustration of Parallel, Anti-Parallel[38] and Perpendicular[37] alignment on devices

2.2.2. Instec commercial cells

These commercial cells are made by two conductive glasses. The cells have a low parasitic capacitance, and the active area can be completely filled with the liquid crystal/oligomer material. The cell gap of each individual cell is 20 µm uniform to ±0.2 µm with 5x5mm ITO area in the middle of the cell and an anti-parallel alignment layer with 1º to 3º pre-tilted angle. The adhesive used in construction of these cells is rated to 200°C.[39] Figure 2.6 shows an illustrative scheme from a LC2-20 cell from Instec Inc.

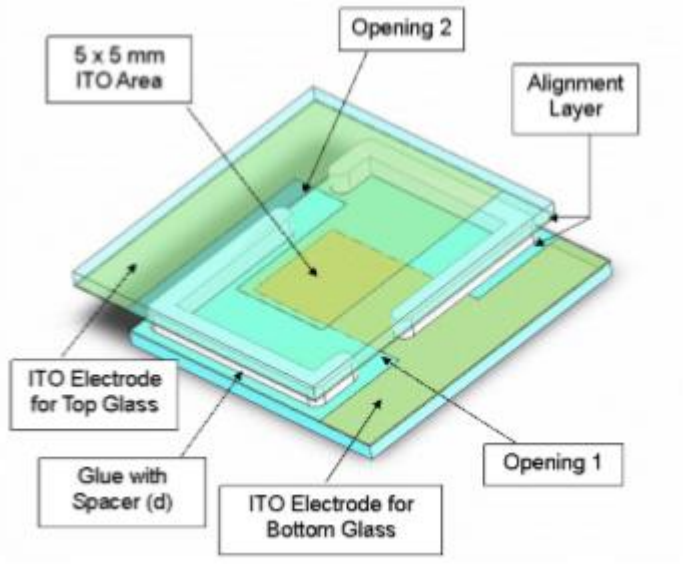

Figure 2. 6 - Scheme of a commercial cell LC2-20 from INSTEC[39]

2.2.3. Instec Glasses

Instec glasses sheets are conductivity glasses with Indium Tin Oxide (ITO) and a rubbing surface with polyimide (PI).[40] These glasses have a size of 25mmx20mmx2.2mm and a sheet resistance of 25ohm/sq. with a small frame which is non-conductive. They were used for made handmade cells in this work. Figure 2. 7 shows an illustrative figure of a substrate glass from Instec.

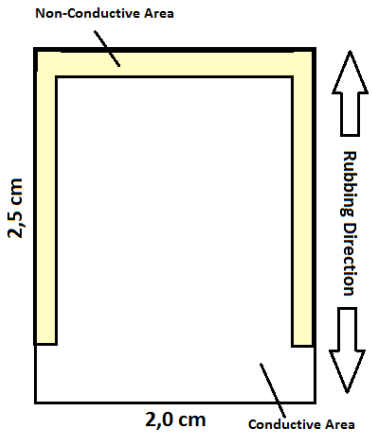

Figure 2. 7 - Illustrative figure of a substrate glass DA256A-PI from Instec Inc.

It is only known the rubbing direction on these glasses, there is no any information about the way: if the rubbing is from up to down or if it is from down to up. Then it was assumed that the glasses have the rubbing in same way and for making the handmade cells with different rubbing types the frame side was the reference.

2.2.4. Handmade Cells

Handmade cells were made with Instec Glasses. The rubbing effect depends how these glasses are used to make a cell. The rubbing has some effect on the liquid crystal molecules, namely in their disposition near the surface

For cells with perpendicular rubbing the whole glass was used to prepare them. For making cells with parallel and anti-parallel rubbing the Instec glasses were coated in small parts to obtain the target rubbing configuration. Perpendicular Rubbing Cells have 4cm^2 area and it was made with the whole Instec glass. Parallel and Anti-Parallel rubbing cells have 1.5cm^2 area and they were made with coated glasses, one glass with 25mmx10mm and other with 20mmx15mm. For the spacing, two Mylar spacers with 23µm of thickness were used. Figure 2.8 shows the three planar rubbing types used on this work.

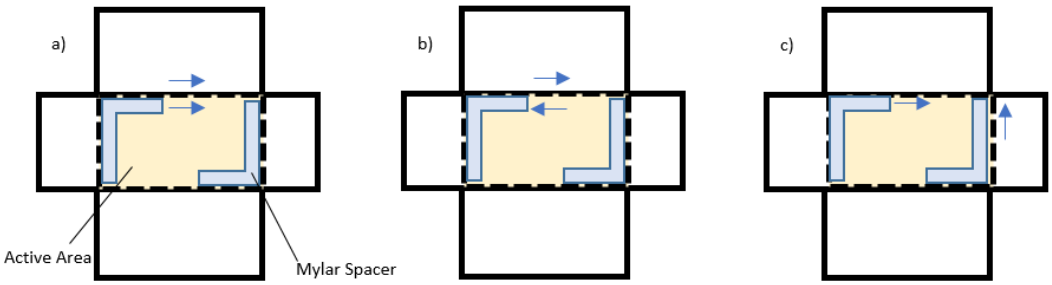

Figure 2. 8 - Illustrative scheme of handmade cells with: a) Parallel; b) Anti-Parallel; and c) Perpendicular Rubbing

Cells without any alignment were also made (Only ITO) and with homeotropic alignment. For these cells conductive glasses XY100T from Xinyan Technologic were used. These glasses have a 500mmx500mmx1.1mm size with an ITO coating and 100 ohm/sq of sheet resistance. For making cells, they were coated in the same proportions of Instec Glasses.

The homeotropic alignment cell was guaranteed with a lecithin layer. The procedure consisted in washing the ITO glasses first with an aqueous nitric acid solution 1:1 and then with ethanol. After washing, the glasses were standing on a desiccator during one day for drying. A lecithin solution with concentration 10g/L was prepared afterwards and the dry glasses were dripped in this suspension solution for 10 minutes. Then the glasses were standing on a desiccator during one day again, for drying.

Figure 2.9. shows a lecithin molecule used for homeotropic alignment:

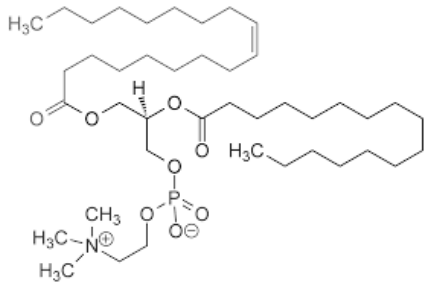

Figure 2. 9 - Lecithin molecule

2.3. Equipment

2.3.1. Measuring Capacitances - LCR Bridge

A Programmable LCR-Bridge from Hameg**.** Programmable LCR-Bridge HM8118 can measure certain values from electric or a conductor display, namely capacitance, impedance, resistivity, inductance and respectively dissipation. In this study LCR-Bridge was used to measure capacitances on cells. Figure 2.10 shows the LCR-Bridge HM8118

Figure 2. 10 - LCR Programmable Bridge HM8118 system from Hameg[41]

Calibration

The Programmable LCR-Bridge HM8118 calibration can be done by two different manners: by open circuit calibration and by short circuit calibration. The open/short circuit calibration compensates for the effects of parasitic impedances of the connections to the component under test.

The LCR bridge HM8118 features a frequency range of 20 Hz to 200 kHz, in 69 steps, with a basic frequency accuracy of 100 ppm.[41] Open circuit calibration was done with clips far each other, and short circuit calibration was done with both clips connected. Figure 2.11 shows the technique used for short circuit calibration:

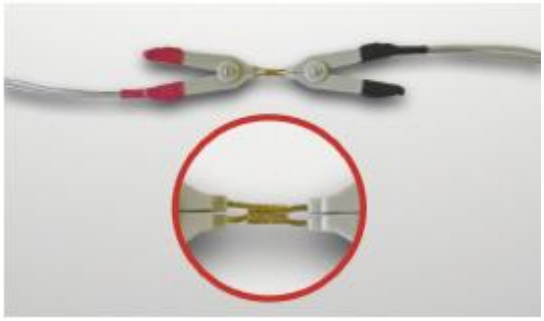

Figure 2. 11 - Short Circuit for LCR Bridge Callibration[41]

The frequency used for measuring capacitances was 1kHz and the sinusoidal voltage was 1V in all studies

2.3.2. Increasing and Decreasing Temperature - FP90 Central Processor

For controlling the temperature variation along the time, a thermoelectric heating (Peltier) system FP90 Central Processor Metler Toledo was used. FP90 can heat and cool with different temperature ratios and it has a temperature range between room temperature values and 375ºC.[42] This equipment was used as a control temperature system for heat and cool the cells. Figure 2.12 shows the FP90 Central Processor.

Figure 2. 12- F90 Central Processor Metler Toledo[42]

2.3.3. Heating with Joule-Heating Effect – TTi EX4210R Power Supply

The Joule-Heating effect can generate heat when an electric current moving across ITO layer of a conducting glass. This is a way to heat a PDLC cell and it can be done by choosing an electric current applied by a TTi EX4210R power supply.

The Joule heating produces heat by an electric current and it was used for clear written information in PDLC with PME devices. When the cell is subject to an electric current with a provide voltage the ITO layer is heated and the molecules of LC lose their preferred orientation. By this, with cooling the PDLC returns to the initial opaque state. The Joule heating is related with the current intensity and resistance of the material:

$$H \alpha RI^2$$

Where H is the energy by heating, R the resistance in one glass, and I the electric current intensity applied. It can be deduced by this correlation that high levels of intensity produces more heat and then the temperature will be higher.[43]

For heating the devices by joule effect the EX4210R from TTi was used. EX4210R is a direct current (DC) power supply and it has a maximum intensity of 10A and a maximum voltage of 42V.[44] Due to security issues, the equipment was adjusted for intensities until 0.5A. Then when the voltage was increased, the current intensity was also increase. Figure 2.13 shows the EX4210R from TTi, the power supply used on this work

Figure 2. 13 - EX4210R power supply from TTi[44]

2.4. Techniques

2.4.1. Capacitance study with Temperature Variation

To measure capacitance values with temperature variation, the hot cooler system FP90 from Mettler was used to increase and decrease temperature, and Programmable LCR-Bridge HM8118 from Hameg for measure capacitance values. It was connected a conductive wire for each cell glass with conductive ink.

The capacitance dependence on temperature was studied when the devices were heated or cooled within an electro-optic cell. These assays were carried out using LCR Bridge and FP90 Central Processor. The capacitance study with temperature have been done firstly for three kind of cells with separated components: empty cells (without dielectric), cells with Liquid Crystal E7 and cells with polymerized oligomer PEGDMA875. Figure 2.14. shows the assemble used for capacitance study with temperature variation

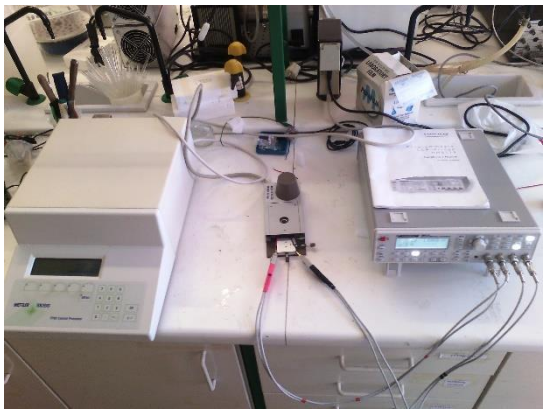

Figure 2. 14 - Assemble used for capacitance measuring with temperature variation

2.4.2. Capacitance-Transmittance study with Temperature Variation

For PDLC devices, the same study was also performed but with an additional diode array spectrophotometer from Avantes (AvaLight-DHS and Ava Spec 2048) to precise the opaque-transparent transition by transmittance variation. These parameters will be very useful to define the PDLC device clarification temperature (Tc) and it respective capacitance. Figure 2.15 shows the assemble used for these study

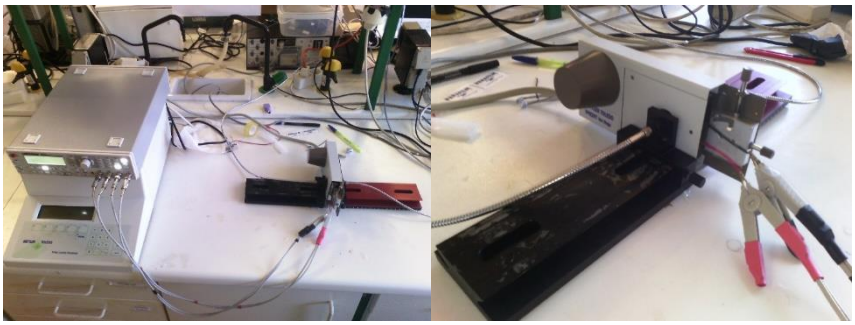

Figure 2. 15 - Assemble for Capacitance-Transmittance study with temperature variation

2.4.3. Capacitance Study with Joule Heating Effect

For capacitance variation studies by Joule-heating effect, the LCR Bridge and the EX4210R were connected one each other by a ground cable. Then it was possible to measure capacitances with different current intensities along time. It is possible to observe the dependence of capacitance with the current used when the PDLC is heated or cooled within an electro-optic cell. When the capacitance reaches a constant value, the current was turned off, and capacitance values were also measured on cooling. If the electric current is enough to reach the Tc, the quantity of electrons that pass through the glass are enough to the cell turns totally transparent. If the electric current is not enough to reach Tc, the electrons that flow the glass will not be enough to turn the cell totally transparent but only a part of it. Figure 2. 16 shows the assemble used on joule heating effect study.

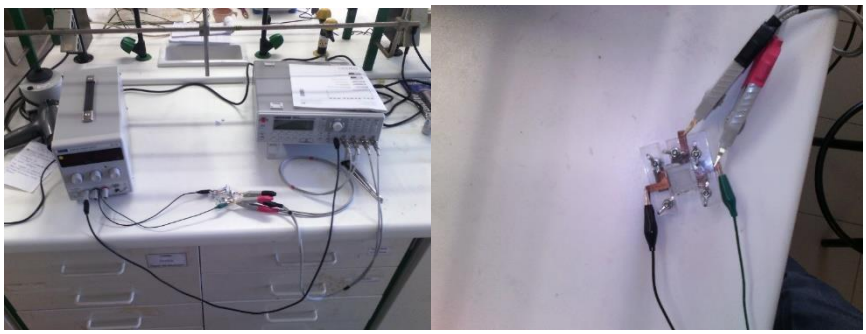

Figure 2. 16 - Assemble for capacitance study with Joule Heating Effect

This assemble was used because it was necessary that current intensity follows the Kirchhoff law for DC circuits[45]. The glass where the heat was applied will work as a resistance and the two glass sandwiched (namely, the cell) will work as a capacitor. The heat flows in one glass and LCR bridge measure capacitances between glasses during heating. By this, the glass can act as a resistor and the cell as a capacitor. Figure 2.17. shows a scheme between Power Supply (PS) and LCR Bridge more precisely:

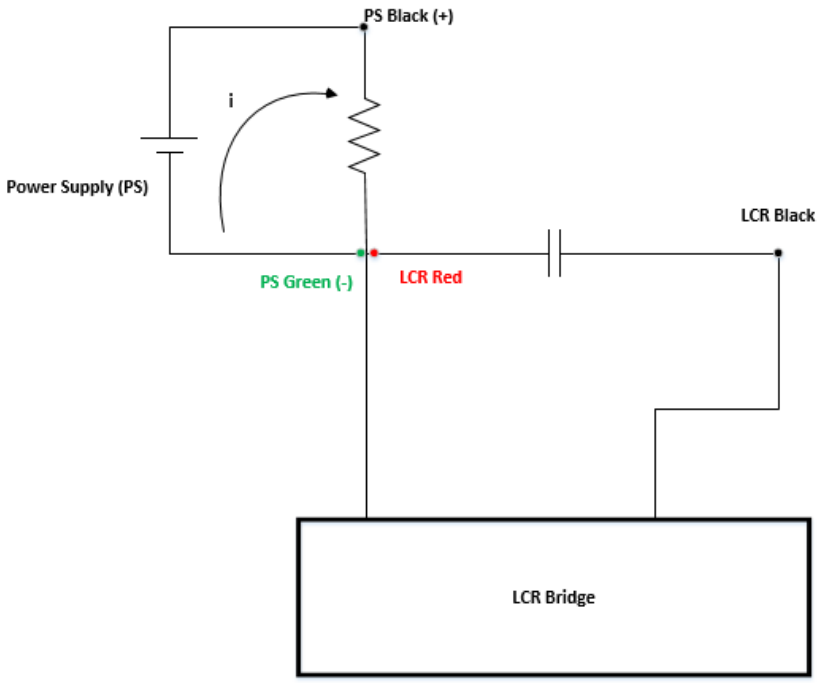

Figure 2. 17 - Scheme for measuring capacitances with Joule-Heating effect

The LCR red clip will work as the input and the LCR black clip will work as the output. With this assemble it was possible to measure the capacitances when a current is passing through one of the glasses.

This method was only used on handmade cells, because it is only possible applying the scheme above if the cells have at least three conductive sides available. Commercial cells have only two sides to connect the crocodile clips from EX4210R and the measuring clips from LCR Bridge.

Perpendicular rubbing cell glasses have the same sizes but in parallel and anti-parallel cells are different. On parallel and anti-parallel cell, the heated glass was the glass with 25mmx10mm. Due contact issues, this study required a technique that can increase the contact area. Therefore these cells were inserted in an acrylic support with a little surface of copper inside for increasing the contact area. Figure 2.18. shows an image of one of these support used.

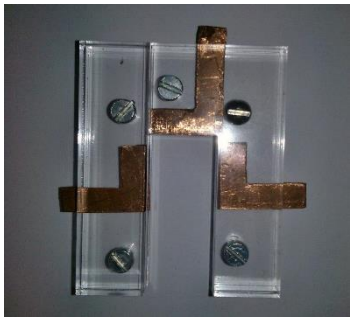

Figure 2. 18 - Acrylic supporters used for heating by joule-effect

2.4.4. Electro-optical (EO) Study

Electro-Optical (EO) study consists in a study based on Transmittance dependence on an applied electric field. This gives important parameters such as the minimum and maximum transmittance, the E90 factor (electric field for 90% of Maximum Transmittance) and then the PME value.

Figure 2.19 shows the EO measuring system used on lab for measuring absorbance when an electric field is being applied in a PDLC cell.

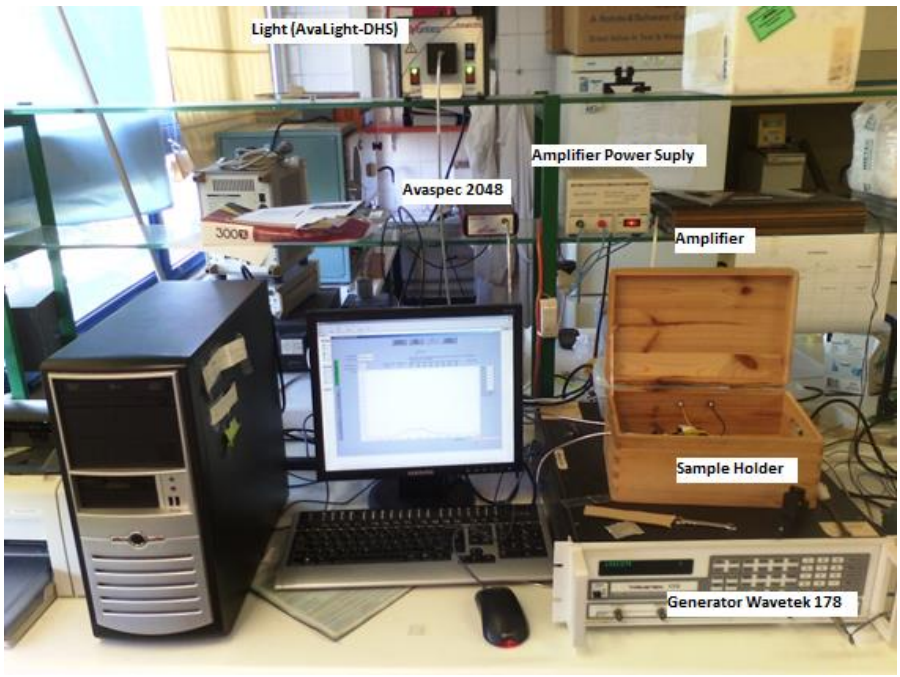

Figure 2. 19 - Electro-optical system

The optical part has a diode array Avantes spectrophotometer (AvaLight-DHS and Ava Spec 2048) using 633 nm light by means a halogen lamp and optical fibber cables that carries the light to the sample holder. The signal generator (Wavetek 178) creates a 1 kHz sine wave with its amplitude varying between 1 mV and 10 V. This signal is, then, converted to an electrical power signal, with a small voltage gain, by an audio amplifier (Vtrek TP-430) which allows the output sine wave to be applied to the transformer's secondary coil. The amplifier is connected to the transformer's secondary coil because it was used a conventional 230V:9V stepdown transformer. With the transformer connected in reverse, one can achieve a 24x voltage gain.

The study was divided into three cycles, which corresponds to 1/3, 2/3 and 3/3 of the maximum applied voltage (400 V). Each cycle consists of 35 experimental points and each point is made in 1.2 seconds. The pulse is applied to the sample activated after 10 ms and lasts for 200 ms and, later, takes 1000 ms to apply new pulse.[46]

2.4.5. Polarized Optical Microscopy (POM)

A polarizing microscopy consists in a microscopy that uses polarized light for investigating the optical properties of specimens. Although originally called a mineral microscope because of its applications in petrographic and mineralogical research, in recent years it has now come to be used in such diverse fields as biology, medicine, polymer chemistry, liquid crystals, magnetic memory, and state-of-the-art materials. [47]

There are two polarisers in a polarized optical microscope and they are designed to be oriented at right angle to each other, which is termed as cross polar. Figure 2.20 shows a schematic figure of a polarized light microscopy

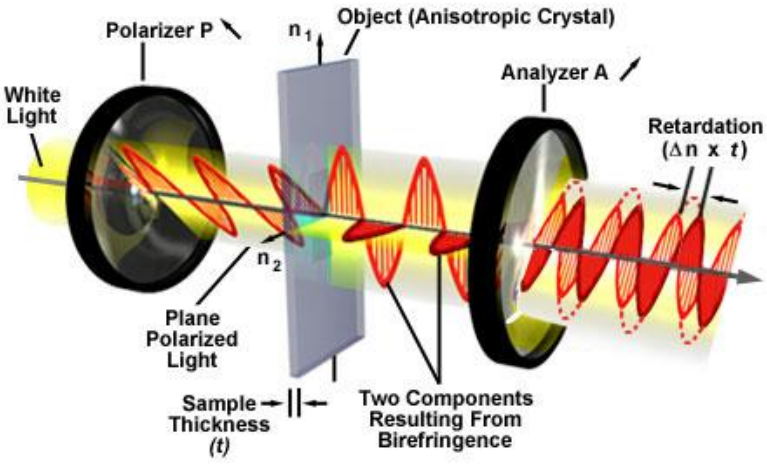

Figure 2. 20 - Crossed Polarizers and Polarized light illustration[48]

In this work the POM images were obtained directly from PDLC films with a Olympus CX-41 microscope with crossed polarisers, equipped with a Olympus Carmedia SC30 camera. Figure 2. 21 shows the POM apparatus used for taking images from cells:

Figure 2. 21 - POM apparatus

2.4.6. Differential Scanning Calorimetry (DSC)

Differential Scanning Calorimetry (DSC) is a thermal analysis technique that looks at how a material's heat capacity is changed by temperature. A sample of known mass is heated or cooled and the changes in its heat capacity are tracked as changes in the heat flow. This allows the detection of transitions such as melts, glass transitions, phase changes, and curing.

The biggest advantage of DSC is the accuracy and speed that it can be used to see transitions in materials. It is a good method for polymeric materials analysis.[49] In this work DSC was used to determine the oligomer polymerisation temperature, the Tg of polymer and E7 and also the Nematic-Isotropic Temperature transition of E7. This is an important way for precise these temperature points, which will be useful to determine the polymer and liquid crystal properties.

Figure 2. 22. shows the DSC q200 from TA apparatus used in this work

Figure 2. 22 - DSC apparatus

During the DSC analysis, the system reproduce a graph which present the different proprieties on substance. The peaks will give information about the glass transition temperatures, crystallization temperatures, melting points and another relevant temperatures. Figure 2.23 shows an example of a typical graph with known peaks after a DSC analysis [50]

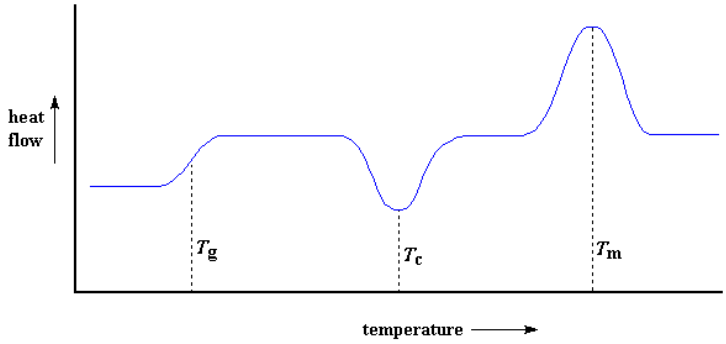

Figure 2. 23 - Heat flow variation with temperature[50]

2.4.7. Atomic Force Microscopy (AFM)

Atomic force microscopy (AFM) is a method to probe a surface in its full, three-dimensional glory, down to the nanometre scale. This method determine the surface heights by "touching" it with a sharp, while measuring the vertical displacement needed to do so. This touching can be very subtle and the whole process is gauged in quite indirect ways.[51]

Figure 2. 24 shows illustrative scheme of a AFM processing analysis

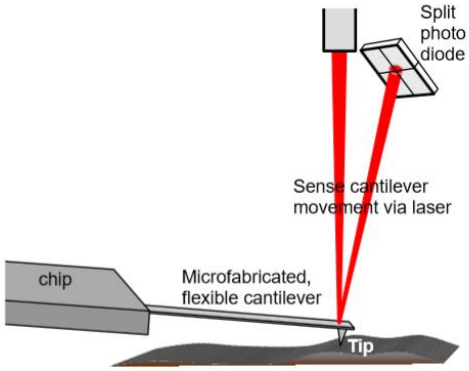

Figure 2. 24 - AFM technique[51]

AFM analysis gives two images: Left image and Right Image. Left Image consists in a height image, which gives information about the surface namely how is reduced height from beam exposure. Right image consists in a phase image, which reveals a lack of stiffness contrast in the exposed region.

In this work AFM was used to find the surface aspect of four samples: ITO covered glass by Xinyan, ITO covered glass with planar alignment layer by Instec, ITO covered glass by Xinyan covered with E7/PEGDMA875 and ITO covered glass with planar alignment layer by Instec covered with E7/PEGDMA875 PDLC. The frequency used was between 300 and 400 kHz, these are the range of values for a 1V peak needed. Figure 2.25 shows the AFM system used on this work.

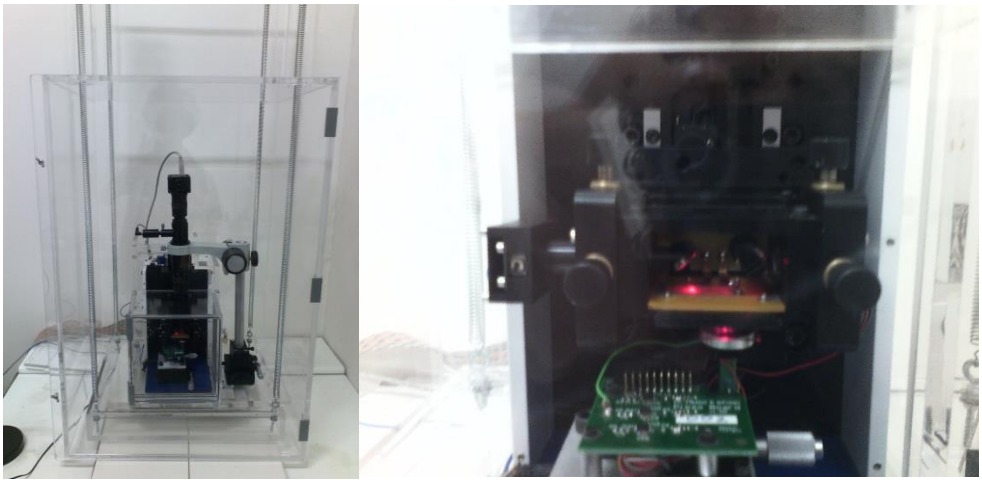

Figure 2. 25 - AFM apparatus

2.4.8. Scanning Electron Microscopy (SEM)

Scanning Electron Microscopy (SEM) was another method to analyse the glass surfaces. SEM requires a system to produce an electron probe, a specimen stage to place the specimen, a secondary-electron detector to collect secondary electrons, an image display unit, and an operation system to perform various operations. The electron optical system consists of an electron gun, a condenser lens and an objective lens to produce an electron probe, a scanning coil to scan the electron probe, and other components.[52] For this analysis it was necessary to remove the liquid crystal from the polymer. Then the glasses were washed with a solvent, acetonitrile, and they were left on a desiccator during one day. Figure 2.26 shows the SEM apparatus from CENIMAT, FCT-UNL.

Figure 2. 26 - SEM apparatus from CENIMAT, FCT-UNL[53]

3

Chapter 3 – Results and Discussion

3.1. DSC analysis

DSC analysis was done to find the thermal properties in liquid crystal E7, oligomer PEGDMA875 + 1% AIBN and mixture 70%/30% E7 PEGDMA875. With this analysis it is possible to understand more about these materials, namely their behaviour during heating and cooling.

A sequential DSC studies were done with heating and cooling. However some of these substances have irreversible transformations, which means that the material properties change during every cooling and heating. In this chapter there are only represented the first heating studies for these materials. The following studies are represented on Appendix A.

3.1.1. E7

Figure 3.1. shows the heating stage for liquid crystal E7

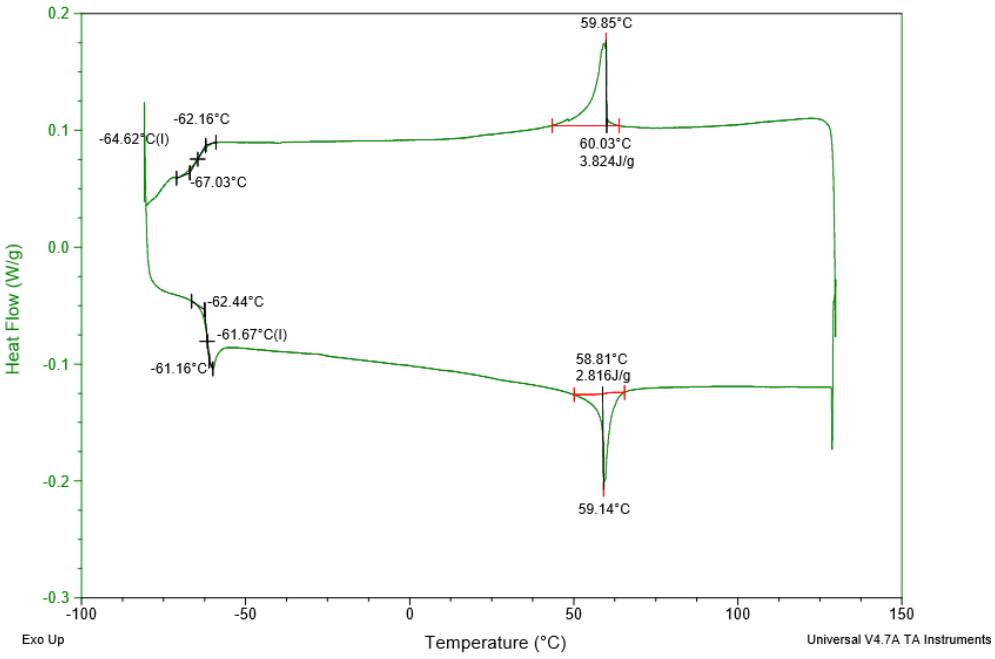

Figure 3. 1 – First heating Stage for E7

From first DSC heating stage it is possible to see two points during heating and cooling. One point is centred at 58.81ºC and matches the liquid crystal Nematic-Isotropic temperature where the nematic liquid crystal turns to isotropic during heating and isotropic to nematic during cooling at 60.03ºC. Another point matches at -61.67ºC on heating curve and at -64,62ºC on cooling curve. These temperatures match the glass transition temperature (Tg).

For other heating stages the results were basically the same, the changes on liquid crystal are reversible and therefore the same points are also present. This stages are represented in Appendix A.

3.1.2. PEGDMA875 + 1%AIBN

Figure 3.2 shows the heating stage for the oligomer PEGDMA875 + 1%AIBN

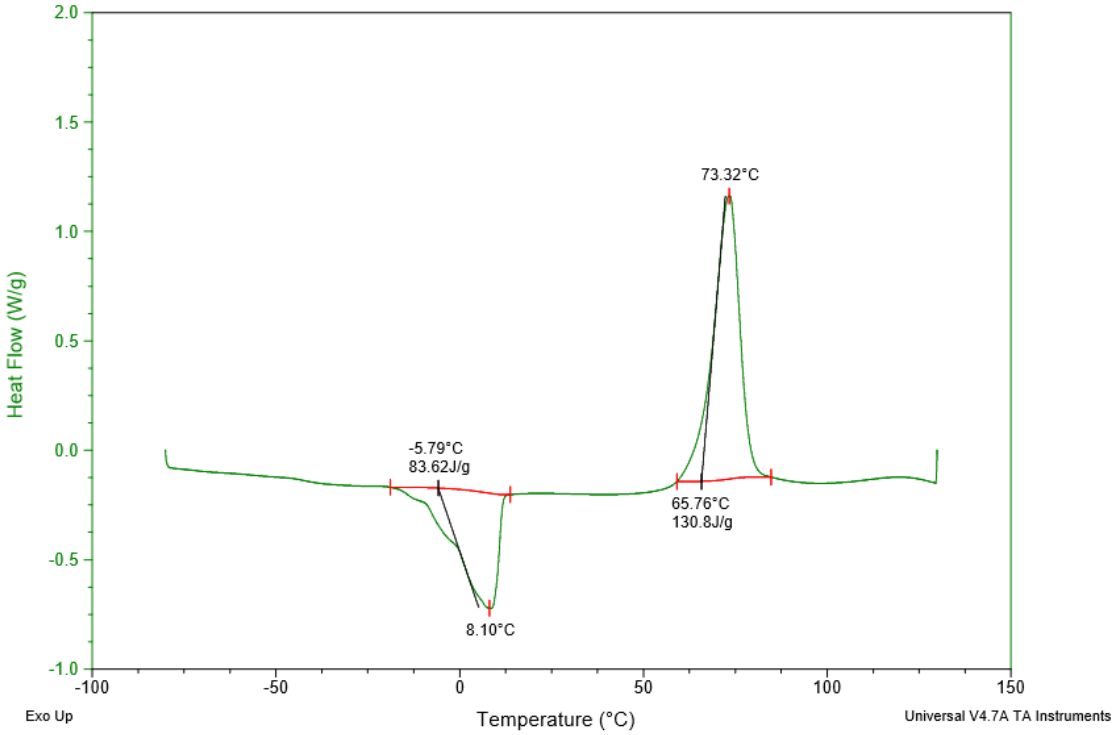

Figure 3. 2 - Heating stage for oligomer PEGDMA875 + 1%AIBN

There are two significant points: a peak at 8.10ºC and a another at 73.32ºC. At 8.10ºC occurs the melting, it turns from solid to liquid, and at 73.32ºC is the peak of polimerisation. After this temperature, the heat is applied to the polymer and there is no return when there is cooling. Oligomer PEGDMA875 has also a Tg around -60ºC but in this case it is diffucult to find it.

Then, the second heating stage was only applied to polimerised PEGDMA875. Figure 3.3 shows the first heating stage for the polimerised PEGDMA875

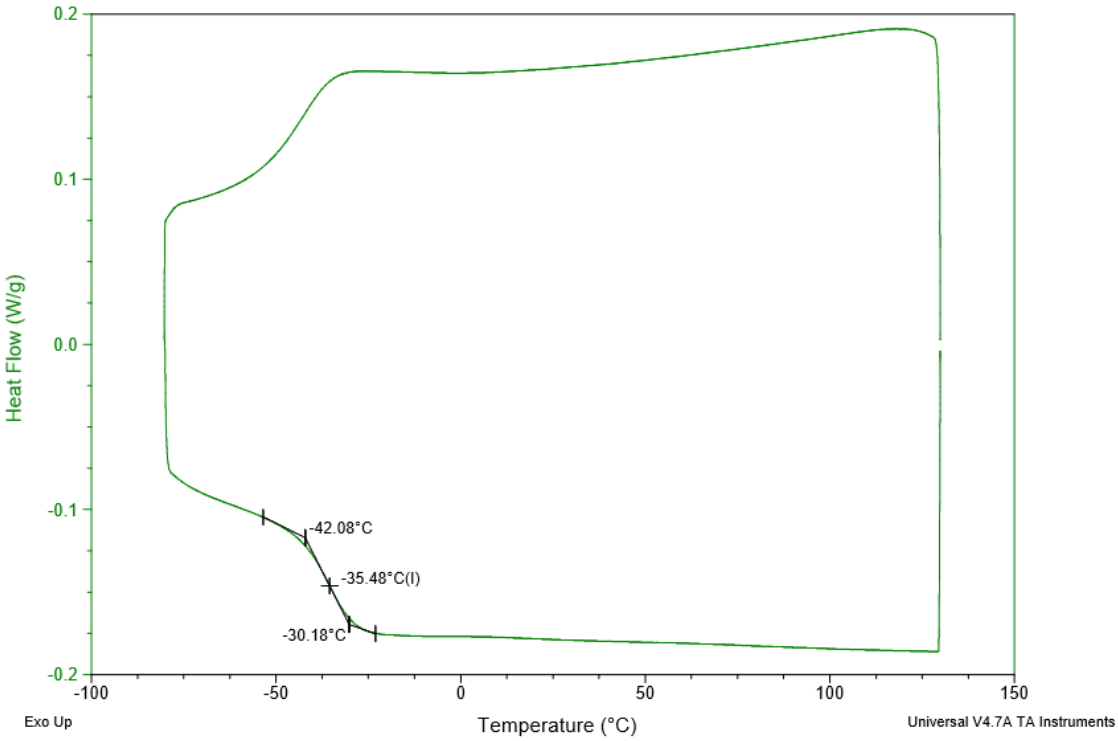

Figure 3. 3 - First Heating cycle for polymerised PEGDMA875

The only point that is visible is the Tg centred at -35.48ºC during cooling and heating.. This is the only relevant temperature point in the analysis of polymerised PEGDMA875 and it means that the polymer is amorphous.

The modifications after and before Tg are reversible, and therefore the following heating stages will be the same. This stages are represent in Appendix A.

3.1.3. Mixture 70% E7 + 30% PEGDMA875

In first heating stage for the mixture 70% E7 plus 30% PEGDMA875 polymerised, the graph is very similar to the E7 DSC analysis. Figure 3.4 shows the first heating stage for this mixture

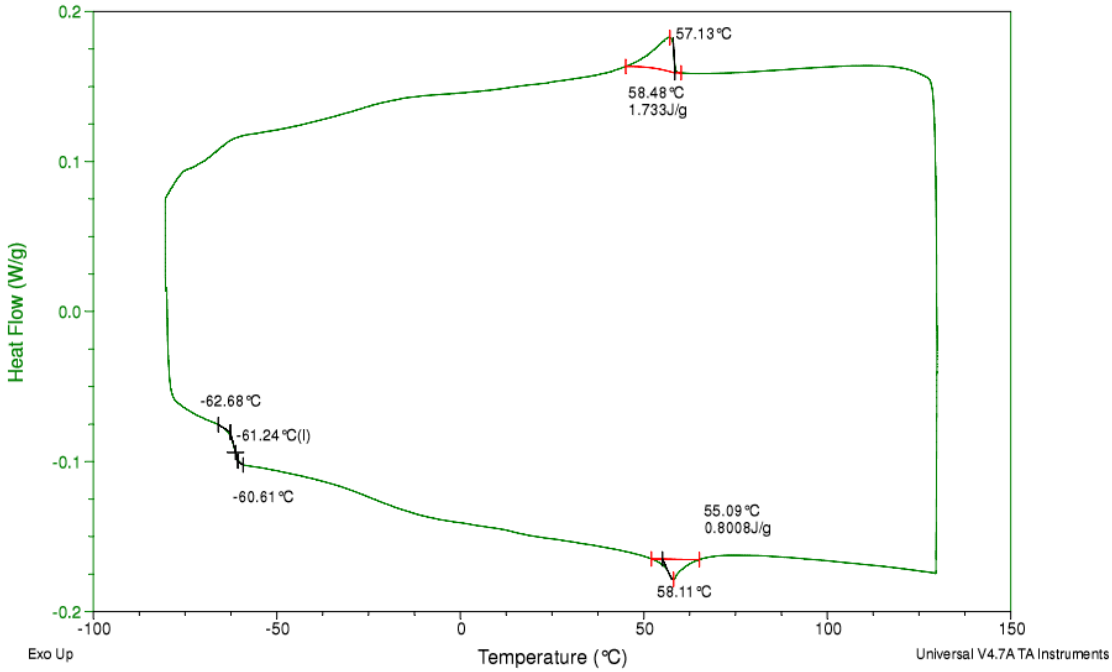

Figure 3. 4 - First Heating cycle for a mixture of 70% E7 and 30% of polymerised PEGDMA875

There are two evident points present in both curves. One at 58.11ºC which matches at 58.48ºC on cooling curve. These temperatures matches the E7 T_{NI} value. The other point is the middle point at 61.64ºC. Despite the PEGDMA875 is polymerised, their Tg is not so evident as the E7 Tg, because liquid crystal proportion is bigger than polymer. This graphic is very similar to the E7 heating cycle. Moreover, the T_{NI} values decrease a little bit on this mixture and, in a nutshell, the mixture presents properties of a polymer and also a liquid crystal.

As the thermal transformations of polymer and liquid crystal are reversible, in a mixture between them will happen the same, as the graph shows. The next heating stage is present on Appendix A.

3.1.4. Discussion

DSC analysis gave the points of the most important thermal properties and transitions of these compounds. When the oligomer polymerises their properties will change in the following heating cycles. The transformations that occur when the temperature reach the Tg in PEGDMA875 and the Tg and T_{NI} in E7 are reversible. In the mixture, due the ratio liquid crystal/polymer, it can be only viewed temperatures that matches the LC Tg and T_{NI}. The polymer temperatures are less evident in the mixture analysis but the heat flow values along the temperature are higher.

3.2. Electro-Optical (EO) Studies

The Electro-Optical studies were done for the six types of cells: four cells with planar alignment layer: commercial cell LC2-20, handmade cell with parallel rubbing, handmade cell with anti-parallel rubbing and perpendicular rubbing; an handmade cell with homeotropic alignment; and one handmade cell without alignment (only conductive glass - ITO). This study can determine the PDLC performance by an applied electric field and, essentially, if it has or not PME.

3.2.1. LC2-20 – Commercial Cell by Instec with planar alignment layer

Figure 3.5. shows the graph for an electro-optical study for a LC2-20 with PDLC.

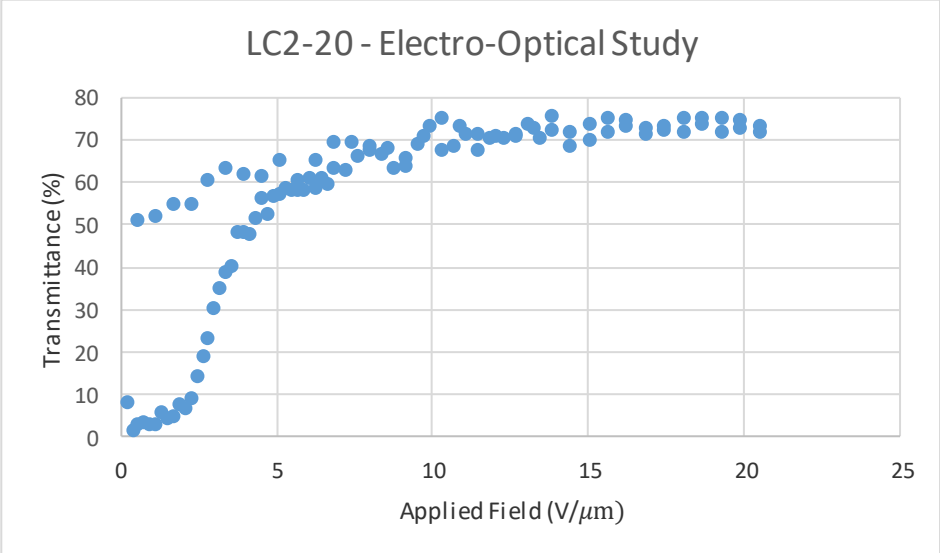

Figure 3. 5 - EO study for a LC-20 cell

Through the graphic above, it is possible to see that there is a high value of transmittance when the electro optic study ends. It means that LC2-20 cell with PDLC has a significant value of PME. Table 3.1. shows the values taken from the electro-optical study for a LC2-20 cell with PDLC

Table 3. 1 - Values from LC2-20 EO study

T_{OFF}	T_{ON}	$T_{OFF'}$	PME (%)	E90 (V/μm)
2	75	51	67	8

The PME is clearly present on a LC2-20 (67%) because the transmittance at the ending is much higher than the transmittance at the beginning. Figure 3.6 shows the POM images with cross polarizers before and after the EO study.

Before EO study **After EO Study**

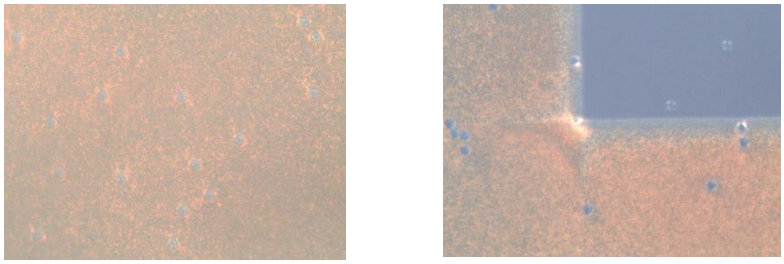

Figure 3. 6 – POM cross polarizers' images from LC2-20 before and after EO study

As it can be seen on Figure 3.6, there is a difference on ITO square after EO study, which means that the memory state is visible by POM. The square is the only conductive part on LC2-20 and the differences between this side and the other are evident.

3.2.2. Handmade cell with parallel rubbing on planar alignment layer (1,5cm^2)

Figure 3.7. shows the EO study for a handmade cell with parallel rubbing on planar alignment layer

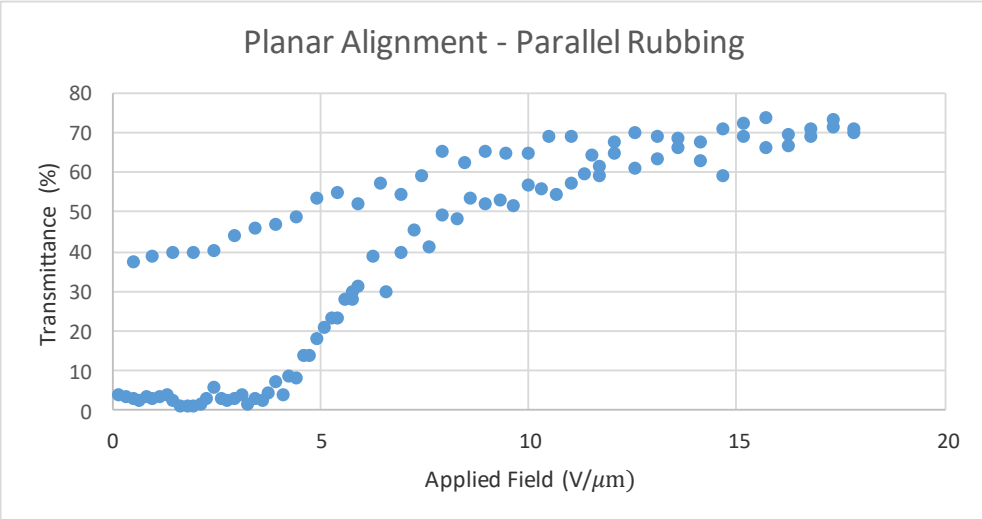

Figure 3. 7 – EO study for the handmade cell with parallel rubbing on planar alignment layer

Through the graphic it can be seen that there is a line with constant transmittances close to 70% when the applied field has great values, and a notable value of transmittance when the electric field is removed. It means that this cell has a considerable value of PME.

Table 3.2. shows the values taken from the electro-optical study for a handmade cell with parallel rubbing on planar alignment layer .

Table 3. 2 - Values from parallel rubbing on planar alignment layer cell EO study

T_{OFF}	T_{ON}	$T_{OFF'}$	PME (%)	E90 (V/μm)
3	74	39	51	15

As the LC2-20, the cell also stars at low values of transmittance, and high values are reached when the applied field have great values. However, this transmittance is not so higher as the LC2-20 cell and it happens the same with the PME, it has a value of 51%.

Figure 3.8 shows the POM images with crossed polarizers from parallel rubbing on planar alignment layer cell before and after EO study.

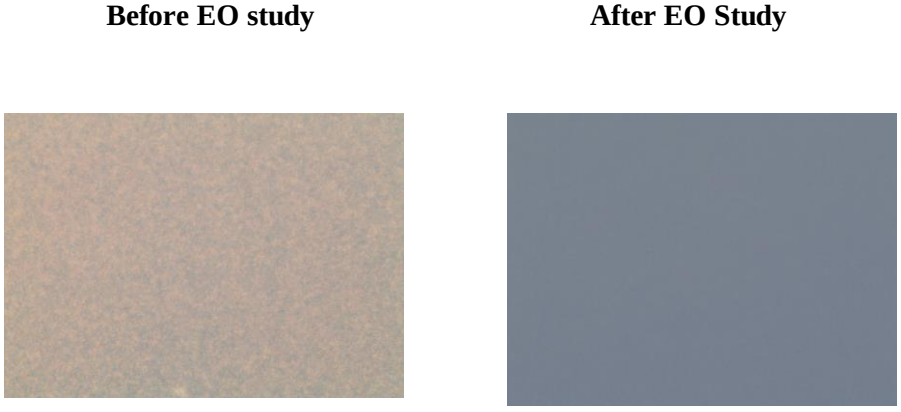

Figure 3. 8 - POM cross polarizers' images before and after EO study for parallel rubbing cell on planar alignment layer

As it can be seen on Figure 3.8. there is a total difference between before and after EO study, which means that the memory state is visible on POM. On these cells, the whole glass will turn transparent instead the square on LC2-20. The glasses are totally conductive, in spite

of the existence of a non-conductive small frame, and due to this the difference is evident in the entire image.

3.2.3. Handmade cell with anti-parallel rubbing on planar alignment layer (1.5cm^2)

Figure 3.9 shows the EO study for the handmade cell with anti-parallel rubbing on planar alignment layer

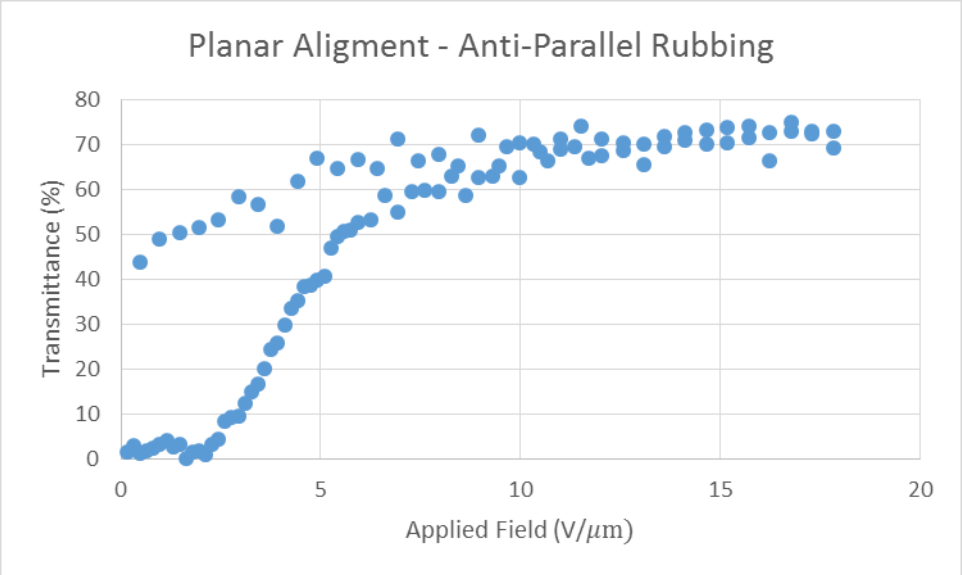

Figure 3. 9 - EO study for the handmade cell with anti-parallel rubbing on planar alignment layer

Through the graph on figure 3.9. it can be seen a stabilisation close to 70% of transmittance when the applied field reach higher values and also a higher transmittance value than the beginning of the study. It means that PME is present on Anti-parallel rubbing on planar alignment layer cell . Table 3.3. shows the most considerable values from this study.

Table 3. 3 - Values from Handmade cell with anti-parallel rubbing on planar alignment layer

T_{OFF}	T_{ON}	$T_{OFF'}$	PME (%)	E90 (V/μm)
2	75	42	55	14

Anti-parallel on planar alignment layer cell has a PME of 55% which means that the transparency is evident after the EO study. Figure 3.10 shows the POM images which can show the differences between before and after the EO.

Before EO study **After EO Study**

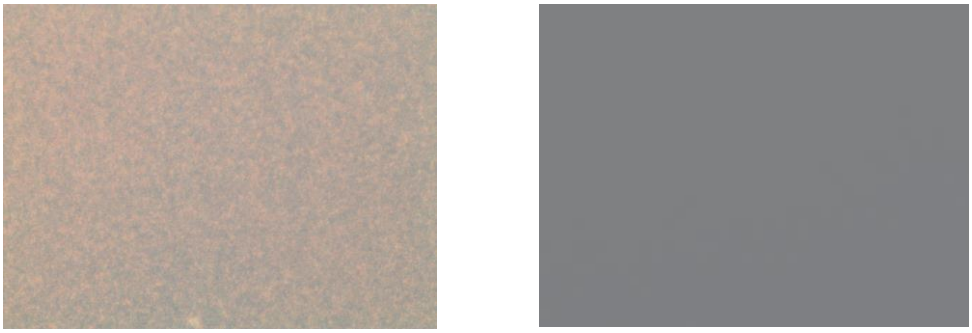

Figure 3. 10 - POM cross polarizers' images from Anti-parallel rubbing on planar alignment layer cell before and after EO study

It happens the same as the parallel rubbing on planar alignment layer cell, it is visible the changing in the whole glass after the EO study due the glasses are all conductive and both images can prove that.

3.2.4. Handmade cell with perpendicular rubbing on planar alignment layer (4cm^2)

Figure 3.11 shows the EO study for a cell with perpendicular rubbing on planar alignment layer and 4cm^2 of active area.

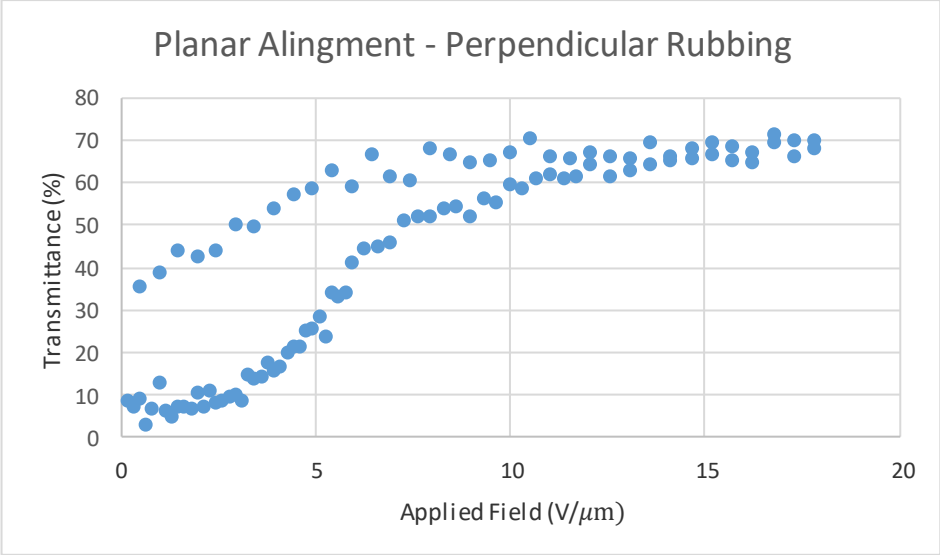

Figure 3. 11- EO study for the perpendicular rubbing on planar alignment layer cell

Through the graphic it can be also seen the transmittance stabilizing when the applied field is considerable, at values close to 70%. The transmittance is higher when the electric is switched off than when the study started. Then it means this cell has PME because the final transmittance is significantly higher than the initial.

Table 3.4. shows the most important values from perpendicular rubbing on planar alignment layer cell EO study:

Table 3. 4 - EO Study values for a perpendicular rubbing on planar alignment layer cell

T_{OFF}	T_{ON}	$T_{OFF'}$	PME (%)	E90 (V/μm)
2	72	37	50	16

As the previous cells, perpendicular rubbing on planar alignment layer cell has also a high PME value, which means that the transparency is visible in this cell after EO. Figure 3.12 shows POM images after and before EO study for this cell

Before EO study **After EO Study**

Figure 3. 12 - POM cross polarizers' images before and after EO study for a perpendicular rubbing on planar alignment layer cell

The POM images from perpendicular rubbing on planar alignment layer cell are very similar as parallel and anti-parallel cells. The differences are evident as the previous cells which means that the transparency after EO is clearly present.

3.2.5. Handmade cell with Homeotropic Alignment layer (4cm^2)

Figure 3.13. shows the EO study for the handmade cell with homeotropic alignment.

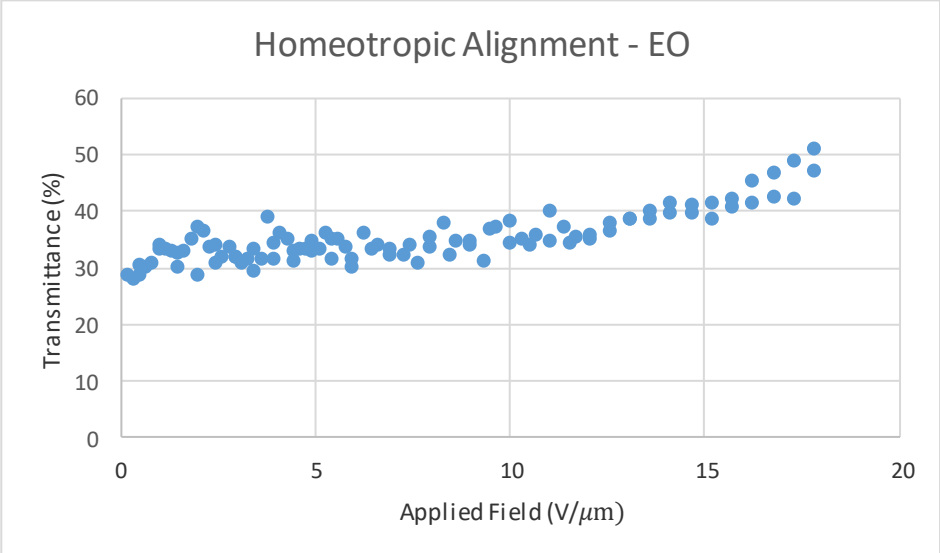

Figure 3. 13- EO study for the handmade cell with homeotropic alignment layer

Homeotropic alignment layer EO study has a different graph than planar alignment cells, the curves are practically constant during the increasing. Table 3.5 shows the values from this study.

Table 3. 5 – Values from EO study for a homeotropic alignment layer

T_{OFF}	T_{ON}	$T_{OFF'}$	PME (%)	E90 (V/μm)
29	≥51	30	-	≥18

The transmittance starts with a higher level than the previous cells, 29%, grows to 51% when the applied field is maximum and returns to their initial transmittance, Moreover the cell do not present any evidence of PME because before EO it starts with some transparency and after EO it returns to same values of transmittance.

Figure 3.14 shows the POM images for the cell with homeotropic alignment layer before and after EO study

Before EO study **After EO Study**

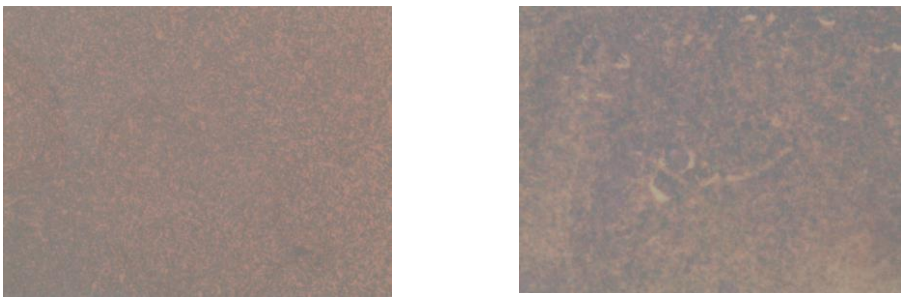

Figure 3. 14 - POM cross polarizers' images for homeotropic alignment layer cell

As it can be seen, POM images after and before EO study do not present significant differences due the low value of PME. It means that there are no significant modifications before the study with an electric field applied.

3.2.6. Handmade cell without alignment layer (4cm^2)

Figure 3.15 shows the EO for a handmade cell without alignment, that means, a cell which glasses have only ITO substrate

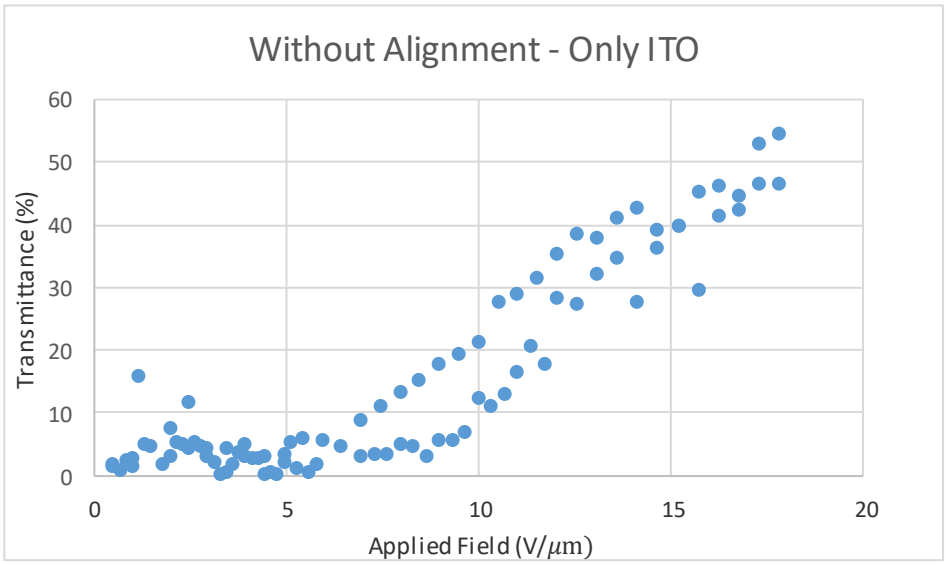

Figure 3. 15 - EO study for a cell without alignment

Through the graphic on Figure 3.8. it can be seen a typical case of hysteresis. The initial and final transmittance at the beginning and ending EO study are the same but the increasing and decreasing curves are different. There is no stabilisation at the ending and therefore the E90 is higher than the other cells with planar alignment, if we consider that the final transmittance matches a constant value if high levels of electric field were applied. Table 3.6. shows the values from the EO study

Table 3. 6 - Values from EO study for a cell without alignment

T_{OFF}	T_{ON}	$T_{OFF'}$	PME (%)	E90 (V/μm)
2	≥55	4	<1	≥18

The cell with no alignment layer has a very low PME value, almost inconsiderable. It means that there is no transparency after an applied field. Figure 3. 16 shows the POM images before and after EO study

Before EO study **After EO Study**

Figure 3. 16 - POM cross polarizers' images for cell without alignment layer

As it can be seen on POM images, there is no significant changes before and after EO. Basically, there is no PME in cells which glasses have no alignment layer.

3.2.7. Discussion

Table 3.7. shows the EO studies comparative results from cells. The most important parameter is the PME, which needs to be considerable.

Table 3. 7 - EO studies comparative results

Cell	T_{OFF}	T_{ON}	$T_{OFF'}$	PME (%)	E90 (V/μm)
LC2-20 commercial cell by Instec	2	75	51	**67**	8
Parallel rubbing on planar alignment layer	3	74	39	**51**	15
Anti-Parallel rubbing on planar alignment layer	2	75	42	**55**	14
Perpendicular rubbing on planar alignment layer	2	72	37	**50**	16
Homeotropic alignment layer	29	≥51	30	**-**	≥18
No alignment layer	2	≥55	4	<1	≥18

It is possible to conclude that only cells with planar alignment can have high values of Permanent Memory Effect, independently the rubbing direction or way. This means that PME is only possible in cells which glasses have a planar alignment treatment. For cells with homeotropic alignment the transmittance values are constant during the applying of the electric field because in the beginning the cell is already fairly transparent. For cells without any alignment the transmittance when the electric field is removed has no significant differences to the transmittance in the beginning and therefore the PME has a very low value.

This study was very important to know that the surface treatment is another factor that influence the PME. Due this, it is necessary to understand how the alignment can influence the PME and why.

3.3. Atomic Force Microscopy on Glasses

After the EO studies it was concluded that alignment layer is important on PME. Then, the glass surfaces need to be analysed, and Atomic Force Microscopy (AFM) was used. AFM analysis was done for four different samples: : ITO covered glass by Xinyan, ITO covered glass with planar alignment layer by Instec, ITO covered glass by Xinyan covered with E7/PEGDMA875 PDLC and ITO covered glass with planar alignment layer by Instec covered with E7/PEGDMA875 PDLC. AFM gives an image of height and an image of phase for each sample and both images can be obtained in 2D and 3D view.

3.3.1 ITO covered glass by Xinyan

It was done the AFM analysis for ITO covered glass by Xinyan only Figure 3.17 shows the 2D height image and figure 3.18 shows the 2D phase image for ITO glass in a 4µm x 4µm area.

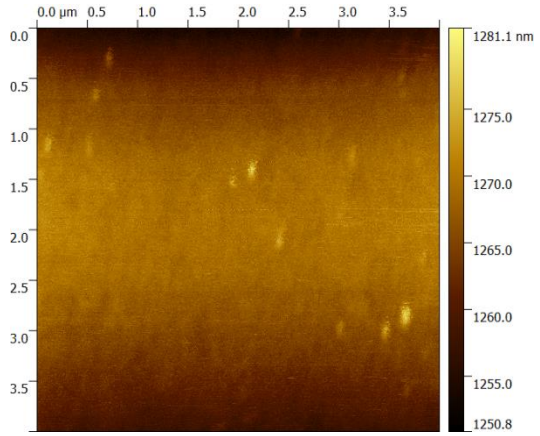

Figure 3. 17- ITO covered glass AFM analysis height image (2D)

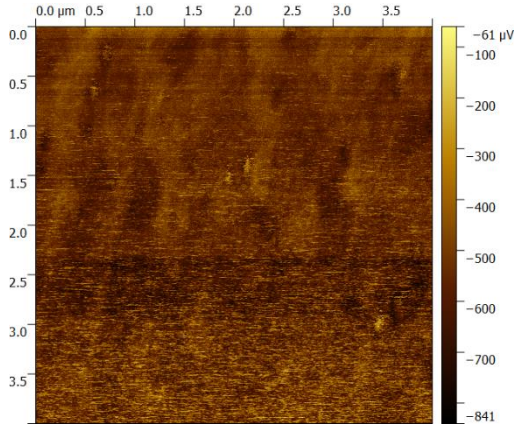

Figure 3. 18 – ITO covered glass AFM analysis phase image (2D)

Figure 3.19 and 3.20 shows the height and right 3D image respectively for AFM analysis for ITO glass surface.

Figure 3. 19 - ITO covered glass AFM analysis height image (3D)

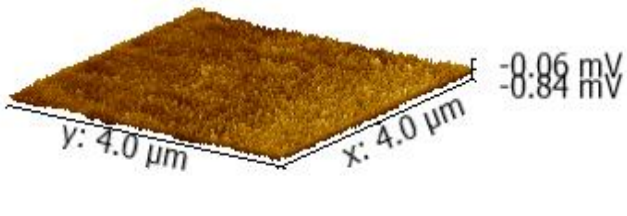

Figure 3. 20 – ITO covered glass AFM analysis phase image (3D)

ITO glasses have a surface with almost homogenous length levels. The ITO grains do not influence the height on a ITO glass.

3.3.2 ITO covered glass with planar alignment layer by Instec

AFM analysis for an ITO covered glass with planar alignment layer by Instec. Figure 3.21 shows the 2D height image and figure 3.22 shows the 2D phase image for ITO covered glass with planar alignment layer by Instec, in a 4µm x 4µm area.

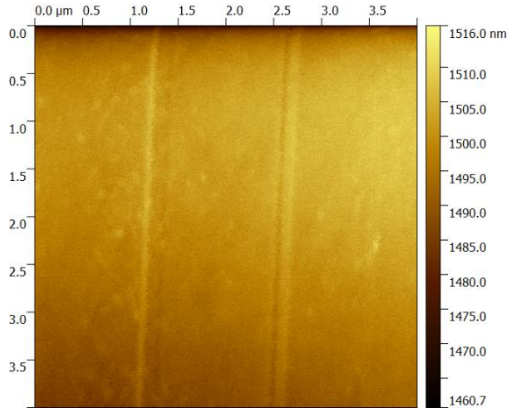

Figure 3. 21 – Instec glass AFM analysis height image (2D)

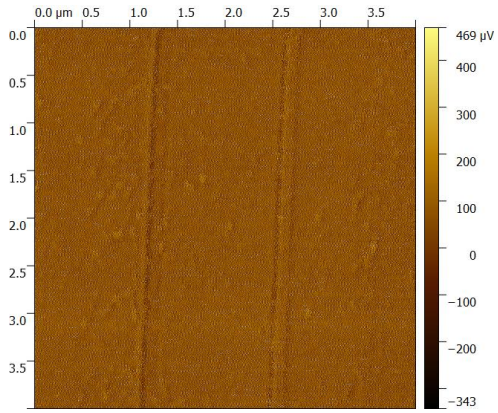

Figure 3. 22 – Instec glass AFM analysis phase image (2D)

Figure 3.23 and 3.24 shows the height and right 3D image respectively for AFM analysis for Instec glass surface.

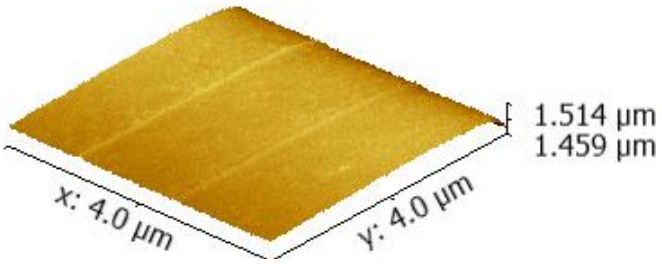

Figure 3. 23 - Instec glass AFM analysis height image (3D)

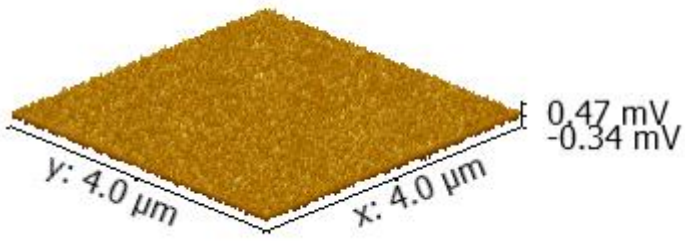

Figure 3. 24 - Instec glass AFM analysis phase image (3D)

AFM analysis gives images of a surface with some stripes that match stretch marks, like a ploughed land. This stripes are due the polyimide rubbing treatment done on glass and the thickness is higher than ITO glass. Despite all the stripes are not spaced by the same distance, in this case the two stripes are separated by 1.5µm each other.

For another perception about these surfaces, in Appendix B there are images for bigger areas where it is visible several stripes.

3.3.3 ITO covered glass by Xinyan covered with E7/PEGDMA875 PDLC

ITO covered glass by Xinyan with E7/PEGDMA875 PDLC analysis was performed. It was not possible to see clearly the PDLC mixture and therefore the resolution used in this study was 20µm x 20µm. Figures 3.25 and 3.26 show the height and phase images

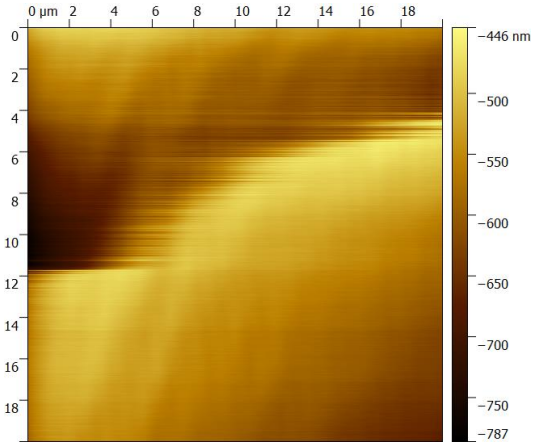

Figure 3. 25 - ITO glass covered with PDLC AFM analysis height image (2D)

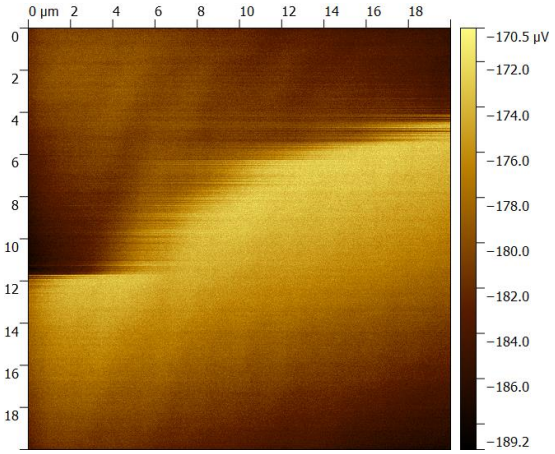

Figure 3. 26 – ITO glass covered with PDLC AFM analysis phase image (2D)

Figure 3.27 and 3.28 shows the height and phase 3D image respectively for AFM analysis ITO glass with PDLC surface.

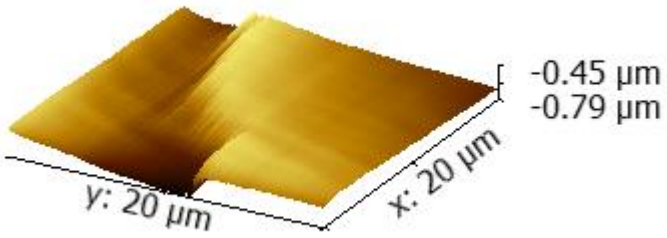

Figure 3. 27 - ITO glass covered with PDLC AFM analysis height image (3D)

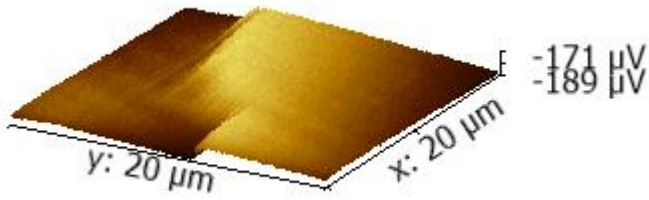

Figure 3. 28 - ITO glass covered with PDLC AFM analysis phase image (3D)

Through the AFM analysis, it can only be observed a huge gelatinous substance and the AFM needle could not make a clear image. On this surface the mixture can align in various orientations and therefore is difficult to see something in these images.

3.3.4 ITO covered glass with planar alignment layer by Instec covered with E7/PEGDMA875 PDLC

ITO covered glass with planar alignment layer by Instec covered with E7/PEGDMA875 PDLC. Figures 3.29 and 3.30 show the height and phase 2D images for this analysis

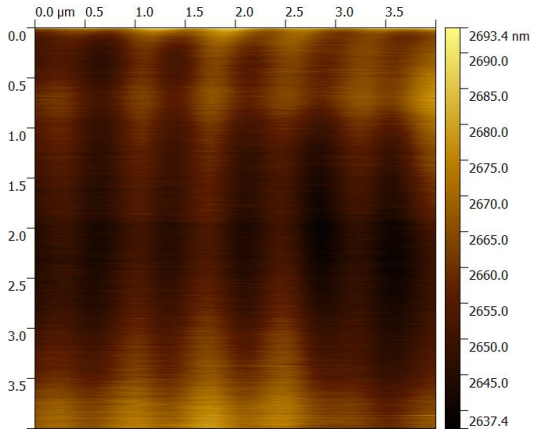

Figure 3. 30 - Instec glass covered with PDLC height image (2D)

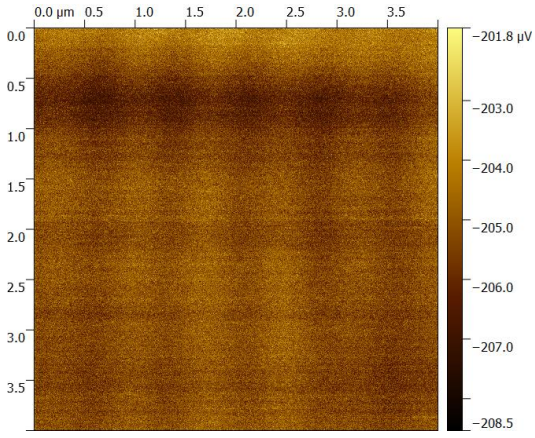

Figure 3. 29 - Instec glass covered with PDLC phase image (2D)

Figures 3.31 and 3.32 show the height and phase 3D image respectively for AFM analysis PI glass with PDLC surface.

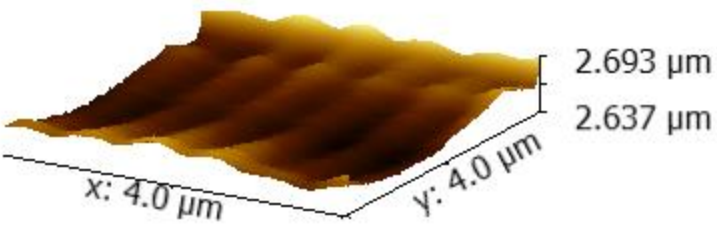

Figure 3. 31 - Instec glass covered with PDLC height image (3D)

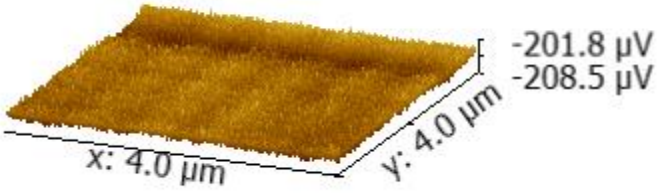

Figure 3. 32 - Instec glass covered with PDLC phase image (3D)

The analysis for an Instec glass covered with PDLC shows that there is a surface with different heights composed by a group of sequential waves separated by 0.75µm each other, a shorter distance than the space between the stretch marks on Instec glass. These waves have the same direction as the rubbing has and then the polymer follows these lines. Due to this, the polymer with LC has a different disposition when the glass has a rubbing treatment, it follows the rubbing direction. Although the images given are wavy, in terms of height the surface it is almost planar.

3.3.5. Discussion

AFM analysis gave important information about the surfaces on these glasses. As the ITO glass have no preferred alignment, the PDLC has no preferential direction but on glasses with alignment it has the preferential direction. These results can prove that alignment is sufficiently strong to align the polymer and liquid crystal mixture in one preferred direction. This preferred direction is the stretch marks direction.

3.4. Scanning Electron Microscopy

SEM analysis was done for the same samples used on AFM analysis but it was necessary to remove the liquid crystal dispersed on polymer. For this reason the samples with PDLC were washed with acetonitrile for removing the liquid crystal and dried for 24h in a desiccator

3.4.1. ITO covered glass by Xinyan

Figure 3.33 shows the SEM analysis for the ITO glass

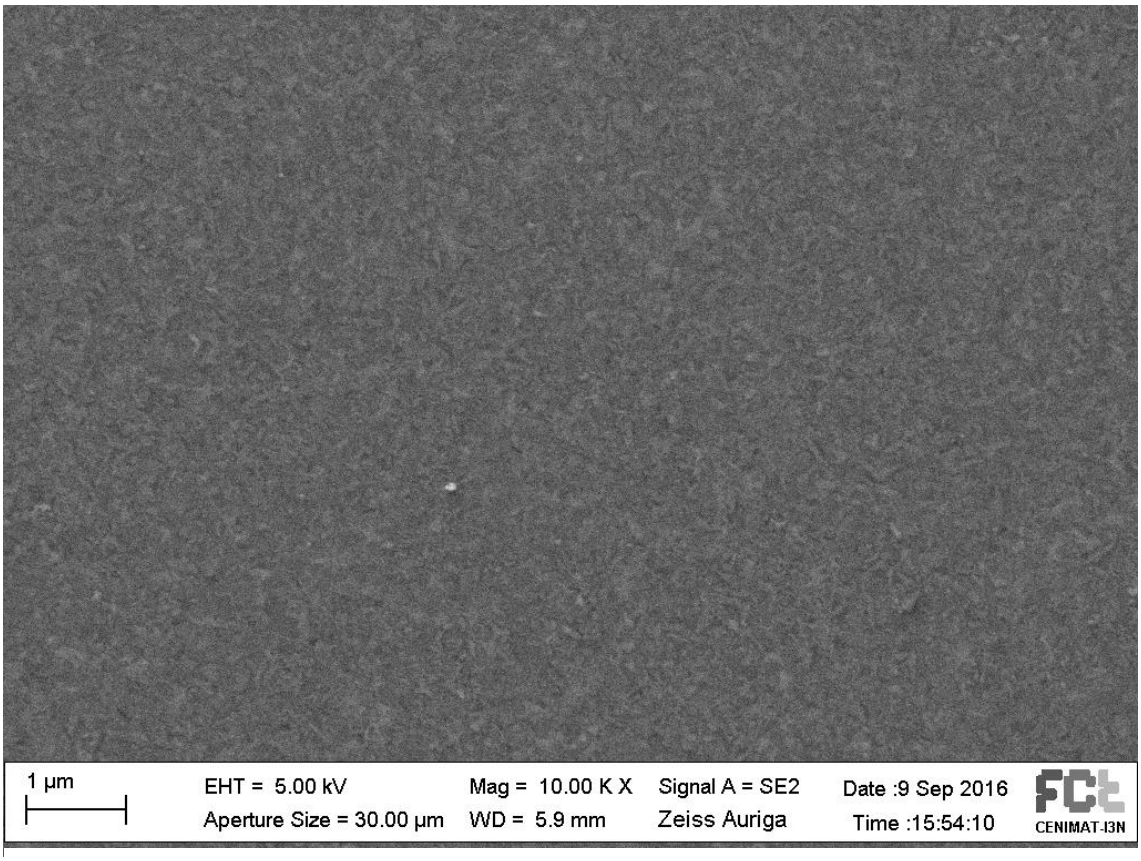

Figure 3. 33 - SEM analysis for ITO covered glass

Such as the AFM analysis, for ITO covered glass by Xinyan it can be seen small particles on the surface. These particles are the ITO grains on glass

3.4.2 ITO covered glass with planar alignment layer by Instec

Figure 3.34 shows the SEM analysis for polyimide planar alignment rubbing glass from Instec

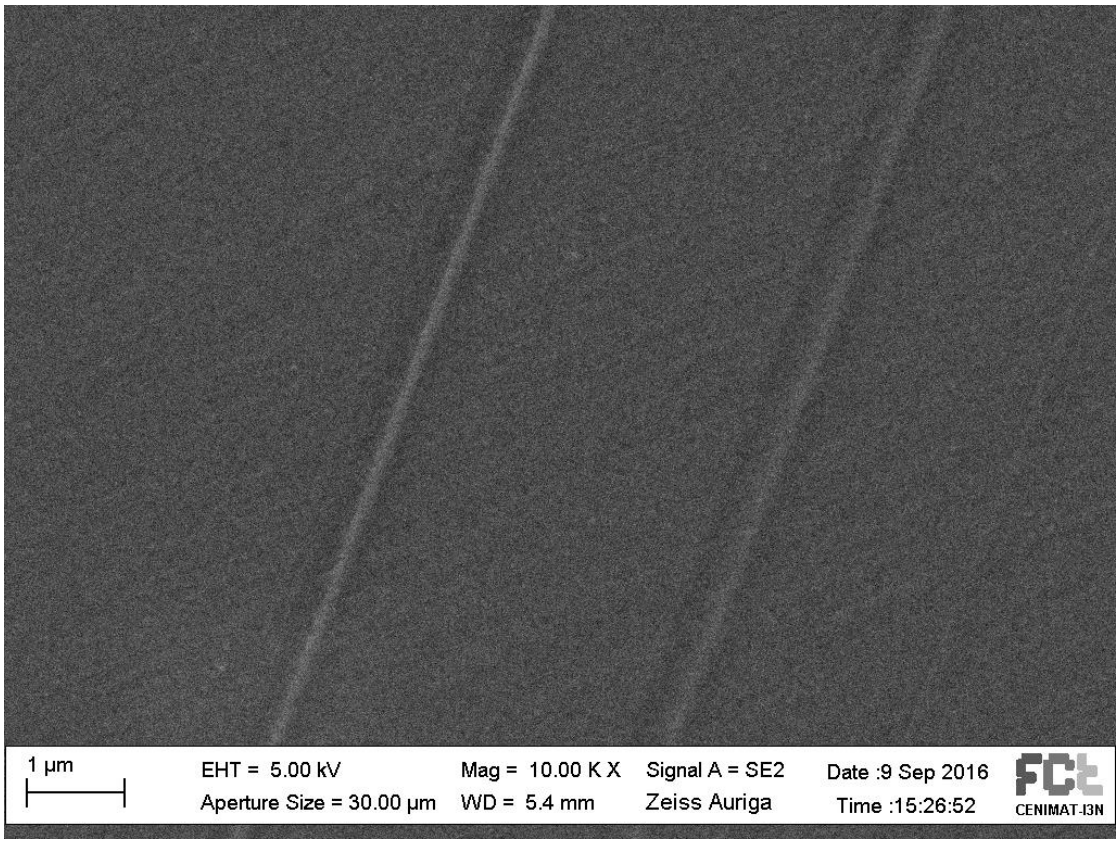

Figure 3. 34 - SEM analysis for Instec glass

By the analysis on polyimide rubbing glass, the stripes with stretch marks aspect can be also seen as the AFM analysis. In this case these two stretch lines are separated by 4µm. These stripes are not all spaced by the same distance and this is was cleared viewed on SEM analysis and on AFM analysis. On Appendix B SEM images with different resolutions shows that there is a great variation of distances between stretch lines.

3.4.3. ITO covered glass covered with E7/PEGDMA875 PDLC

Figure 3.35 shows the SEM analysis for ITO covered glass covered with E7/PEGDMA875 PDLC

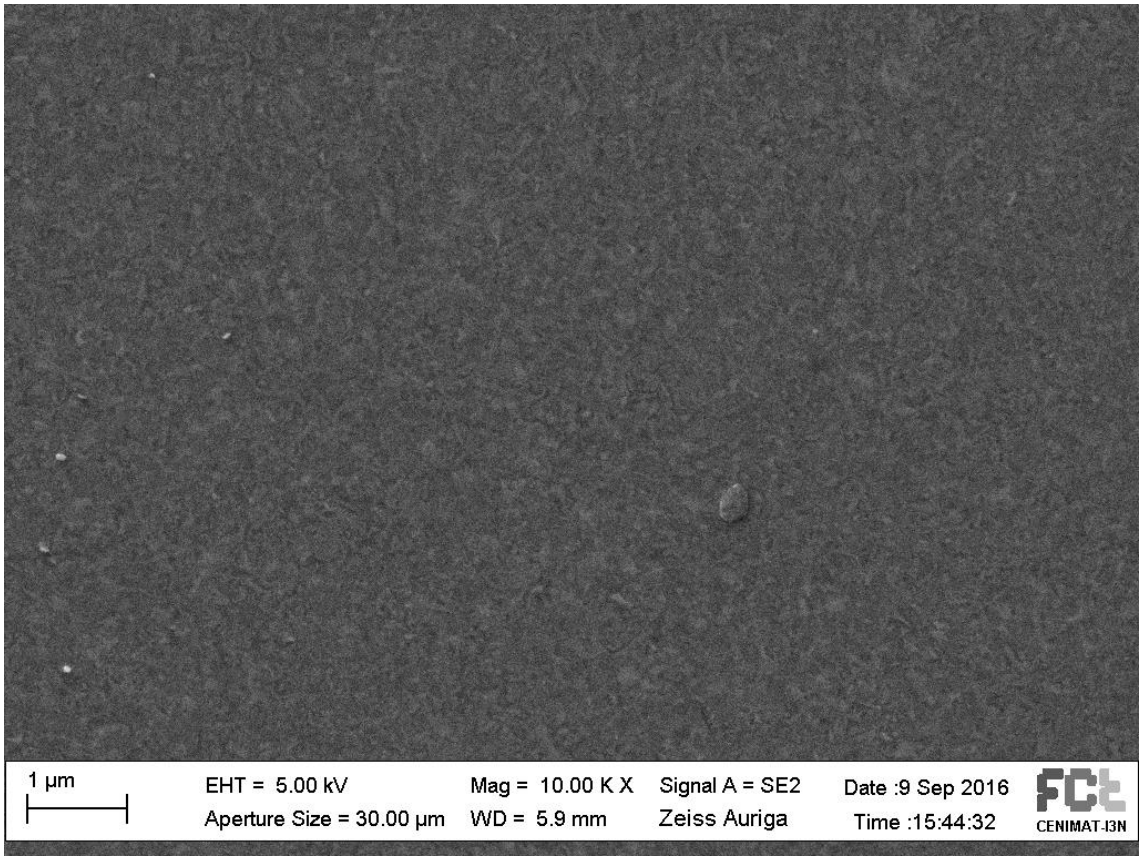

Figure 3. 35 - SEM analysis for ITO glass covered with PDLC

For ITO Glass with PDLC, the same analysis give us an image very similar to the ITO glass analysis but with some particles on it. These particles are polymer remains. Unfortunately the acetonitrile removed a big part and it was no possible to see with more detail the polymer on this glass.

3.4.4 ITO covered glass with planar alignment layer by Instec covered with E7/PEGDMA875 PDLC

Figure 3.36 shows the SEM analysis for a ITO covered glass with planar alignment layer by Instec covered with E7/PEGDMA875 PDLC

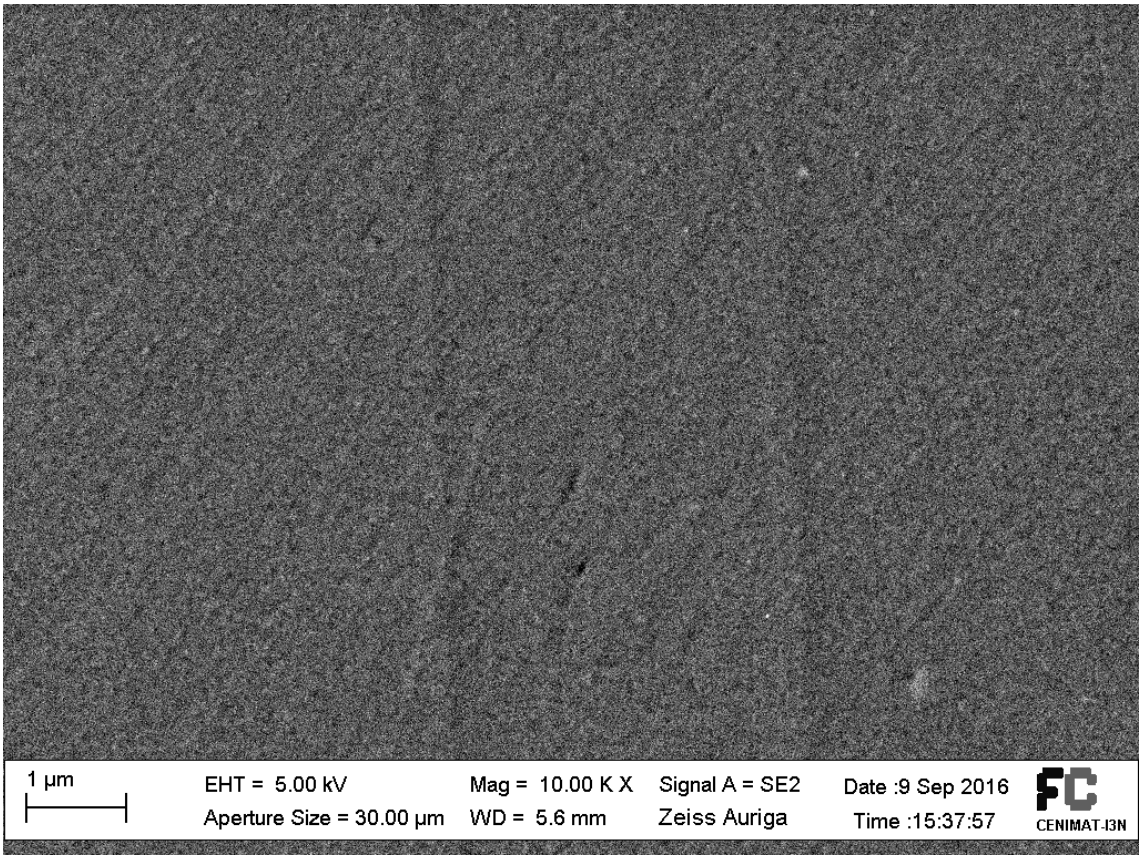

Figure 3. 36 - SEM analysis for Instec glass covered with PDLC

The stretch lines are less evident than SEM analysis for ITO covered glass with planar alignment layer by Instec. Actually, instead this stripes have an aspect of stretch lines, they are filled by the polymer and therefore it is possible to see a relief. This means that polymer fills the stretch marks and there is a strong probably that their chains align in their direction. In this case these two lines are separated by 4µm.

It happened the same as the ITO glass with PDLC during the washing, part of the polymer was also removed. It is only can be observed the stretch lines filled by the polymer.

3.4.5. Discussion

Through SEM images, it is possible to take some conclusions about the surfaces. The images from ITO glass and Instec glass have the same aspect as the AFM analysis. However, and because part of the polymer was removed by the solvent, in ITO glass with PDLC to find something that can give relevant information. Only on Instec glass covered by PDLC it is possible to see the stretch lines filled by the polymer.

Nevertheless, the SEM and AFM results are enough to verify there is a clear influence on PDLC mixture and that can be also viewed on other resolutions. In Appendix C more surfaces SEM images can be seen.

3.5. Capacitance study with Temperature variation

Only commercial cells LC2-20 and handmade cells with planar alignment layer show PME after the EO study. Therefore it was done the capacitance study along temperature for these cells for trying to understand the capacitance behaviour with temperature variation.

The capacitance study along temperature for three types of cells were accomplished: empty cells, cells with E7 and cells with PEGDMA875 polymerized. The temperature rates used for these studies were 5ºC/min and 2ºC/min on increasing and decreasing steps. The results from these studies will be very important for determining how the capacitance varies in a cell with PDLC.

3.5.1. Empty cells

Empty cells have no dielectric inside, which means that capacitance must be constant along temperature. Figures 3.37 shows the temperature variation in this four types of cells.

LC2-20

Figure 3. 37 shows the capacitance study for an empty LC2-20 cell

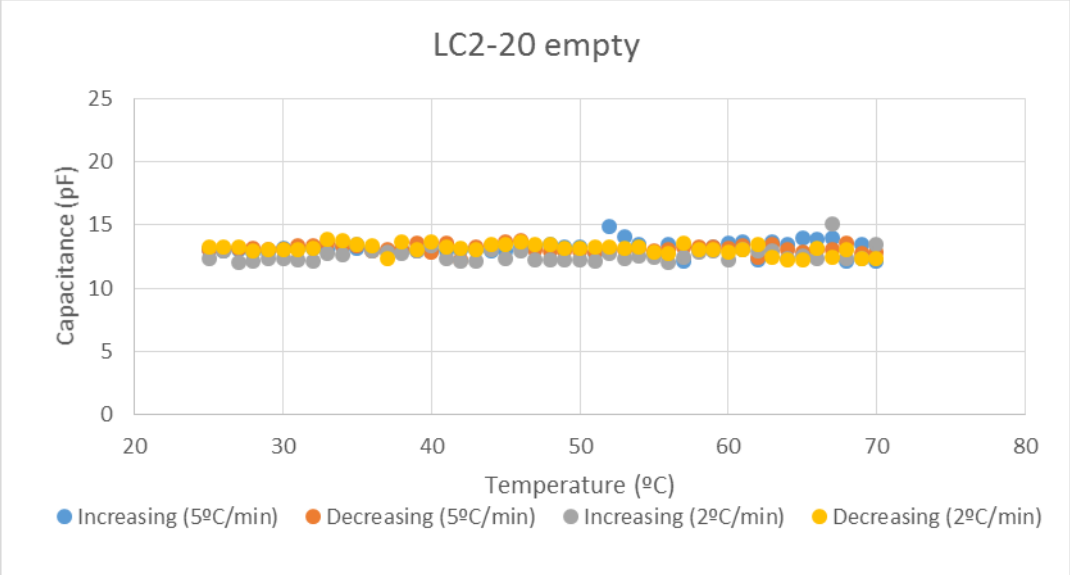

Figure 3. 37 - Empty LC2-20 capacitance study with temperature

In LC2-20, the capacitance seems to be constant during temperature increasing and decreasing with a average value of 12pF.

Parallel rubbing on planar alignment layer cell 1.5cm^2

Figure 3.38 shows the capacitance study along temperature for an empty handmade cell anti-parallel rubbing on planar alignment layer cell

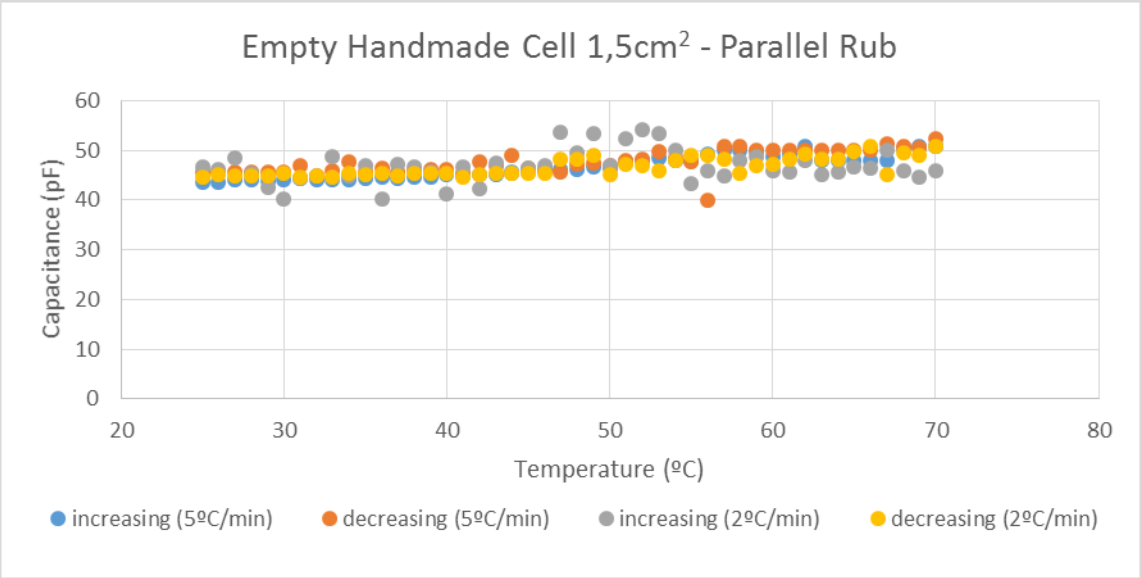

Figure 3. 38 – Empty handmade cell with parallel rubbing on planar alignment layer capacitance study

The capacitance of the empty handmade cell with parallel rubbing on planar alignment layer with 1.5cm^2 was to be constant with temperature increasing and decreasing with some oscillation points. Despite these points, it has an average measured value of 48pF.

Anti-parallel rubbing on planar alignment layer cell 1.5cm^2

Figure 3.39 shows the capacitance study along temperature for an empty anti-parallel rubbing on planar alignment layer handmade cell

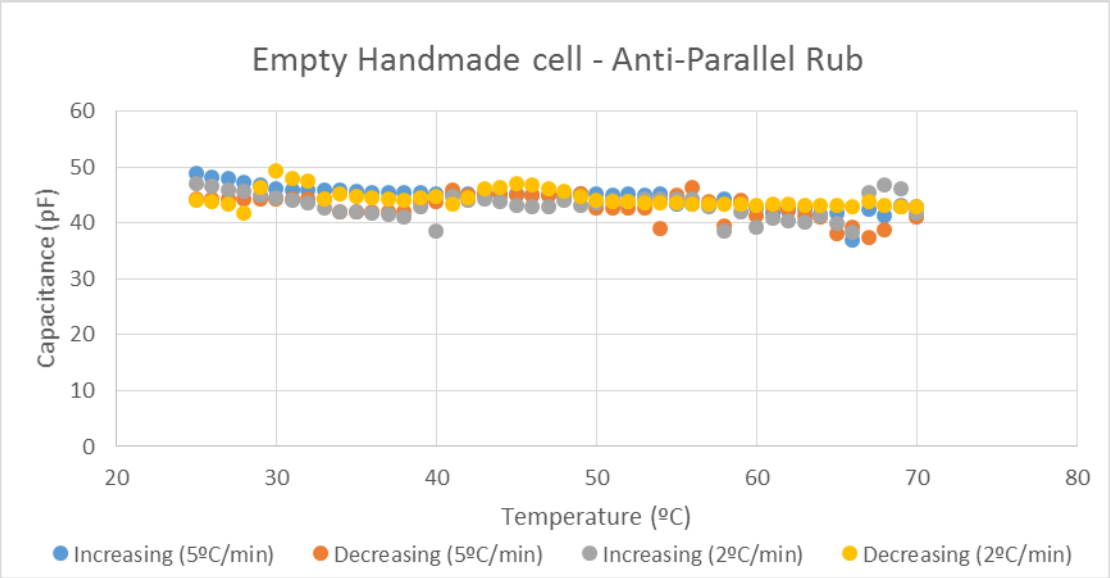

Figure 3. 39 - Empty handmade cell with anti-parallel rubbing on planar alignment layer capacitance study

As the parallel, the anti-parallel rubbing on planar alignment layer cell has also a capacitance values constant with small oscillations. The average measured capacitance is about 46pF, a value very close to the measured value in parallel rubbing on planar alignment layer cell. The areas are the same and then it was expected equal capacitance values or values very close each other

Perpendicular rubbing on planar alignment layer cell 4cm^2

Figure 3.40 shows the capacitance study along temperature for an empty perpendicular rubbing on planar alignment layer handmade cell

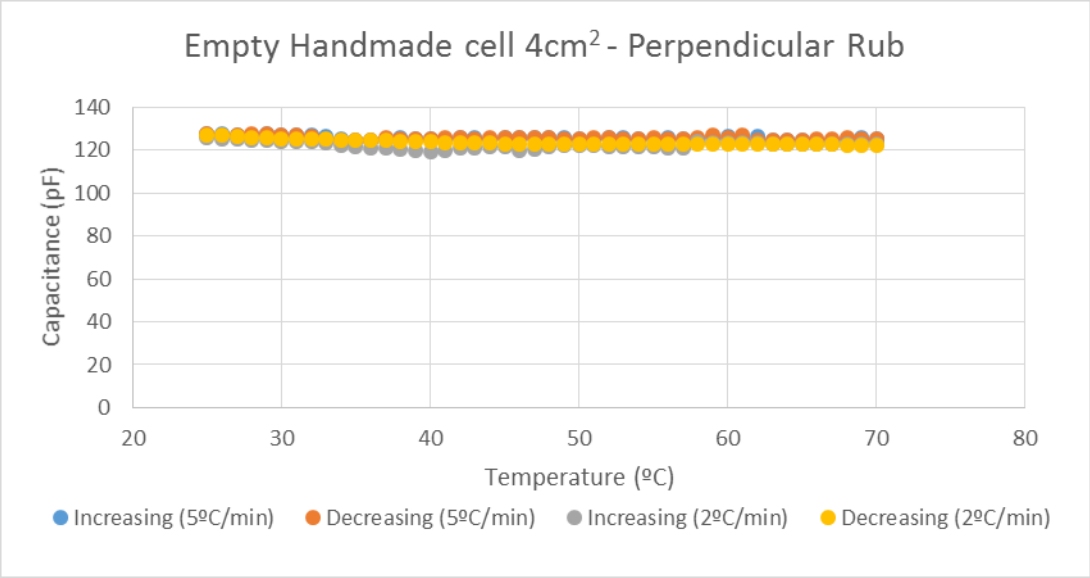

Figure 3. 40 - Empty handmade cell with perpendicular rubbing on planar alignment layer capacitance study

Perpendicular rubbing on planar alignment layer cell has a bigger area than the other cells, the capacitance values are therefore higher. Without a dielectric it presents an average value of 127pF, in spite of there are some oscillations values during the study.

3.5.2. Cells with E7

After the study in empty cells, the study on cells with E7 were performed. It was expected aa discontinuously point at nematic-isotropic temperature transition, namely at 58ºC. At this point the LC permittivity turns constant along the temperature and then for temperatures above the capacitance shall be also constant. Figure 3.41 shows the graph for the LC2-20 with E7 capacitance study with temperature

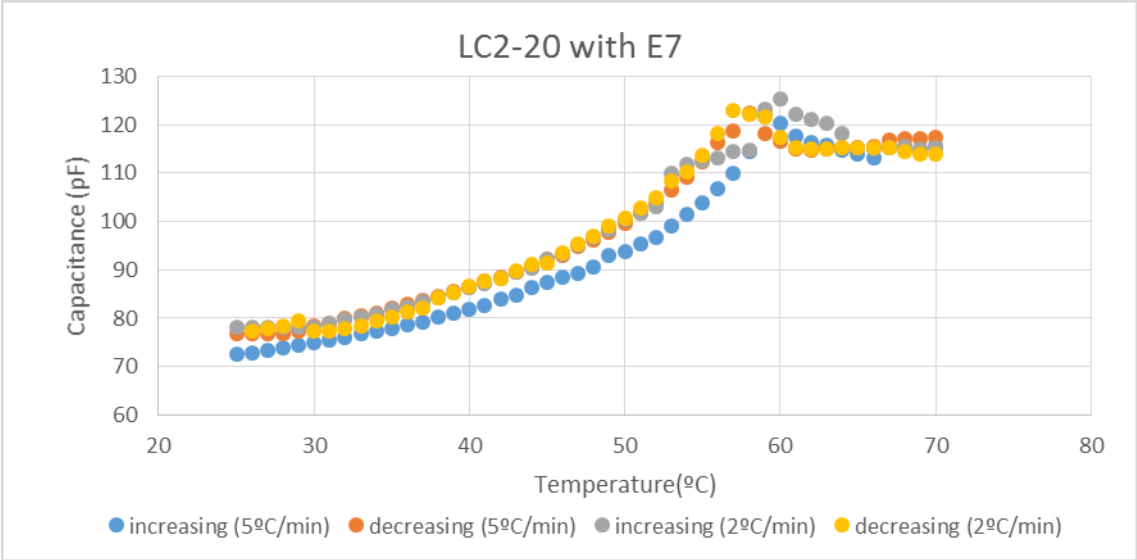

Figure 3. 41- LC2-20 with E7

Figure 3.23 shows four curves for LC2-20 heating with E7. It is possible to see a point at 58ºC which is the maximum curve of capacitance. This value is the T_{NI} of E7 and matches a values of nearly 125pF on LC2-20 cell. Above this temperature, capacitance decreases and stabilises at 115pF until 70ºC.

Parallel rubbing on planar alignment layer cell (1.5cm^2)

Figure 3.42 shows the capacitance study for the parallel rubbing on planar alignment layer cell with E7

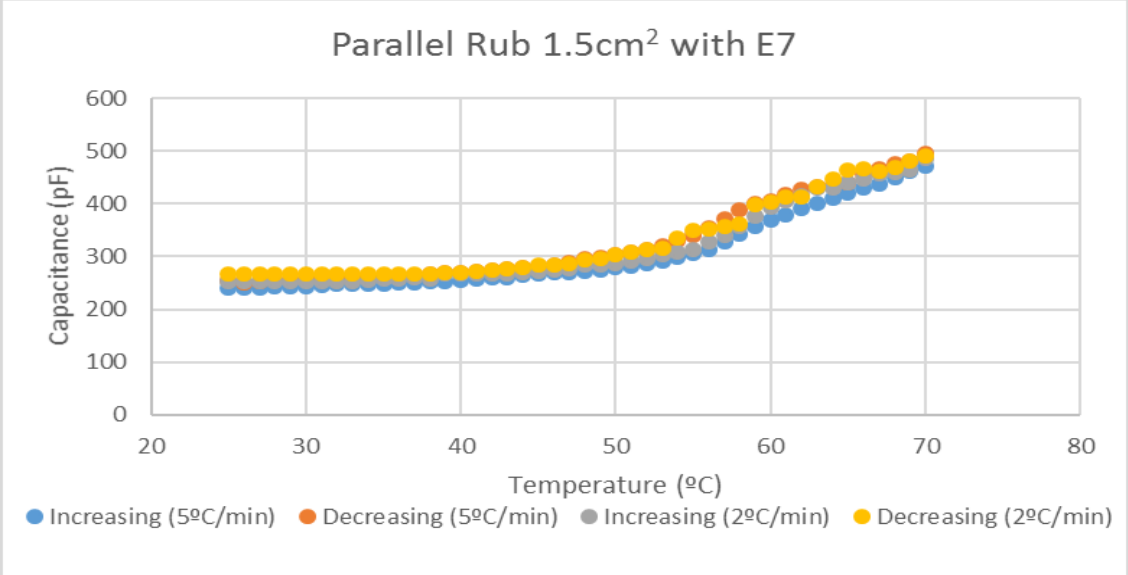

Figure 3. 42 - Handmade parallel rubbing on planar alignment layer cell with E7 capacitance study with temperature

In handmade parallel rubbing on planar alignment layer cell it is also visible a point at 58ºC which matches a capacitance value of 370pF. However, after this temperature the capacitance values increase slowly until 70ºC and it is not possible to see a stabilization as a LC2-20 cell

Anti-parallel rubbing on planar alignment layer cell (1.5cm^2)

Figure 3.43 shows the capacitance study with temperature for an anti-parallel rubbing on planar alignment layer cell

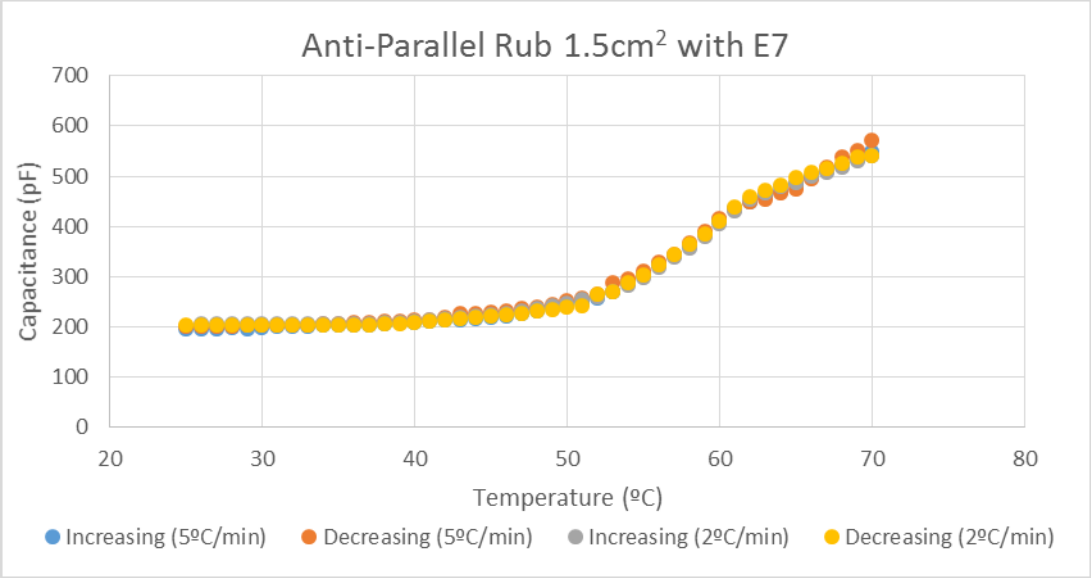

Figure 3. 43 - Handmade anti-parallel rubbing on planar alignment layer cell with E7 capacitance study with temperature

In handmade anti-parallel rubbing on planar alignment layer cell, values are very similar as the parallel rubbing on planar alignment layer cell due the same areas. At 58ºC the same point is visible and it has a capacitance value of 383pF. Above this temperature the capacitance increases slower than before, in other words, the slope of capacitance decreases.

Perpendicular rubbing on planar alignment layer cell (4cm^2)

Figure 3.44 shows the capacitance study with temperature for the perpendicular rubbing on planar alignment layer cell with E7

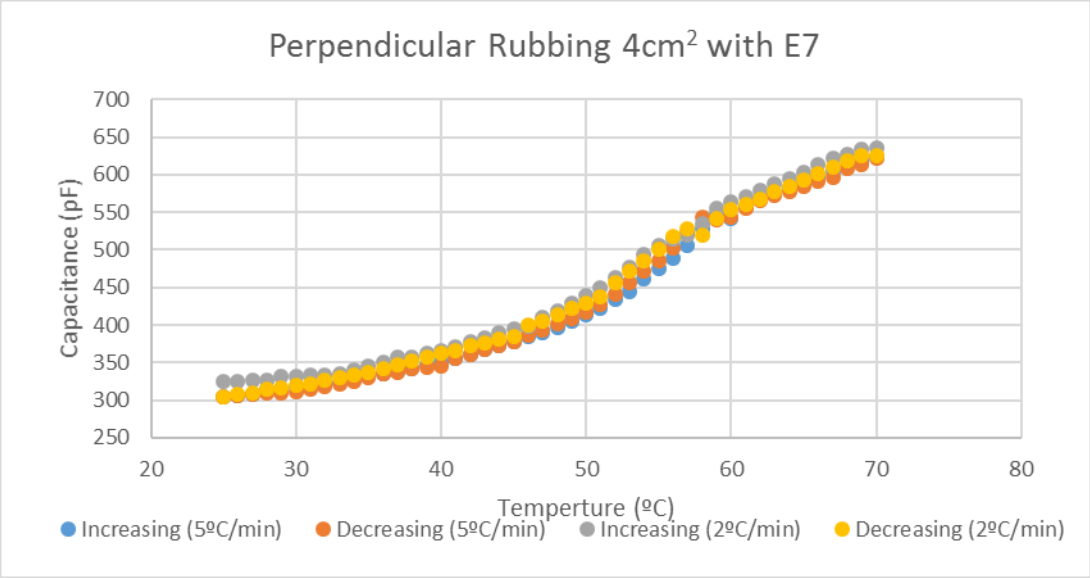

Figure 3. 44 - Handmade perpendicular rubbing on planar alignment layer cell with E7 capacitance study with temperature

The capacitance at 58ºC is about 540pF and this value is higher on perpendicular rubbing on planar alignment layer cell because the area is also higher. Above this temperature, like the previous cells, the capacitance increases slower.

3.5.3. Cells with polymerised PEGDMA875

The same procedure was done for cells with only polymerised PEGDMA875. Instead E7 curves, it was expected a curve with no discontinuously points.

LC2-20

Figure 3.45 shows the capacitance study with temperature for a LC2-20 with polimerised PEGDMA8

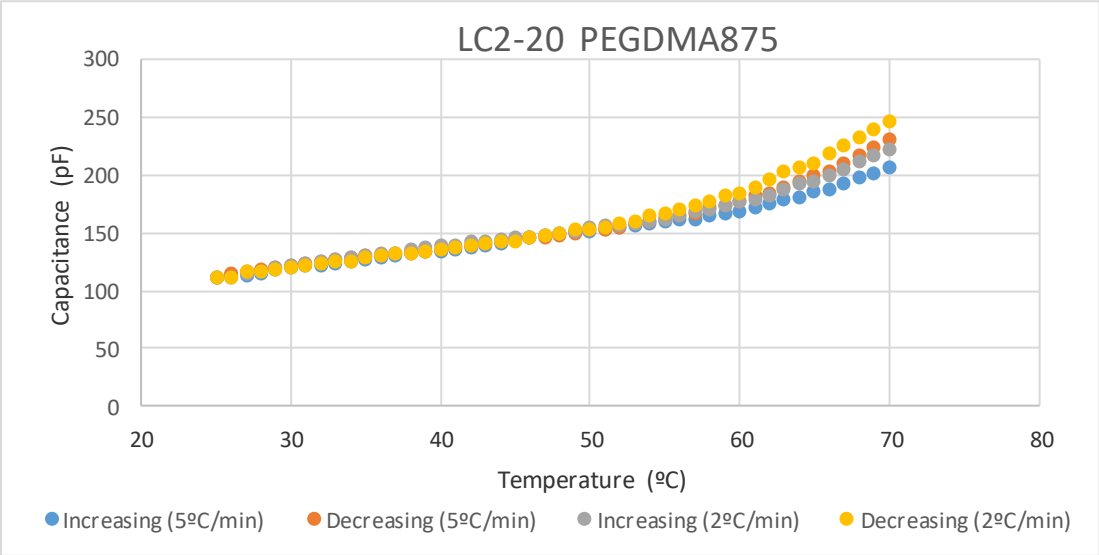

Figure 3. 45 - LC2-20 with PEGDMA875 capacitance study with temperature

For LC2-20 with PEGDMA875, de capacitance increases with temperature and it has an almost linear response. It starts with capacitances at 114pF at room temperature and reaches values of 250pF at 70ºC.

Parallel rubbing on planar alignment layer cell (1.5cm^2)

Figure 3. 46 shows the capacitance variation with temperature for the parallel rubbing on planar alignment layer cell with PEGDMA875

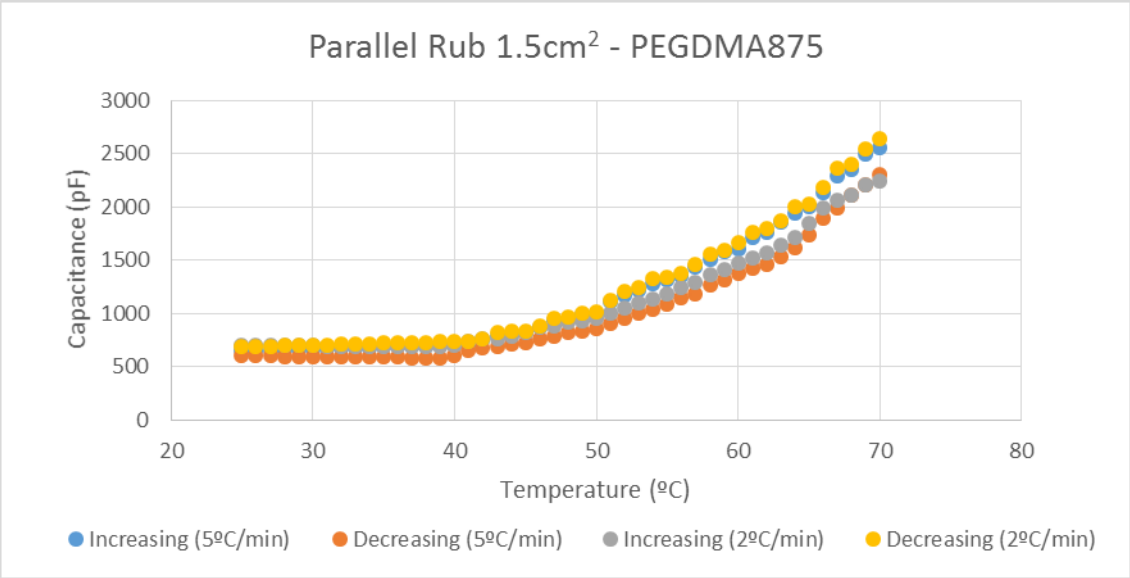

Figure 3. 46 - Parallel rubbing on planar alignment layer cell with PEGDMA875 capacitance study with temperature

In the parallel rubbing on planar alignment layer cell, the capacitance starts at 613pF at room temperature, starts growing slowly until 40ºC and above this temperature the growing slope will be higher, and it can reach the 2800pF at 70 º C.

Anti-parallel on planar alignment layer rubbing cell (1.5cm^2)

Figure 3.47 shows the capacitance variation with temperature for the anti-parallel rubbing on planar alignment layer cell with PEGDMA875

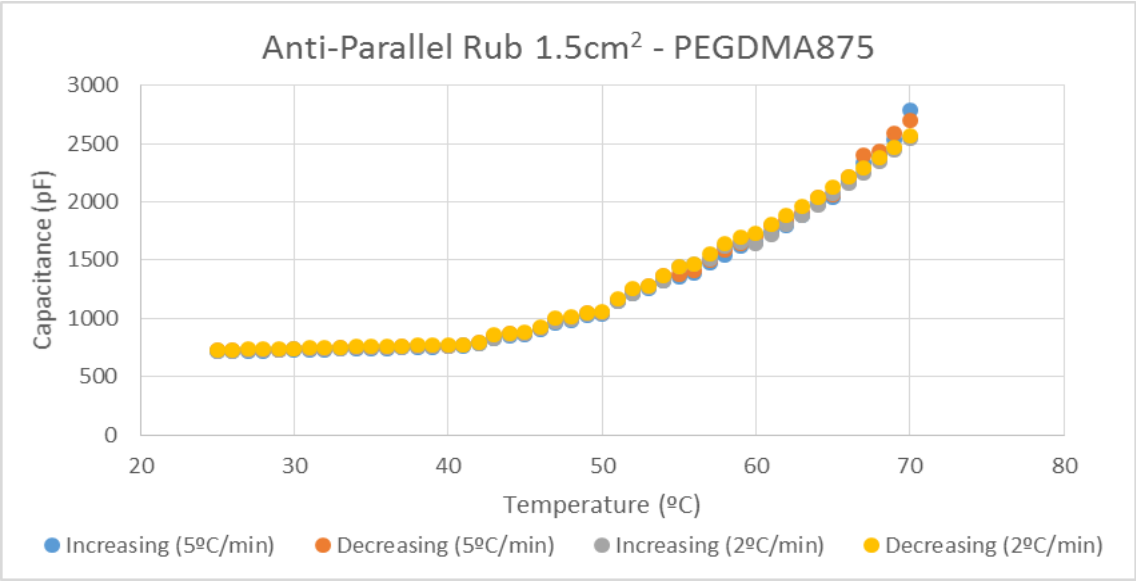

Figure 3. 47 - Handmade anti-parallel rubbing on planar alignment layer cell with PEGDMA875 capacitance study with temperature

For handmade cell with anti-parallel rubbing the capacitance starts at 760pF and it is almost constant until 42ºC. Above this temperature capacitance starts to increase linearly and it reaches values of 2700pF at 70ºC.

Perpendicular rubbing on planar alignment layer cell (4cm^2)

Figure 3.48 shows the capacitance variation handmade perpendicular rubbing on planar alignment layer cell with PEGDMA875

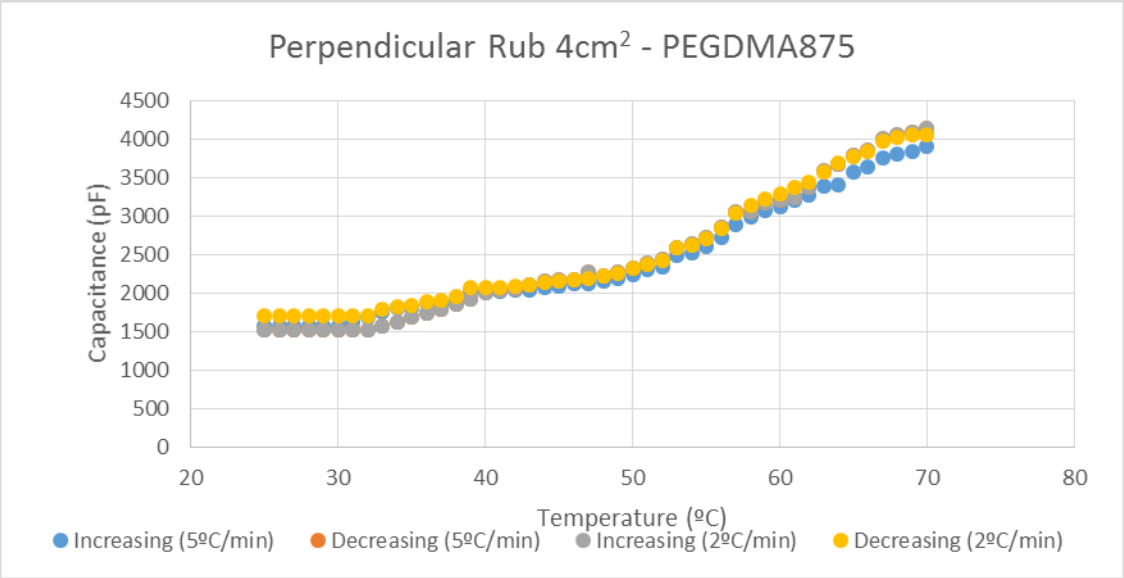

Figure 3. 48 - Handmade perpendicular rubbing on planar alignment layer cell with PEGDMA875 capacitance study with temperature

For the perpendicular rubbing on planar alignment layer cell, the capacitance starts to grow slowly until 40ºC. Above this temperature the capacitance values start to grow faster and the curve is very similar as an exponential. At room temperature the capacitance is about 1650pF and it reach a capacitance of 4100pF at 70ºC.

3.5.4 Discussion

The capacitance values are nearly constant along temperature for the four empty cells. However, some values are different than expected values. The expected values were obtained by the expression from gauss law which can calculate the capacitance knowing the area, the distance between plates and in this case the air permittivity which is very close to the vacuum permittivity[28] (ε_0 = 8.854 x 10^{-12} F m^{-1}). It is possible to verify if these values are some different than expected by applying the capacitance expression using the area and thickness of each cell. Table 3.8 shows the measured and expected values for empty cells:

Table 3. 8 – Measured and capacitance values from empty cells

Empty Cell	*Area (cm^2)*	*Thickness (μm)*	*C Measured (pF)*	*C Expected (pF)*	*Difference*
LC2-20 commercial cell by Instec	0.25	20	13	12	+8%
Parallel rubbing on planar alignment layer	1.5	23	48	57	-16%
Anti-Parallel rubbing on planar alignment layer	1.5	23	46	57	-19%
Perpendicular rubbing on planar alignment layer	4	23	129	153	-16%

The mean measured capacitance values are close to the expected. When the handmade cells are heated, mylar spacers can have some influence on capacitance values. This can explain the oscillations in some of the handmade cells. Nevertheless, in four cells the values are nearly constant with the temperature variation.

On cells with E7 there is an evident point at 58ºC where the liquid crystal turns to isotropic during temperature increasing and to nematic during temperature decreasing. Only in LC2-20 cell, the capacitance stabilizes after the T_{NI}. In handmade cells the capacitance does not stabilize, there is a drop on growing slope after this temperature. The mylar spacers interference can be the explanation by the values do not stabilize on handmade cells.

So, the next step was analysing the PDLC capacitance behaviour with the temperature increasing and decreasing.

3.6. Capacitance-Transmittance study with temperature

The same study as for the empty cells, cells with E7 and cells with PEGDMA875 were performed for cells with PDLC with an additional curve for the transmittance variation. With this two curves it is possible to find the Tc on each cell by a great increasing on transmittance, when occurs the opaque-transparent transition, as well as a point on capacitance curve, like the nematic-isotropic transition point on cells with liquid crystal but less evident.

These studies were all done before EO study, by other words they were done when the cells have no PME on them.

3.6.1. LC2-20 cell with PDLC

Figures 3.49 and 3.50 shows the capacitance and transmittance variation in a LC-20 with temperature increasing and decreasing

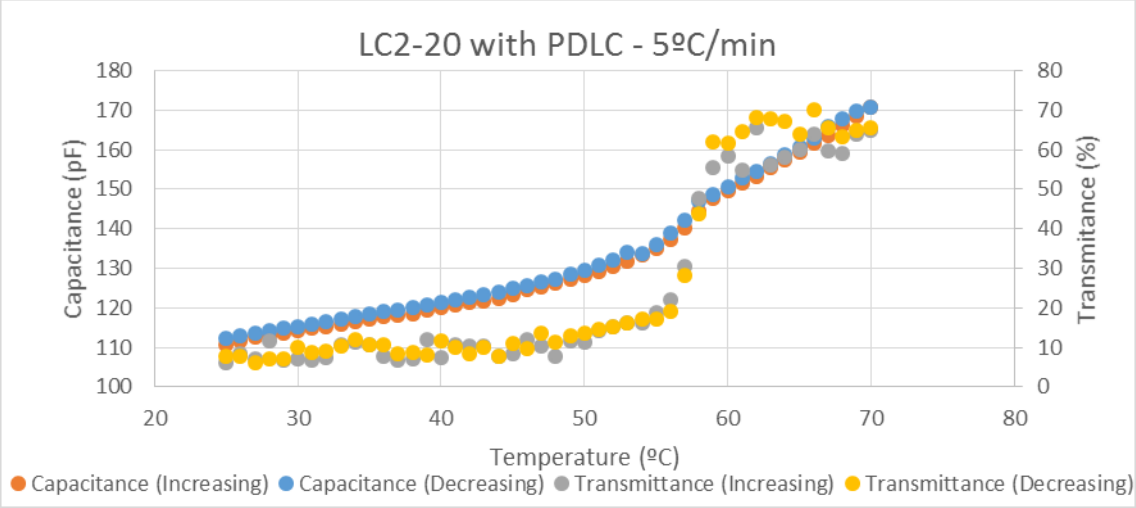

Figure 3. 49- Capacitance-Transmittance study along temperature for LC2-20 cell with PDLC– Rate 5ºC/min

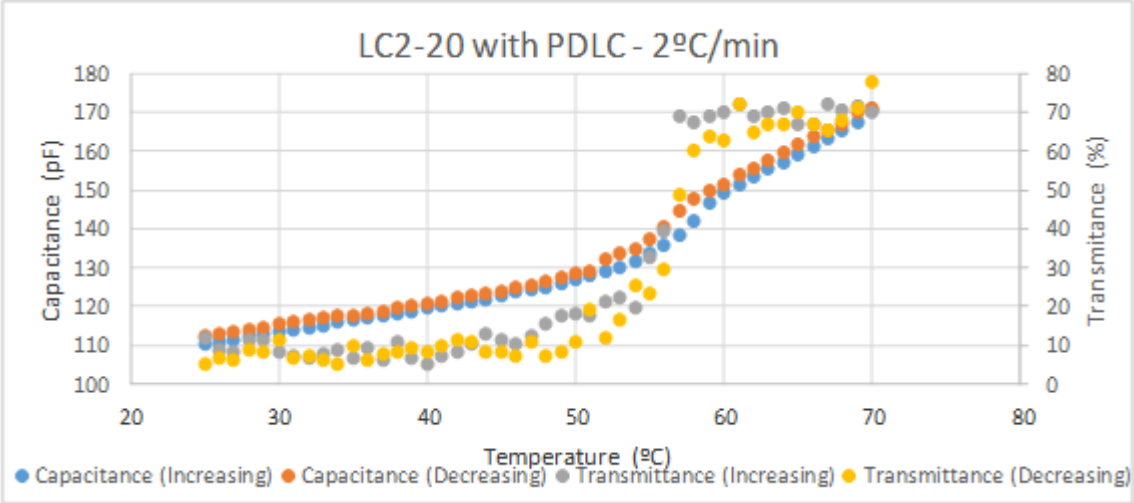

Figure 3. 50 Capacitance-Transmittance study along temperature for LC2-20 cell with PDLC – Rate 2ºC/min

In both studies, there is a point at 57ºC on capacitance curves which matches the transmittance inflection. This is the Tc temperature and it has a value of 147pF. However, in terms of capacitance, this point is not so clear as the Nematic-Isotropic transition on a LC cell. The fact that a PDLC is a mixture between a LC and a polymer, it was expected that this point was not so manifest like the LC cells.

Table 3.9 shows the most important capacitance and transmittance values from this study

Table 3. 9 - Values from LC2-20 Capacitance-Transmittance study

Temperature	***Room (25ºC)***	***Tc (57ºC)***	***70ºC***
Capacitance (pF)	111	147	172
Transmittance (%)	4	-	74

At room temperature the capacitance has value of 111pF and reach to 172pF at 70ºC with a maximum transmittance of 74ºC. At 57ºC the capacitance is about 147ºpF and there is the opaque-transparent transition. At 70ºC it reaches 172pF of capacitance and 74% of transmittance

3.6.2. Parallel rubbing on planar alignment layer cell (1.5cm^2) with PDLC

Figures 3.51 and 3.52 shows the capacitance and transmittance variation at 5ºC/min and 2ºC/min respectively:

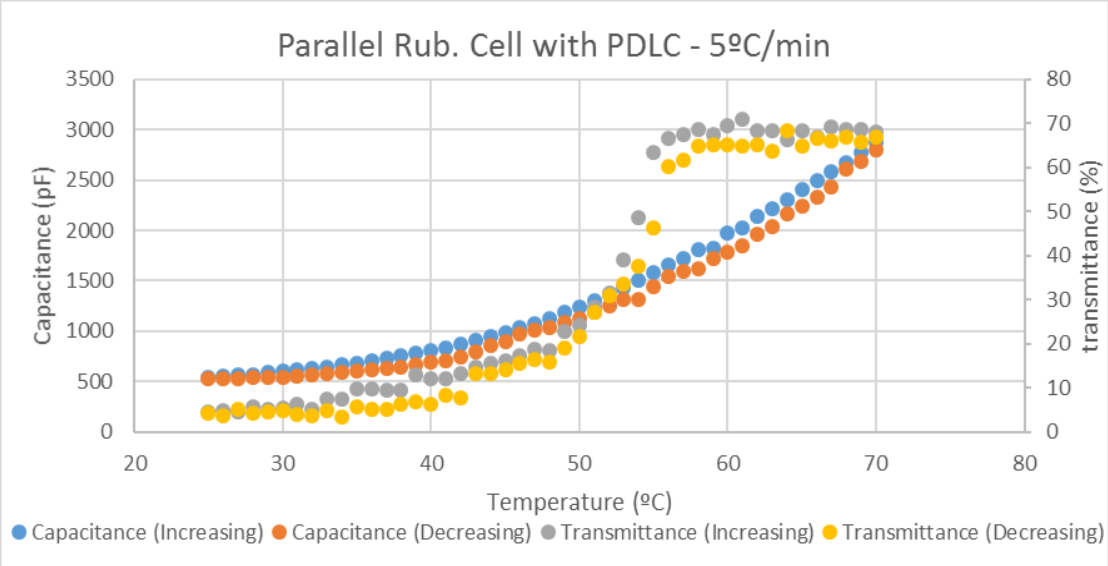

Figure 3. 51- Capacitance-Transmittance study along temperature for parallel rubbing on planar alignment layer cell with PDLC – Rate 5ºC/min

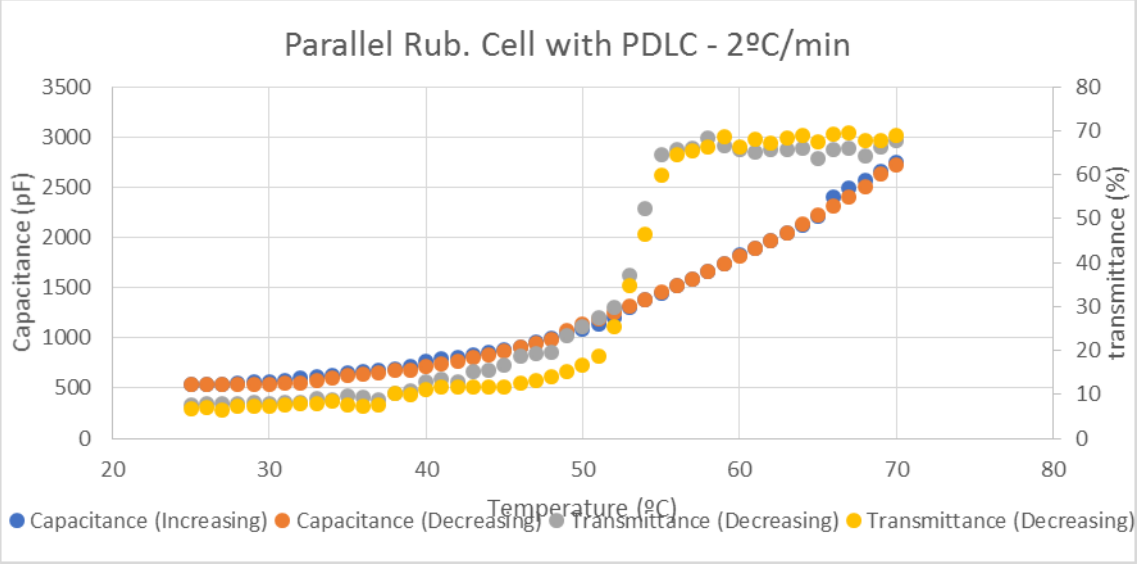

Figure 3. 52 - Capacitance-Transmittance study along temperature for parallel rubbing on planar alignment layer cell with PDLC – Rate 2ºC/min

The Tc on parallel rubbing on planar alignment layer cell it is very difficult to find on capacitance curves, the only curve which has a point is the decreasing curve with 5ºC/min ratio at 54ºC, which matches the transmittance deflection in this case.

Table 3.10 shows the most relevant values from this study

Table 3. 10 - Values from parallel rubbing on planar alignment layer cell Capacitance-Transmittance study

Temperature	*Room (25ºC)*	*Tc (54ºC)*	*70ºC*
Capacitance (pF)	505	1400	2780
Transmittance (%)	4	-	72

The capacitance starts with 505pF at room temperature. Then it starts to increase and at clarification temperature it presents a value of 1400pF and matches the transmittance inflection. When it reach the 70ºC it has value of 2780pF where the transmittance is about 72%.

3.6.3. Anti-parallel rubbing on planar alignment layer cell (1.5cm^2) with PDLC

Figures 3.53 and 3.54 shows the capacitance and transmittance variation at 5ºC/min and 2ºC/min rates respectively

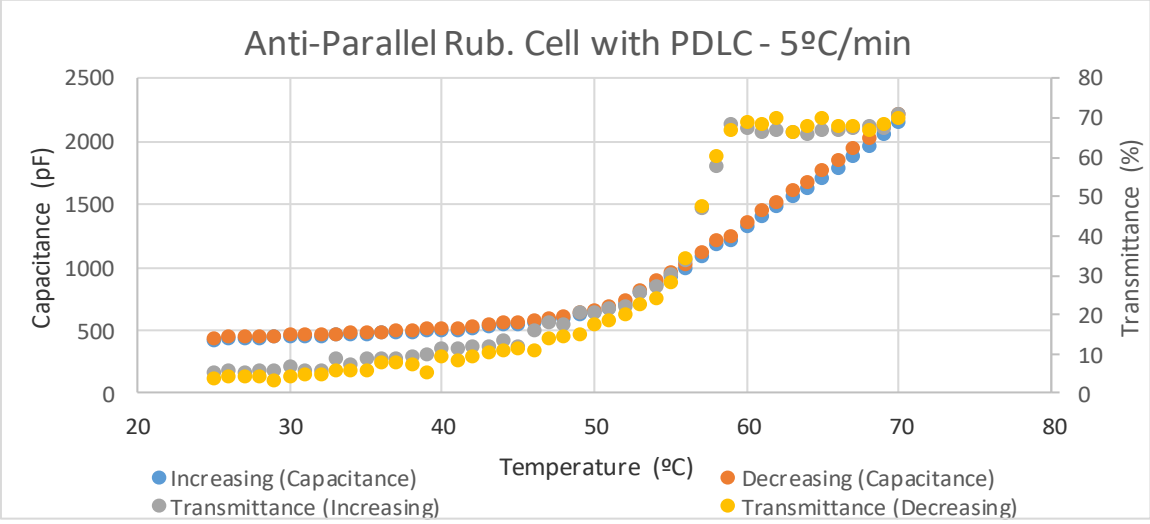

Figure 3. 53 - Capacitance-Transmittance study along temperature for anti-parallel rubbing on planar alignment layer cell with PDLC – Rate 5ºC/min

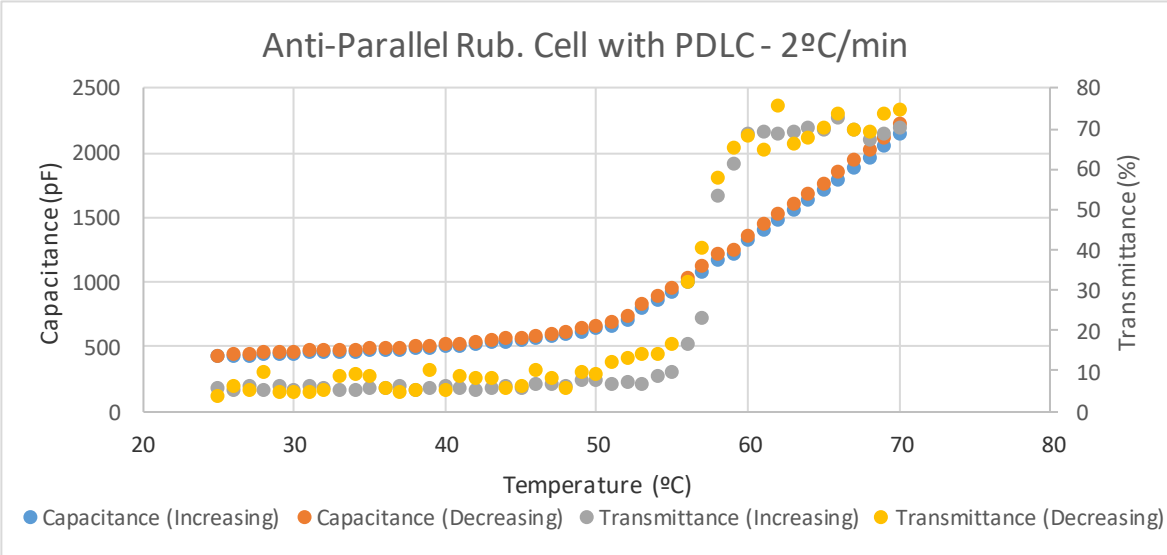

Figure 3. 54 Capacitance-Transmittance study along temperature for anti-parallel rubbing on planar alignment layer cell with PDLC – Rate 2ºC/min

In anti-parallel rubbing on planar alignment layer cell, there is a point on capacitance curves at 57ºC where transmittance reach a maximum value which is coincident with the transmittance great increasing. This point can be seen in both studies, in spite of it is not so evident as the LC2-20. Table 3.11 shows the values from this study.

Table 3. 11 - Values from anti-parallel Capacitance-Transmittance study

Temperature	***Room (25ºC)***	***Tc (57ºC)***	***70ºC***
Capacitance (pF)	484	1200	2450
Transmittance (%)	3	-	72

At room temperature the cell presents a capacitance of 484pF and a transmittance value of 3%. The Tc point has a capacitance value of 1200pf, where occurs the transmittance inflection. At 70ºC the capacitance is about 2450pF and transmittance 72%.

3.6.4. Perpendicular rubbing on planar alignment layer cell (4cm^2) with PDLC

Figures 3.55 and 3.56 shows the Capacitance-Transmittance study for a cell with perpendicular rubbing and 4cm^2 of area

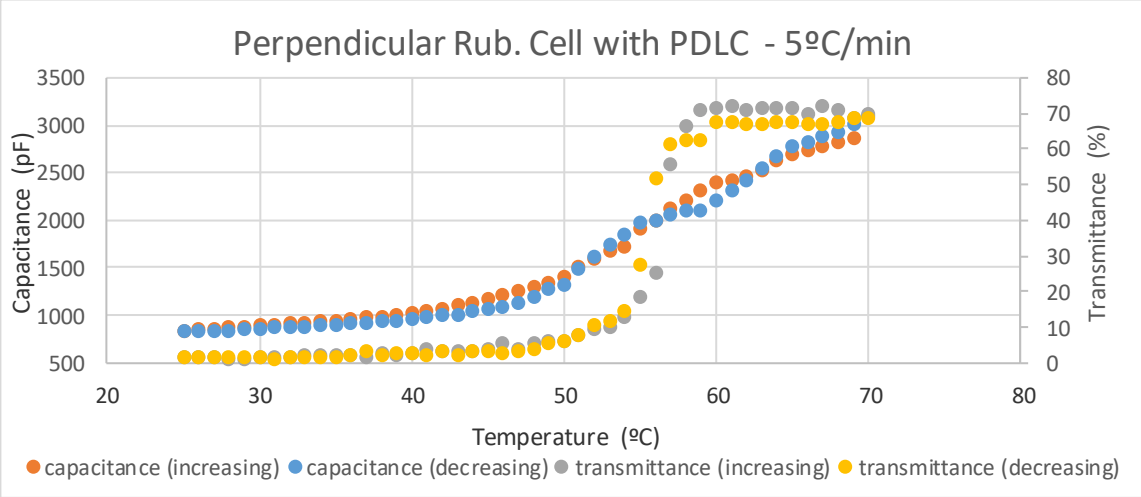

Figure 3. 55 - Capacitance-Transmittance study along temperature for perpendicular rubbing on planar alignment layer cell with PDLC – Rate 5ºC/min

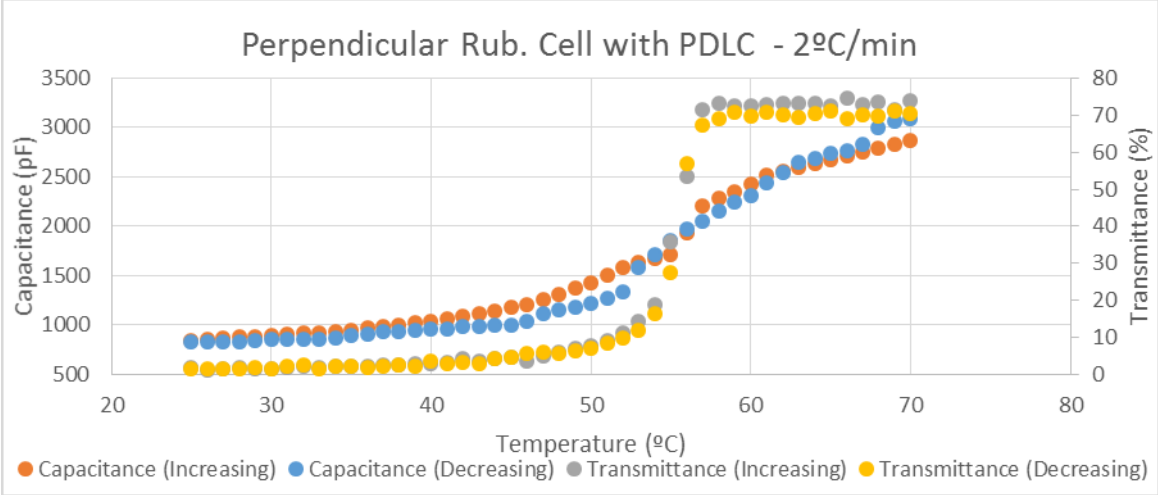

Figure 3. 56 - Capacitance-Transmittance study along temperature for perpendicular rubbing on planar alignment layer cell with PDLC – Rate 2ºC/min

In perpendicular rubbing on planar alignment layer cell, there is a point in capacitance curves at 56ºC where the transmittance inflection occurs. This will be the Tc. Table 3.12 shows the values from this study.

Table 3. 12 - Values from perpendicular rubbing Capacitance-Transmittance study

Temperature	*Room (25ºC)*	*Tc (56ºC)*	*70ºC*
Capacitance (pF)	859	2200	3195
Transmittance (%)	2	-	73

It starts with 859pF at room temperature and reach values close to 3200pF at 70ºC. The Tc matches a value of 2200pF at 56ºC.

3.4.5. Discussion

The Tc values on these cells are all lower than liquid crystal E7 T_{NI}. This can be explained by the different orientation of liquid crystal molecules in each polymer microdomain. For different microdomains with different orientations less energy will be needed to change to isotropic. In a LC there is no microdomains, and it takes more energy to change it to isotropic.

The capacitance study results in empty cells, cells with E7, cells with PEGDMA875 and cells with PDLC can also be comparable by capacitance values at same temperatures. Thereby, the temperatures used for compare this results were the room temperature (25ºC), Clarification Temperature in PDLC cell and the final temperature (70ºC). Tables 3.13 to 3.16 shows the results for each case in this study

LC2-20 cell

Table 3. 13 - Comparative capacitance results for LC2-20

	Room (25ºC)	*Tc (57ºC)*	*70ºC*
E7 (pF)	74	106	116
PEGDMA875 (pF)	120	165	220
PDLC (pF)	**111**	**147**	**172**

For LC2-20 cell, the PDLC capacitance values are between E7 and PEGDMA875 capacitance values along all the curve. At 25ºC the capacitance are closer to PEGDMA875 values than at Tc or at 70ºC.

Parallel rubbing on planar alignment layer (1,5cm^2)

Table 3.14 shows the comparative results for parallel rubbing on planar alignment layer cell

Table 3. 14 - Comparative capacitance results for parallel rubbing on planar alignment layer cell

	Room (25ºC)	*Tc (54ºC)*	*70ºC*
E7 (pF)	204	338	530
PEGDMA875 (pF)	715	1664	2810
PDLC (pF)	**505**	**1400**	**2780**

Parallel rubbing on planar alignment cell presents values between E7 and PEGDMA875 but in this case, with the temperature increasing, the values will be closer to PEGDMA875 capacitance values than E7.

Anti-parallel rubbing on planar alignment layer cell (1,5cm^2)

Table 3.15 shows the comparative results for anti-parallel rubbing on planar alignment layer cell

Table 3. 15 - Comparative capacitance results for anti-parallel rubbing on planar alignment layer cell

	Room (25ºC)	*Tc (57ºC)*	*70ºC*
E7 (pF)	264	361	491
PEGDMA875 (pF)	730	2352	2790
PDLC (pF)	**484**	**1200**	**2450**

For anti-parallel rubbing on planar alignment layer cell , the values still between PEGDMA875 and E7 cells during temperature increasing and decreasing, as the previous cells. In this cell the values are clearly between E7 and PEGDMA875 cells, as it can be seen in the table 3.15.

Perpendicular on planar alignment layer cell (4cm^2)

Table 3.16 shows the comparative results for perpendicular rubbing on planar alignment layer cell

Table 3. 16 - Comparative capacitance results for perpendicular rubbing on planar alignment layer cell

	Room (25ºC)	*Tc (56ºC)*	*70ºC*
E7 (pF)	310	510	625
PEGDMA875 (pF)	640	2996	4013
PDLC (pF)	**859**	**2200**	**3195**

For perpendicular rubbing on planar alignment layer cell the capacitance at room temperature is a little bit higher than PEGDMA875 and E7 cells. However, when the temperature increases the values starts to be between E7 and PEGDMA875 cells, namely at Tc and at 70ºC.

In every cells the PDLC capacitance values are between E7 and PEGDMA875 cells values in spite of the room temperature capacitance in perpendicular rubbing on planar alignment layer cell is higher than the value on PEGDMA875. As the PDLC is a mixture of E7 and PEGDMA875 in 70%/30% proportions respectively, the capacitance values should be lower than PEGDMA875 values and higher than E7 values as was expected.

3.7. Capacitance study with Temperature variation after EO study

After Electro-Optical study, these cells are in a PME state and then the liquid crystal molecules disposition is different. When a cell is heated until a temperature equal or higher than Tc, the LC disposition will return to the initial disposition. Therefore, the capacitance values will change and, in these cases, the heating curve must be different than the cooling curve.

3.7.1. LC2-20 cell with PDLC

Figure 3.57 shows the capacitance variation with temperature graph after EO study for the LC2-20 cell with PDLC

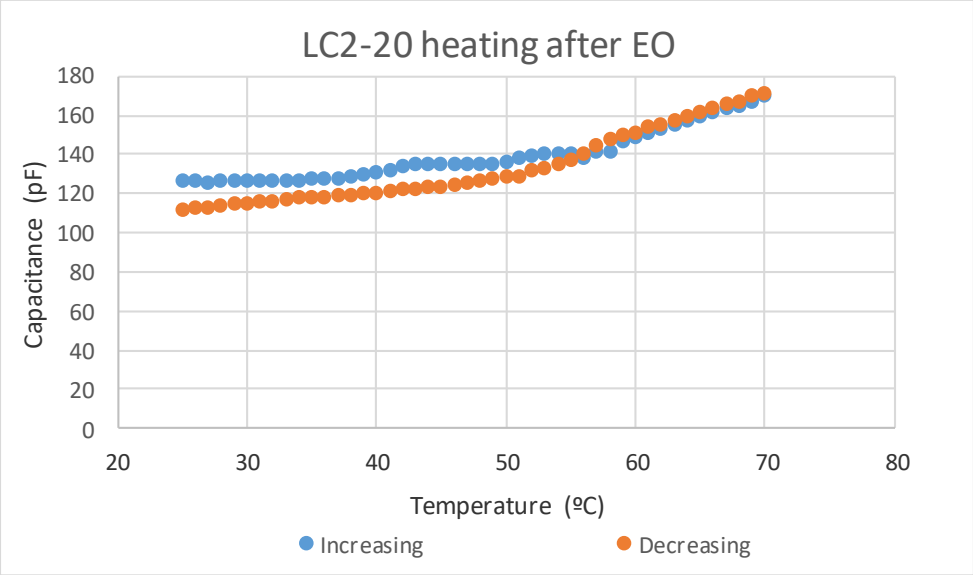

Figure 3. 57 - LC2-20 cell with PDLC capacitance study with temperature after EO study, 2ºC/min rate

.Table 3.17 shows the relevant values from this study, during the increasing and decreasing temperature.

Table 3. 17 - Values from capacitance study after EO cycle for LC2-20 cell with PDLC

	Room T (25ºC)	***Tc (57ºC)***	***70ºC***
Increasing (pF)	133	141	171
Decreasing (pF)	112	143	172

There is a difference about 21pF between the PME state and cleared state in the beginning. This difference will decrease with the temperature increasing until 54ºC, where the capacitance values are almost the same values in decreasing curve. Then, after the decreasing, the values at room temperature are closer to the values before the EO study.

3.7.2. Parallel rubbing on planar alignment layer cell (1.5cm^2) with PDLC

Figure 3.58 shows the capacitance variation with temperature graph after EO study for the parallel rubbing on planar alignment layer cell with PDLC

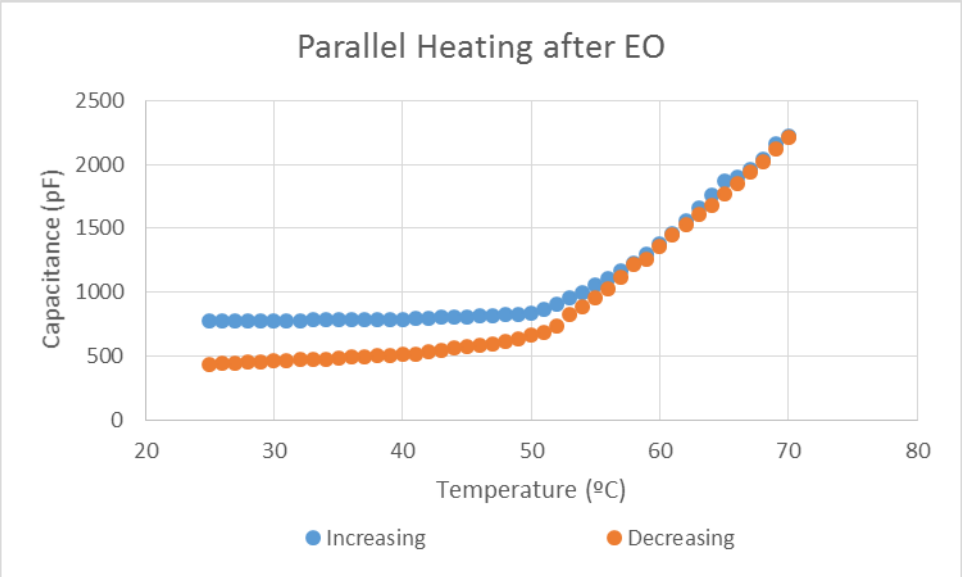

Figure 3. 58 - Parallel rubbing on planar alignment layer cell with PDLC capacitance variation with temperature after EO study, 2ºC/min rate

Table 3.18 shows the values from this study, during the increasing and decreasing temperature.

Table 3. 18 - Values from capacitance study for parallel rubbing on planar alignment layer cell after EO study

	Room (25ºC)	***Tc (54ºC)***	***70ºC***
Increasing (pF)	762	1112	2220
Decreasing (pF)	478	1178	2215

The difference between capacitances in the beginning is 287pF. Like the LC2-20 the values between the curves after and before EO are getting closer with temperature increasing. After the temperature of 52ºC the values in both curves are almost the same. At the end of the decreasing, the values return to capacitance values before EO study.

3.7.3. Anti-parallel rubbing on planar alignment layer cell (1.5cm^2) with PDLC

Figure 3.59 shows the capacitance variation with temperature graph after EO study for the anti-parallel rubbing on planar alignment layer cell with PDLC

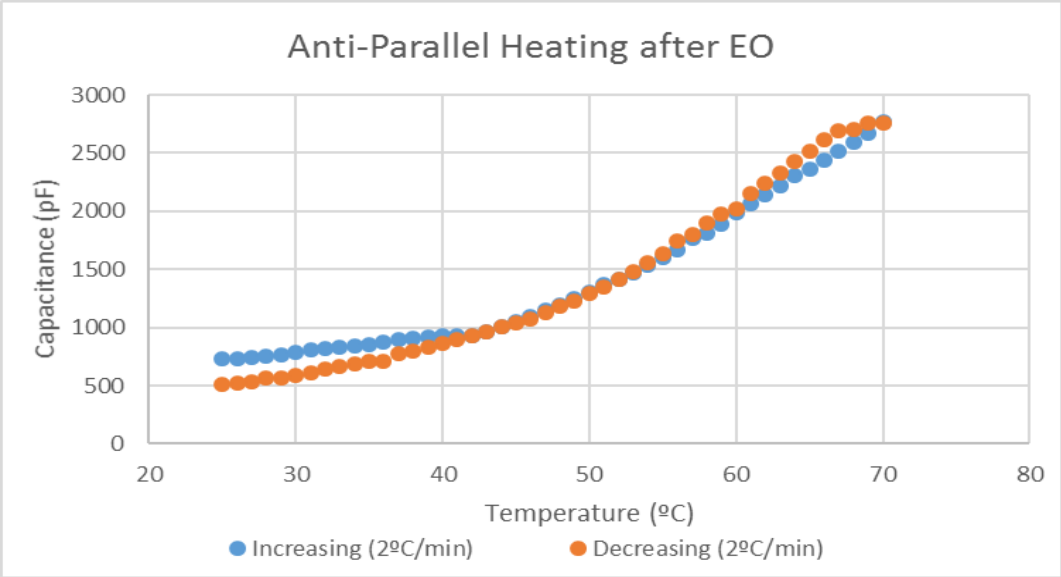

Figure 3. 59 – Anti-parallel rubbing on planar alignment layer cell capacitance variation with temperature after EO study, Rate 2ºC/min

Table 3.19 shows the values from this study, during the increasing and decreasing temperature.

Table 3. 19 - Values from capacitance study for anti-parallel rubbing on planar alignment layer cell after EO study

	Room T (25ºC)	***Tc (57ºC)***	***70ºC***
Increasing	731	1824	2808
Decreasing	510	1871	2801

In this case, the difference between both curves is 221 pF at room temperature, and it reduces during temperature increasing, namely until 42ºC. After this point, the increasing curve have almost the same aspect as the decreasing curve. In the end, after decreasing, the values return to the same values before EO.

3.7.4. Perpendicular rubbing on planar alignment layer (4cm^2) with PDLC

Figure 3.60 shows the capacitance variation with temperature graph after EO study for the perpendicular rubbing on planar alignment layer cell with PDLC

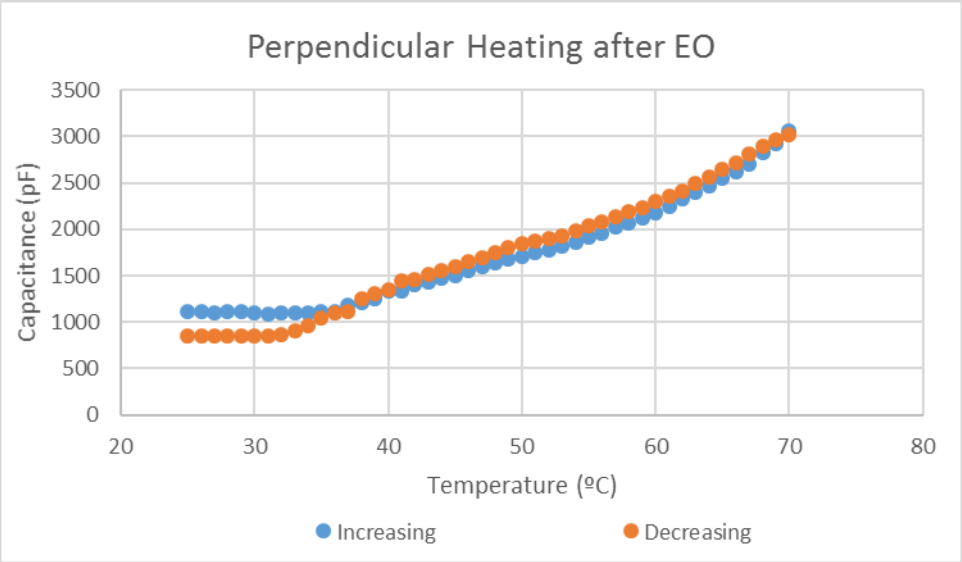

Figure 3. 60 - Perpendicular rubbing on planar alignment layer cell capacitance variation with temperature after EO study, Rate 2ºC/min

Table 3.20 shows the values from the graph during the increasing and decreasing temperature

Table 3. 20 - Values from perpendicular rubbing on planar alignment layer cell capacitance variation with temperature after EO study

	Room T (25ºC)	*Tc (56ºC)*	*70ºC*
Increasing	1143	2182	3213
Decreasing	851	2224	3204

There is a difference of 292pF between the increasing and decreasing curves at room temperature. With the temperature increasing, the differences between both curves reduce and at Tc and at 70ºC the capacitances are basically the same. When the temperature returns to the room, the values are almost the same as the cell before EO.

3.7.5 Discussion

As was expected, the capacitance values in every cells are higher after EO than before. The director changes the orientation and then the capacitance increases. When a PDLC cell is heated the director will return to the initial orientation. Then the capacitance will return to the same values that it had before EO study.

In some cells the curves coincide with lower temperatures but always before Tc point. The fact that increasing and decreasing curves in some cells coincide each other earlier or later must be irrelevant for the information erasing on devices with memory.

This study was done for trying to understand what happened to the capacitance after the EO study and their behaviour when the PME is erased. Then it is possible to known when the written information is totally cleared if the capacitance return to values before EO study.

3.8. Capacitance study with Joule-Heating Effect

After the capacitance studies along temperature it was possible determine which capacitance level matches the Tc on a PDLC cell. Then it is possible to heat the cell by joule-heating effect with different current intensities and find which current values must be used to erase the written information. For each handmade cell it was applied four current intensities with different values to find which currents are able to clear the PME. When the capacitance reaches constant values the Power Supply was turned off and the cell temperature decreases.

This was a study only applied on handmade cells and it was done a study before the EO study where the cells are totally opaque and after EO study where cells have written information.

3.8.1. Parallel rubbing on planar alignment layer cell (1.5cm^2) with PDLC

For cells with 1.5cm^2, the currents applied were 0.11A; 0.13A; 0.15A and 0.17A. Figure 3.61 shows the graph for Joule-heating before EO study for the parallel rubbing on planar alignment layer cell, where the Tc matches the 1400pF.

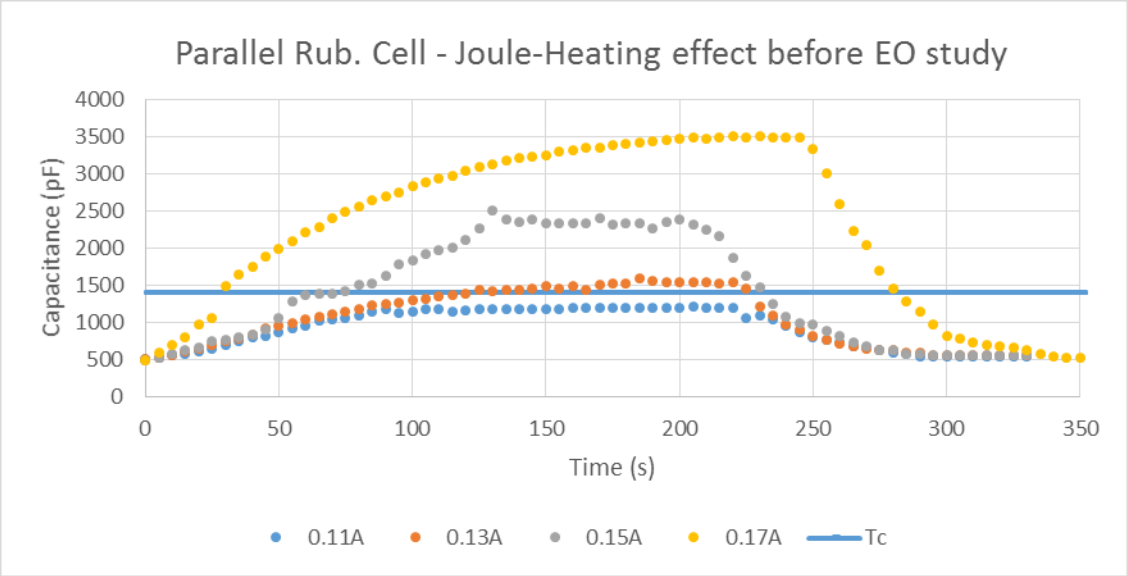

Figure 3. 61 – Joule-heating effect for parallel rubbing on planar alignment layer cell before EO study

It can be seen that a Joule-heating effect current of 0.11A is not enough to reach the Tc but currents higher than 0.13A can do. Table 3.21 shows the capacitance values from this study.

Table 3. 21 – Capacitance values from Joule heating effect before EO study – Parallel rubbing on planar alignment layer cell

Capacitance (pF)	*0.11A*	*0.13A*	*0.15A*	*0.17A*
Beginning	503	505	512	507
Maximum	1310	1585	2509	3512
Ending	513	524	517	505

High values of current intensity reach high temperature values and then high values of capacitance. As was expected the capacitance maximum values increase with the current. The currents above 0.13A can reach easily the Tc, and then it the PDLC cell can totally turn to the transparent state.

Table 3.22 shows the time values of heating until stabilization and cooling when the current was turned off. The most important value is the time that a current needs to PDLC cell reach the Tc.

Table 3. 22 - Time values from Joule heating effect before EO study – Parallel rubbing on planar alignment layer cell

Time (s)	*0.11A*	*0.13A*	*0.15A*	*0.17A*
Heating	100	110	125	160
Cooling	50	75	75	80
Time to reach Tc	-	105	60	30

Small intensities cannot reach the Tc value. Then the capacitance value in PDLC are below than capacitance value for Tc. The time for heating until stabilization is directly proportional to the capacitance values, as well as the cooling time. The time to reach Tc decrease with high values of intensity. This means that high current intensities will reach faster the Tc than lower levels of current intensity.

Then it was also done the study after EO, is this, when the information was written on PDLC. Figure 3.62 shows the graph for heating when the PDLC has PME:

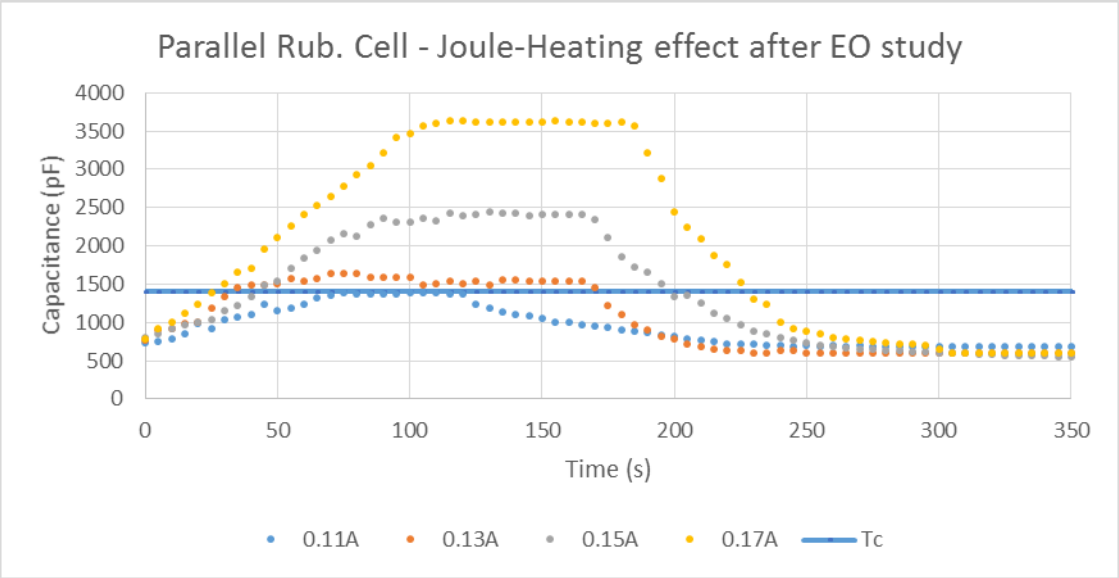

Figure 3. 62 - Joule-Heating effect for parallel rubbing on planar alignment layer cell after EO study

Through the graph it can be seen that capacitance initial values are higher than before EO study. If the intensities are enough to reach the Tc the written information is totally erased. If the current intensities cannot reach the Tc value, the heat is not enough to clear the PME. When the current is turned off, if the capacitance values at ending are the same than before EO it means that the written information was totally erased. Table 3.23 shows the capacitance values from this study

Table 3. 23 – Capacitance values from Joule-heating effect after EO study Parallel rubbing on planar alignment layer cell (1.5cm^2) with PDLC with PME

Capacitance (pF)	*0.11A*	*0.13A*	*0.15A*	*0.17A*
Beginning	791	788	794	788
Maximum	1350	1585	2509	3624
Ending	685	549	536	532

The maximum capacitances are close to the study before EO. However, the ending capacitances of intensities which are above than 0.11A return to the same that the cell had before the EO study. This means that these intensities can erase completely the written information in this cell.. The clarification temperature value cannot be reached with this current intensity, and then, the erasing will be not enough to clear all written information. Therefore, the capacitance value did not decrease until values before EO study.

Table 2.24 shows time values for heating until the stabilization, cooling and time to reach the Tc.

Table 3. 24 - Time values from Joule-heating effect after EO study - Parallel rubbing on planar alignment layer cell

Time (s)	*0.11A*	*0.13A*	*0.15A*	*0.17A*
Heating	55	60	80	95
Cooling	65	75	80	95
To reach Tc	-	40	40	30

After the EO study, the cell has PME and the time to reach Tc and the heating time until the capacitance stabilises are lower than before EO study. However, the cooling times increase. As the capacitance values are higher than the capacitances before EO study, it is faster to heat the cell.

3.8.2 Anti-parallel rubbing on planar alignment layer cell (1.5cm^2) with PDLC

For Anti-parallel rubbing on planar alignment layer cell it was also applied the same intensity values as the parallel rubbing on planar alignment layer cell. This cell has a capacitance value of 1200pF on Tc. Figure 3.63 shows the capacitance variation before EO for the Anti-parallel rubbing on planar alignment layer cell

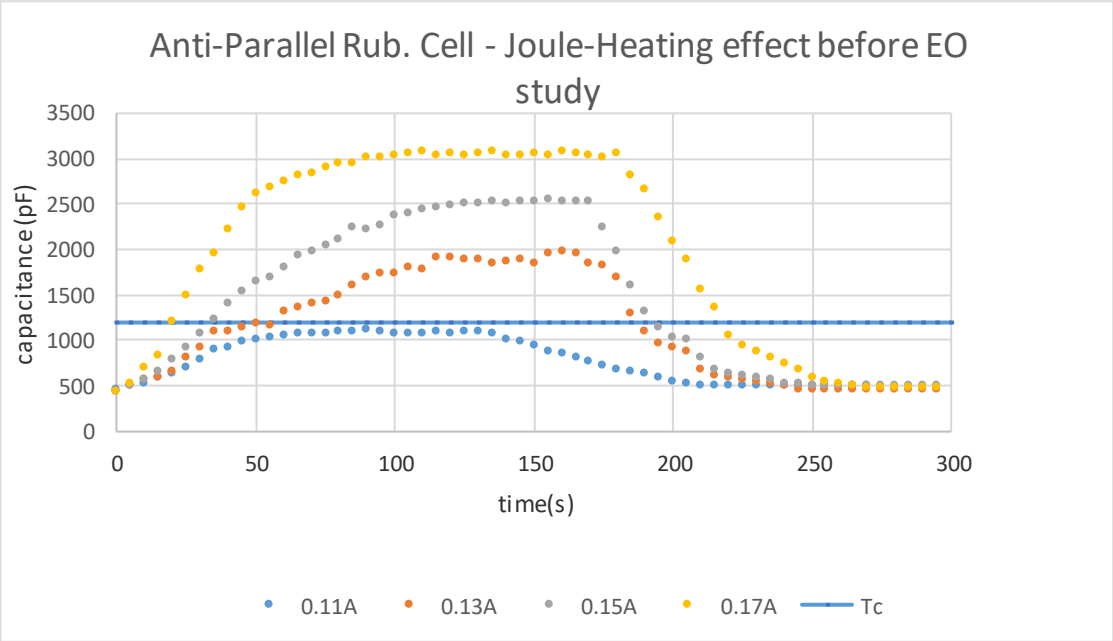

Figure 3. 63 - Joule-Heating Effect for anti-parallel rubbing on planar alignment layer cell before EO study

Like the parallel rubbing on planar alignment layer cell, a 0.11A intensity is not enough to reach the Tc but values higher than 0.13A can do. Table 3.25 shows important values from this study on anti-parallel rubbing on planar alignment layer cell

Table 3. 25 – Capacitance values from Joule-heating effect before EO study - Anti-parallel rubbing on planar alignment layer cell

Capacitance (pF)	*0.11A*	*0.13A*	*0.15A*	*0.17A*
Beginning	455	425	438	423
Maximum	1100	1950	2520	3200
Ending	482	424	438	422

As the parallel rubbing on planar alignment layer cell the 0.11A is not enough to reach the Tc and currents higher than 0.13A can reach the Tc in this devices. The values are similar than the previous cell.

Table 3.26 shows the time values for the Anti-parallel rubbing on planar alignment layer cell

Table 3. 26 - Time values from Joule-heating effect before EO study - Anti-parallel rubbing on planar alignment layer cell

Time (s)	*0.11A*	*0.13A*	*0.15A*	*0.17A*
Heating	100	120	130	130
Cooling	65	75	75	80
To reach Tc	-	60	45	25

As the parallel rubbing on planar alignment layer cell, 0,11A cannot reach the Tc and for higher instensities the heating and cooling times increase and the time to reach Tc decreases. The 0.15A and 0.17A have almost the same heating times but the time to reach Tc is bigger at 0.15A than 0.17A. The order of values are similar as the previous cell.

Figure 3.64 shows the joule-heating effect after EO study

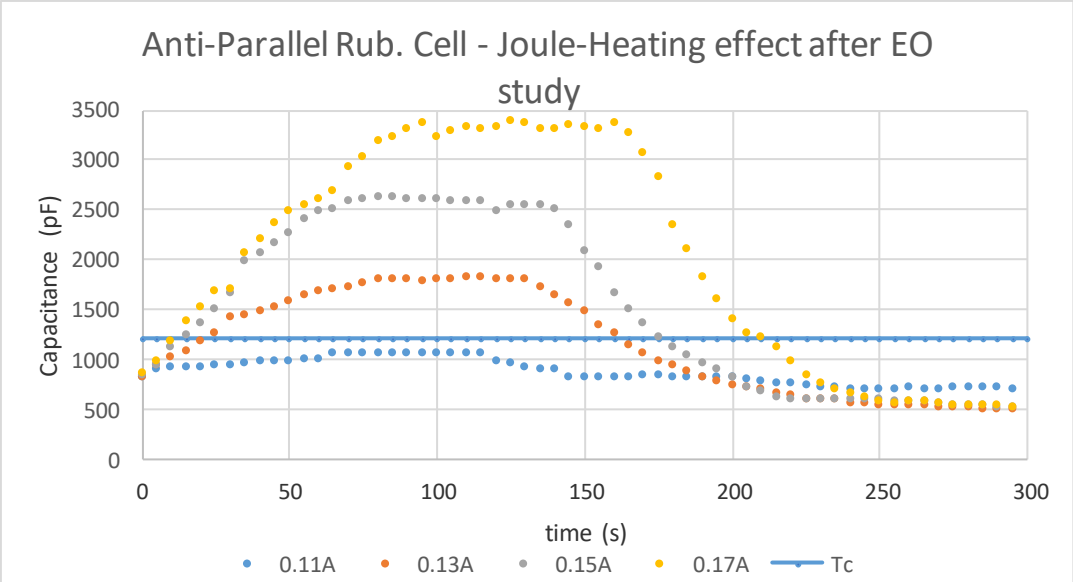

Figure 3. 64 - Anti-parallel rubbing on planar alignment layer cell - Joule-Heating effect after EO study

It is clearly evident that in the beginning, the capacitances are higher than before EO study. When the current is turned off it was waiting for a stabilization and for intensities that can reach the Tc the capacitance stabilises at the same values before the EO study. Table 3.27 shows the results from this study in terms of capacitance

Table 3. 27 – Capacitance values from Joule-heating effect after EO study - Anti-parallel rubbing on planar alignment layer cell

Capacitance (pF)	*0.11A*	*0.13A*	*0.15A*	*0.17A*
Beginning	783	774	769	770
Maximum	1090	1800	2625	3370
Ending	705	483	477	466

The ending capacitances of intensities which are above than 0.11A return to values closer to values before the EO study. Intensities higher than 0.13A can erase completely the written information on cells. The 0.11A intensity ending capacitance presents a value higher than other ending capacitances and close to the initial. The clarification temperature value cannot be reached with this current intensity, and then, the heat will be not enough to clear all written information. Therefore, the capacitance value did not decrease until values that the cell had before EO study. Table 3.28 shows the time values for this study

Table 3. 28 – Time values from Joule-heating effect after EO study - Anti-parallel rubbing on planar alignment layer cell

Time (s)	*0.11A*	*0.13A*	*0.15A*	*0.17A*
Heating	75	75	80	100
Cooling	85	105	115	125
To reach Tc	-	30	20	10

The heating time and time to reach Tc are lower than before the EO study. The cooling times are bigger due the waiting time for reaching a baseline and as the capacitance values drop at the end, the cooling is a little bit higher because there is a decreasing until a baseline

3.8.3. Perpendicular rubbing on planar alignment layer cell (4cm^2) with PDLC

As the perpendicular rubbing cell has a bigger area than parallel and Anti-parallel rubbing on planar alignment layer cells, high intensities were applied. Figure 3.65 shows the heating by joule effect graphic for a handmade cell with perpendicular rubbing alignment layer with different intensities: 0.15A; 0.18A; 0,21A; 0,24A. It is also represented the capacitance value for Tc at 2400pF.

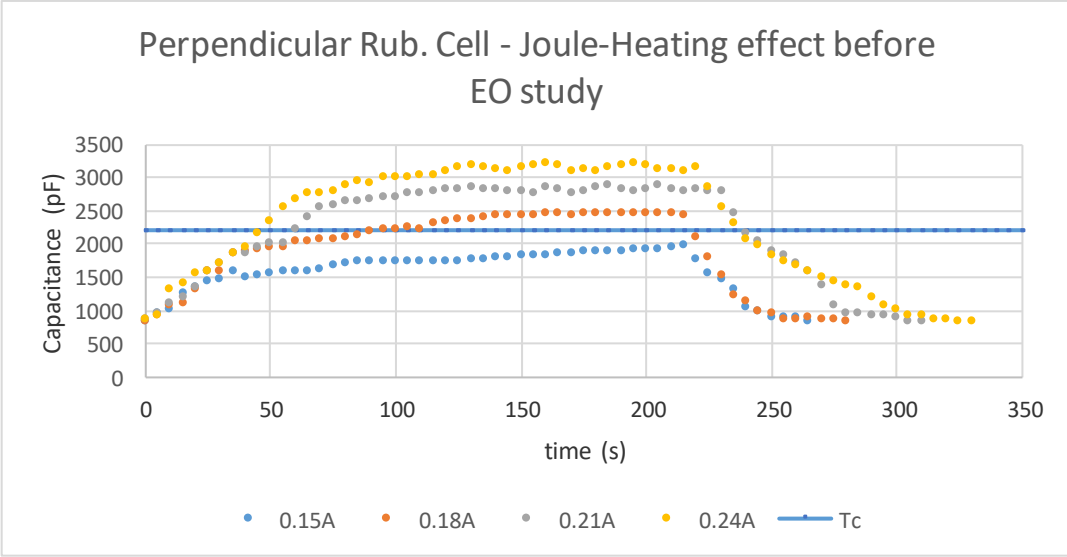

Figure 3. 65 - Perpendicular rubbing on planar alignment layer cell with PDLC- Joule-heating effect before EO study

In the case of the perpendicular rubbing on planar alignment layer cell, a 0.15A intensity is not enough to reach Tc and the other intensities can reach it. The Table 3.29 shows the capacitance values at beginning, ending and maximum.

Table 3. 29 – Capacitance values from Joule-heating effect before EO - Perpendicular rubbing on planar alignment layer cell with PDLC

Capacitance (pF)	*0.15A*	*0.18A*	*0.21A*	*0.24A*
Beginning	844	847	863	854
Maximum	1982	2475	2894	3213
Ending	849	849	837	823

By heating, the capacitance values can increase and return to values at the beginning the values at beginning of heating in all studies with different current intensities. The current of 0.15A never reaches the Tc capacitance value.

Table 3.30 shows the time values for Joule-heating effect before EO study

Table 3. 30 - Time values from Joule-heating effect before EO - Perpendicular rubbing on planar alignment layer cell with PDLC

Time (s)	*0.15A*	*0.18A*	*0.21A*	*0.24A*
Heating	150	150	120	100
Cooling	45	55	85	100
Reach Tc	-	90	60	45

When a 0.15A current is applied, the cell cannot reach the Tc value and the heating will be not enough to occur the opaque-transparent transition totally. The current intensities higher than 0.18A can reach the Tc and then the cell turns totally transparent and the cooling time will be greater for great levels of intensities.

The same procedure it was done after EO for the perpendicular rubbing on planar alignment layer cell with PDLC. Figure 3.66 shows the joule-heating after EO study.

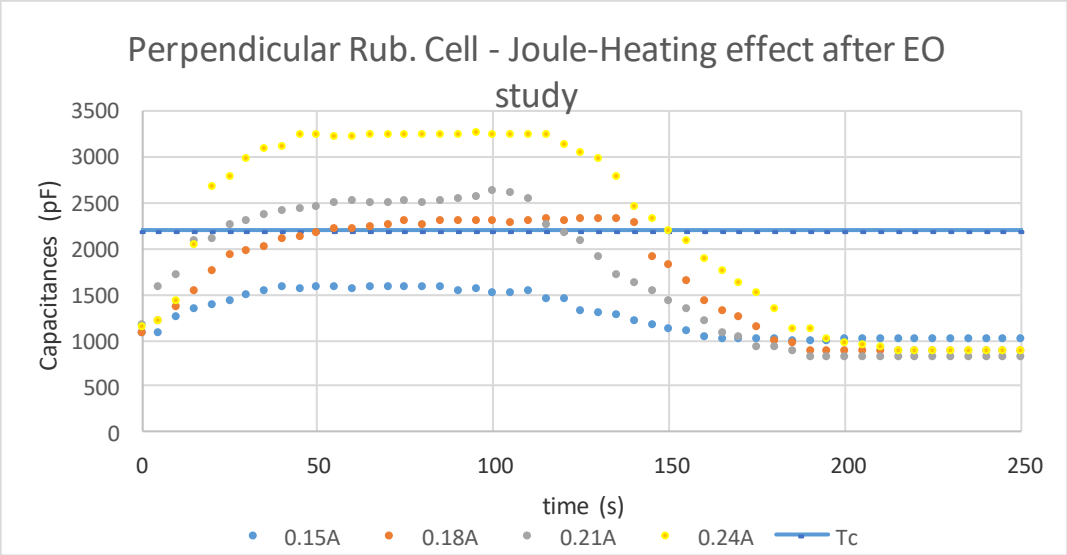

Figure 3. 66 - Perpendicular rubbing on planar alignment layer cell with PDLC - Joule-heating effect after EO study

As it can be seen, an intensity of 0.15A still not enough to reach the Tc and then the written information will be not totally cleared. Before the EO study this intensity was not enough to turn the cell totally transparent and therefore currents higher than 0.18A can reach the Tc and then clear the written information on the device.

Table 3.31 shows the capacitance values from joule-heating effect after EO study

Table 3. 31 – Capacitance values from Joule-heating effect after EO study - Perpendicular rubbing on planar alignment layer cell with PDLC

Capacitance (pF)	*0.15A*	*0.18A*	*0.21A*	*0.24A*
Beginning	1088	1075	1175	1135
Maximum	1615	2340	2690	3270
Ending	1002	848	826	853

The 0.15A is not enough to erase the written information totally and therefore, at the ending, the capacitance is little smaller than the beginning. For the other intensities, the capacitance decreases until values before EO study. This means that currents higher than 0.18A current are enough to clear all the written information in this cell as was verified on study before EO.

Table 3.32 shows the time values from joule-heating effect after EO study

Table 3. 32 - Time values from Joule-heating effect after EO study - Perpendicular rubbing on planar alignment layer cell with PDLC

Time (s)	*0.15A*	*0.18A*	*0.21A*	*0.24A*
Heating	55	55	50	45
Cooling	55	65	85	115
To reach Tc	-	55	25	15

As the other cells, after EO the heating time and time to reach Tc decreases but the cooling time increases. The 0.15A current do not reach the Tc and the other currents can reach it faster than they reach before EO study.

3.8.4. Discussion

When a Joule-Heating Effect current is not enough to reach the Tc before EO, the written information is not totally erased. For erasing all the written information it will be need at least currents of 0.13A in parallel and anti-parallel rubbing on planar alignment layer cells and 0.18A on perpendicular rubbing on planar alignment layer cell with PDLC. This can be observed by analysing the capacitance values in the beginning and ending, when they return values before EO it means that the written information was totally erased.

Another important aspect is the time that the cells need for heating, reaching Tc and cooling before and after EO. The heating time and time to reach Tc decreases but the cooling time increases. This can be explained by an existence of a great mobility on LC molecules after an electric field be applied. If the mobility is higher than before, the energy need will be also lower. Then the times for heating and reaching the Tc will be reduced.

The PME can only be erased since certain levels of current intensities and capacitance is a good physical quantity to know where opaque-transparent transition occurs and if the heating is enough.

4

Chapter 4 – Conclusions

With the results of this work, it can be concluded that PME is only present in PDLC cells which glasses having a planar alignment treatment, independently the direction and way. This is another important factor that determines the PME value on PDLC cells, and the AFM and SEM analysis can prove that the polymer follows the alignment. Although the alignment is known by aligning the LC molecules, it is strong enough to also align the polymer and then the polymer/liquid crystal mixture.

When a PDLC cell is submitted to an EO study and it presents a high PME value the capacitance values increases due the LC director alignment. The written information is completely erased if the capacitance values decrease until values closer before EO study. When not, it means that the heat applied was not enough to reach the clarification temperature, and then, the written information is not completely erased.

Another important aspect is that it is possible to find the transparent-opaque transition if we measure capacitances. The capacitance study can give to us a usefully information about how the PDLC device can be heated for erasing the written information instead transmittance study. Moreover, during EO study we can also measure capacitances and the graph of capacitance variation applied field must be very similar to the graph of transmittance variation applied field.

The results of this work can be very determinant in a next step of smart windows development. If the glasses have planar alignment treatment it is possible to develop a system that turn the window transparent by an applied electric field and return to the opaque state by heating with an electric current for a few seconds. This system can be very advantageous, it reduces the energetic waste and then it can be more economical and environmentally friendly.

5

Chapter 5 – Bibliography

1. Case Western Reserve University; *Liquid Crystal Phases* http://plc.cwru.edu/tutorial/enhanced/files/lc/phase.
2. *Chemistry of Liquid Crystals and their Industrial Applications* http://shodhganga.inflibnet.ac.in/bitstream/10603/12732/7/07_chapter%201.pdf
3. Barrett Research Group; *Introduction to Liquid Crystals*; McGill University http://barrett-group.mcgill.ca/tutorials/liquid_crystal/LC02.htm.
4. Palffy-Muhoray P.; *The Diverse World of Liquid Crystals*; Physics Today, September 2003; 54-60.
5. Nobel Prize; *History and Properties of Liquid Crystals*; http://www.nobelprize.org/educational/physics/liquid_crystals/history/.
6. Pierre-Gilles de Gennes; *Soft matter;* Nobel Prize Lectures 1991; 1-6.
7. Martins AF; *Os Cristais Líquidos*. Colóquio/Ciências; 1972; 3-25.
8. Kosuge M.; *Liquid crystal display device and driving method of the same* - US 20110164072 A1 Patent. 2011; http://www.google.ch/patents/US7471275
9. Kumar S. et al.; *Experimental Study of Physical Properties and Phase Transitions*; Cambridge University Press, Cambridge; 2001; 1-9.
10. Shakhashiri B.; *Liquid crystals*; Chemical Week; 2007; 4-5.
11. Andrienko D.; *Introduction To Liquid Crystals*. International Max Planck Research Schools – Max Plank Society; 2006; 1-32.
12. Materials Research Science and Engineering Centers Education; *Textures of Liquid Crystal Phases*; http://education.mrsec.wisc.edu/courses/colorsymp/park/index.html.
13. Sedumpa A.; *Topological Microfluidics*; Springer Science & Business Media; Switzerland SIP, ed.; 2013; Chapter 2; 1-9
14. Dabrowski R, Przemyslaw K, Herman J.; *High Birefringence Liquid Crystals*; Crystals; 2013; 443-482.

15. Stanford University; *Refractive index discontinuities due to birefringence*; http://web.stanford.edu/group/scintillators/ceramicprocessing.html.
16. University of Cambridge; *DoITPoMS - TLP Library Liquid Crystals - Birefringence in nematics;* http://www.doitpoms.ac.uk/tlplib/liquid_crystals/birefringence_nematics.php.
17. Zakerhamidi MS, Ara MHM, Maleki A. *Dielectric anisotropy , refractive indices and order parameter of W-1680 nematic liquid crystal*; Journal of Molecular Liquids. 2013;181:77-81.
18. Alla R. *On the Control of Nematic Liquid Crystal Alignment On the Control of Nematic Liquid Crystal Alignment*. 2013, Thesis for the Degree of Doctor of Philosophy in Physics; University of Gottenburg
19. University of Kent; *Liquid Crystals - a Simple View on a Complex Matter*; http://www.personal.kent.edu/~bisenyuk/liquidcrystals/emfield1.html.
20. Drzaic P; *Putting Liquid Crystal Droplets To Work : A Short History of Polymer Dispersed Liquid Crystals*; Liquid Crystals; 2006; 1281-1285;
21. Hakemi H.; *Industrial Development of Plastic PDLC : Is There a Plastic PDLC : Is There A Future ?;* Liquid Crystals Today; 1998; 7-12
22. Technology - Smart Films International; http://smartfilmsinternational.com/pdlc/.
23. Silva MC, Figueirinhas J, Sotomayor J; *Effect of an Additive on the Permanent Memory Effect of Polymer Dispersed Liquid Crystal Films*; Journal of Chemical Technology and Biotechnology, Vol. 90, Issue 9; 2005; 1565-1568
24. Mouquinho AI, Petrova K, Barros MT, Sotomayor J.; *New Polymer Networks for PDLC Films Application;* INTECH. 2012;140-164.
25. West JL, Kelly JR, Jewell K; *Effect of Polymer Matrix Glass-Transition Temperature on Polymer Dispersed Liquid-Crystal Electrooptics*; Applied Physics Letter;1992; 3238-3240.
26. University of Cambridge; *DoITPoMS - TLP Library Dielectric materials - Capacitors*. http://www.doitpoms.ac.uk/tlplib/dielectrics/capacitors.php?printable=1.
27. Freedman R, Young H; *Sears and Zemansky's University Physics with Modern Physics*. 12th edition (Pearson, ed.), San Francisco, 2008; 788-809
28. HP Hewlett Packard; *Agilent Measurement of Capacitance Characteristics of Liquid Crystal Cell Application*; http://www.hpmemoryproject.org/an/pdf/an_369-7.pdf.
29. Polytronix Inc. Applications http://www.polytronixglass.com/pdlc-smart-film/.
30. Luís N.; *Efeito de Memória na Gravação de Informação em PDLCs*. 2014. Dissertação para obtenção do Grau de Mestre em Engenharia Química e Bioquímica, FCT-UNL
31. Cooper J, Glass WA; *Compositional Analysis of Merck E7 Liquid Crystal Intermediates Using UltraPerformance Convergence Chromatography (UPC 2) with PDA Detection*. Waters Corporation. 2013; 1-7.
32. Wu S-T, Meucci R, Faetti S.; *Infrared refractive indices of liquid crystals*. Journal of Applied Physics. 2005; 073501-073505.
33. Sigma Aldrich. Sigma Aldrich: Product Specification Poly(ethylene glycol) dimethacrylate.
34. Sigma Aldrich. Sigma Aldrich: Product Specification 2,2′-Azobis(2-methylpropionitrile)
35. Holland CD; Anthony RG.; *Fundamentals of Chemical Reaction Engineering*. 2nd

Edition. (Hall P, ed.) Englewood Cliffs, NJ; 1977; 354-383

36. Samant MG, Sto J.*; Liquid crystal alignment by rubbed polymer surfaces : a microscopic bond orientation model.;* Journal of Electron Spectroscopy and Related Phenomena; 1999; 189-207.
37. INSTEC Inc; *Solutions for Precision Temperature Control and Liquid Crystal Property Measurement*; http://www.instec.com/support.php?id=&num=3.
38. INSTEC Inc; *Liquid Crystal Consumables and Accessories*; www.instec.com/products1.php?sid=26
39. INSTEC Inc.; *Precision Instruments for TFT-LCD Industry R&D and Education Since 1984*. www.instec.com
40. Hameg; *Programmable LCR Bridge HM 8118*, from Hameg
41. The European Synchroton; *FP90 Central Processor Manual*
42. Alonso & Finn. *Física, Um Curso Universitário Vol.2*.; 2.ª edição. Edgard Blucher, São Paulo - Brasil; 1987; 152-153;
43. Instruments TT. *THURLBY THANDAR INSTRUMENTS EX Series single , dual and triple output models*; http://www.tti-new.com/pdf-files/psu-ex-series-4p.pdf
44. Bird J. *Electrical Circuit Theory and Technology*. 2nd edition. (Newnes, ed.), Oxford, 167-170; 2003.
45. Silva MC; *Effect of surfactant on PDLC films with and without permanent memory effect*; 2013; Dissertação para obtenção do Grau de Mestre em Engenharia Química e Bioquímica, FCT-UNL
46. OLYMPUS; *Basics of Polarizing Microscopy*. http://research.physics.berkeley.edu/yildiz/Teaching/PHYS250/Lecture_PDFs/polarization microscopy.pdf.
47. Microscopy U; *Introduction to Optical Birefringence*; http://www.microscopyu.com/techniques/polarized-light/principles-of-birefringence.
48. PerkinElmer Inc.; *Differential Scanning Calorimetry (DSC) - A Beginner's Guide*. :1-9. https://www.perkinelmer.com.cn/CMSResources/Images/46-74542GDE_DSCBeginnersGuide.pdf
49. Polymer Science Learning Center; *Differential Scanning Calorimetry;* http://pslc.ws/macrog/dsc.htm
50. Haugstad G.; *Atomic Force Microscopy: Understanding Basic Modes and Advanced Applications*; Wiley ed.; New Jersey; Chapter 1; 2012 ; 1-18
51. JEOL - Serving Advanced Technology; *Scanning Electron Microscope A To Z*; 1-13. http://www.jeolusa.com/RESOURCES/Electron-Optics/Documents-Downloads/EntryId/598
52. Laboratory of Nanofabrication - CENIMAT. http://www.cenimat.fct.unl.pt/services/laboratory-nanofabrication.

A

Appendix A – DSC analysis

E7

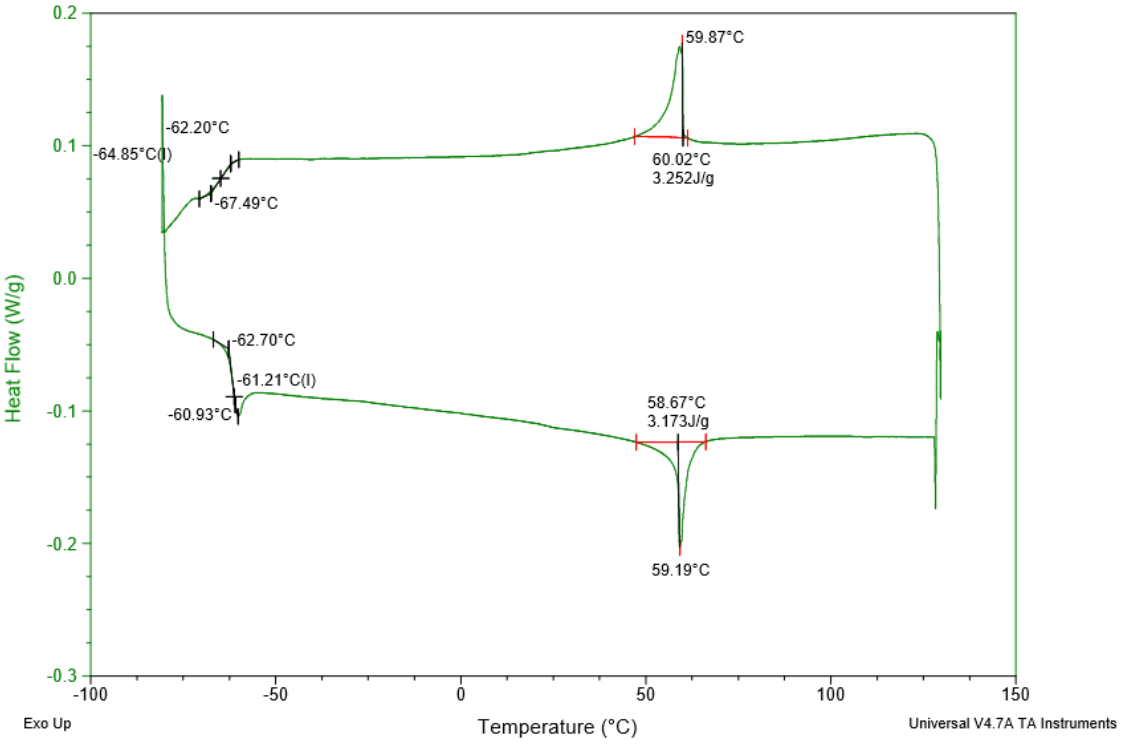

Figure A. 1 - Second Heating stage for E7

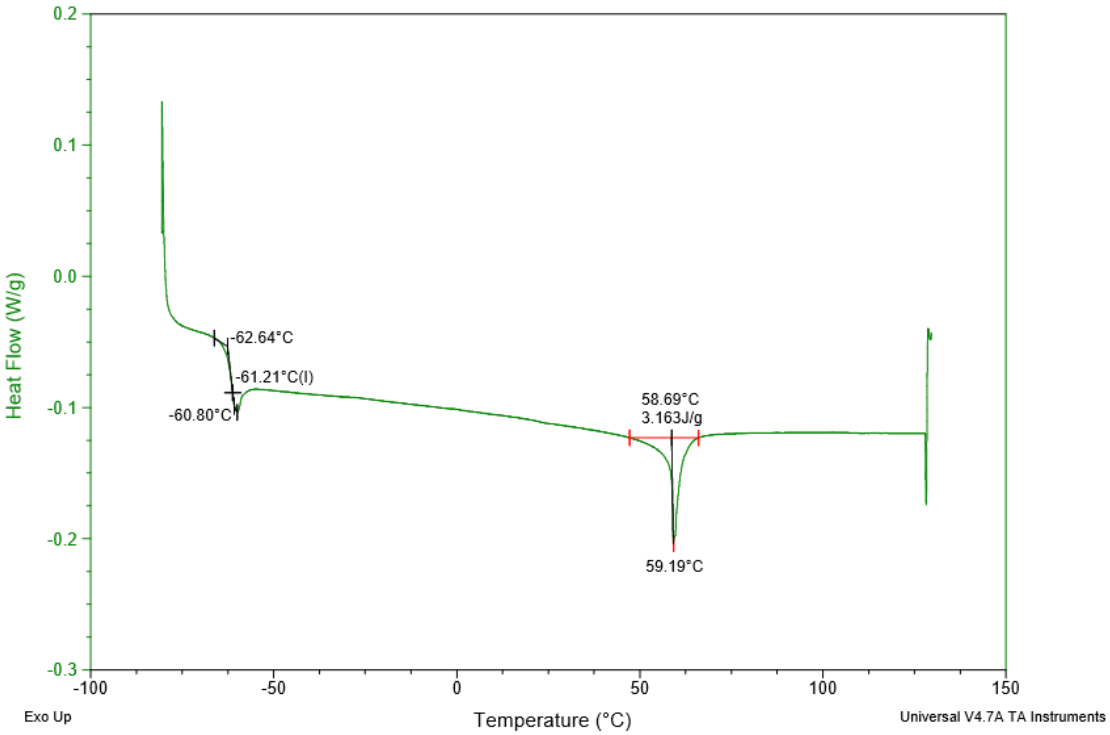

Figure A. 2 - Third heating stage for E7 (Only Heating)

PEGDMA875 polymerised

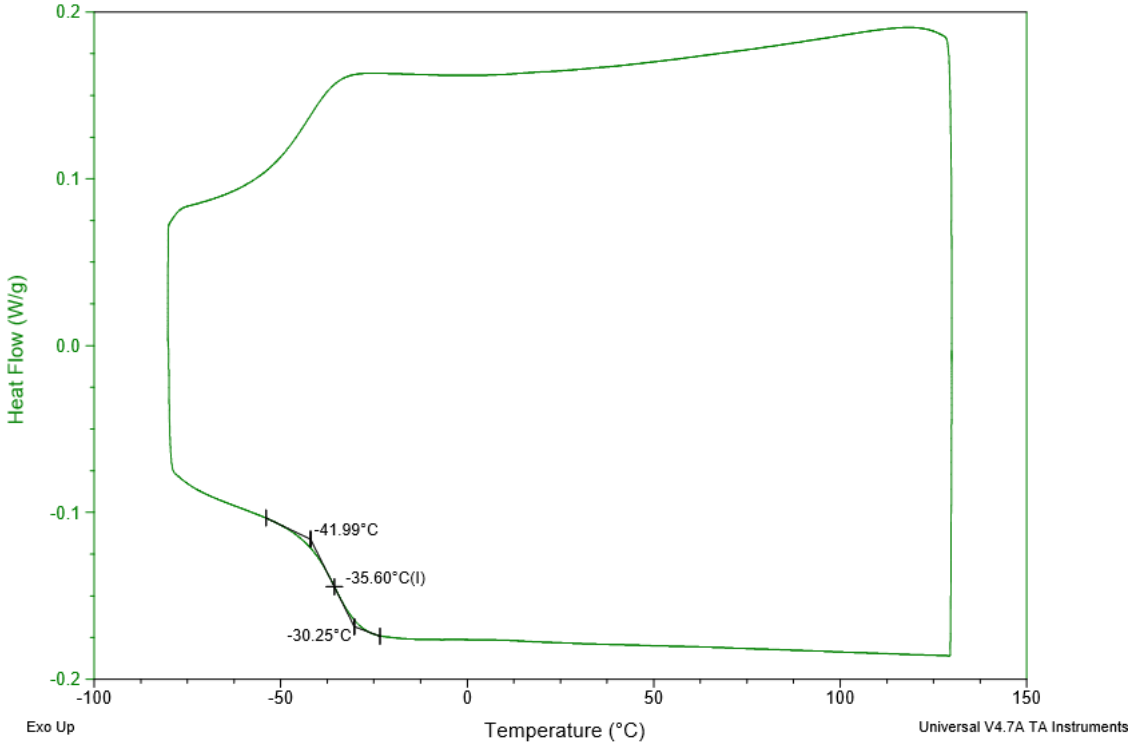

Figure A. 3 - Second Heating stage for PEGDMA875 polymerised

Mixture: 70%E7 + 30%PEGDMA875

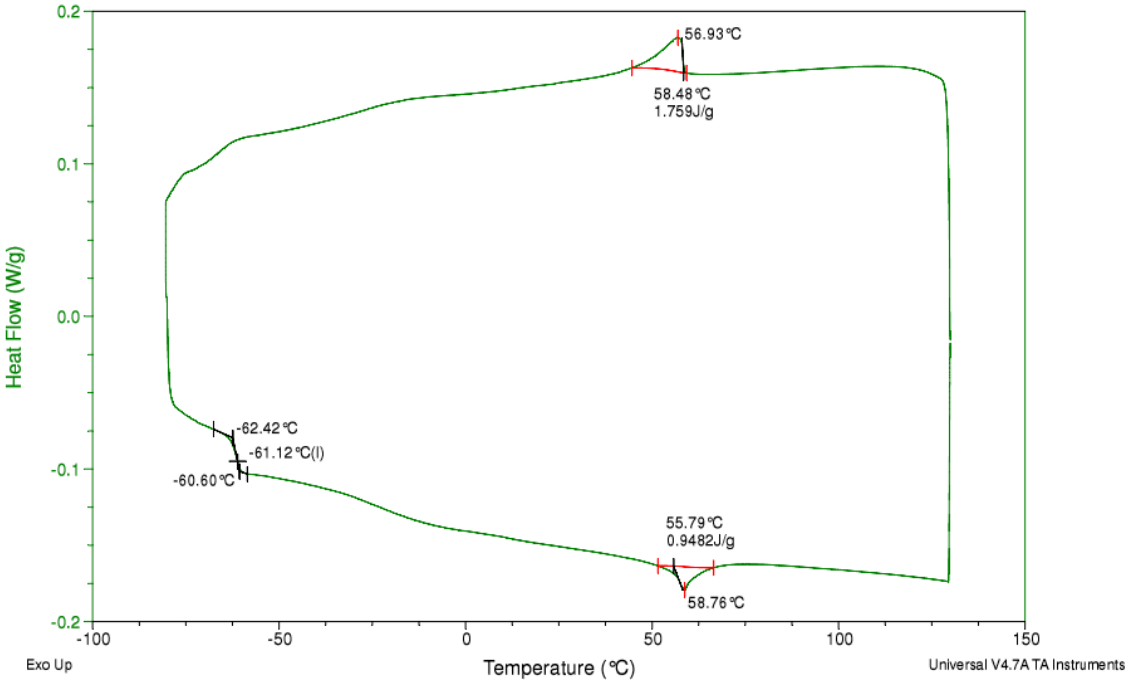

Figure A. 4 - Second Heating Stage for the Mixture 30% E7 70% PEGDMA875

B

Appendix B – AFM images

ITO Glass: 20µm x 20µm

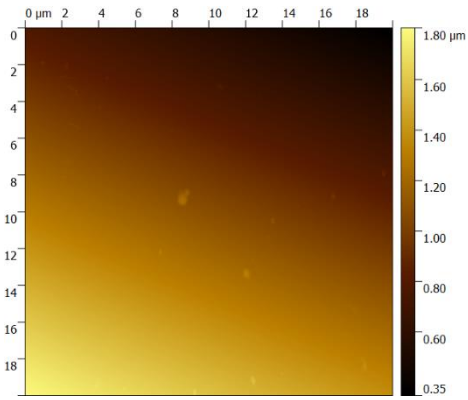

Figure B. 1 - ITO covered glass AFM analysis height image (2D)

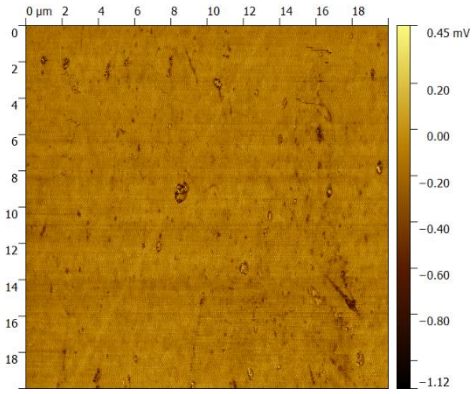

Figure B. 2 - ITO covered glass AFM analysis phase image (2D)

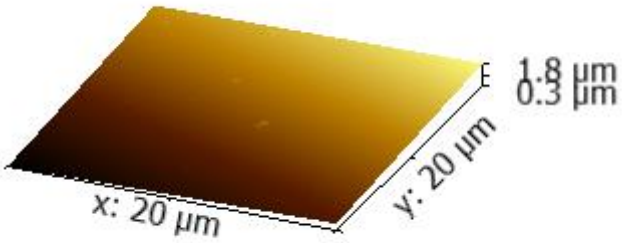

Figure B. 3 - ITO covered glass AFM analysis height image (3D)

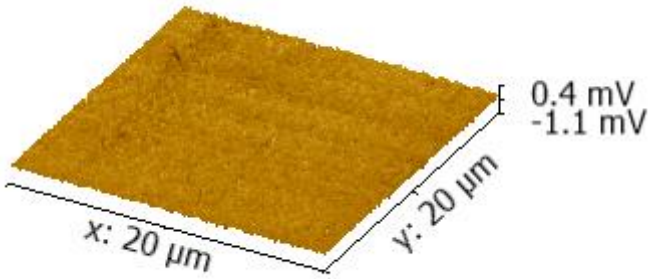

Figure B. 4 - ITO covered glass AFM analysis phase image (3D)

Instec Glass: 20µm x 20µm

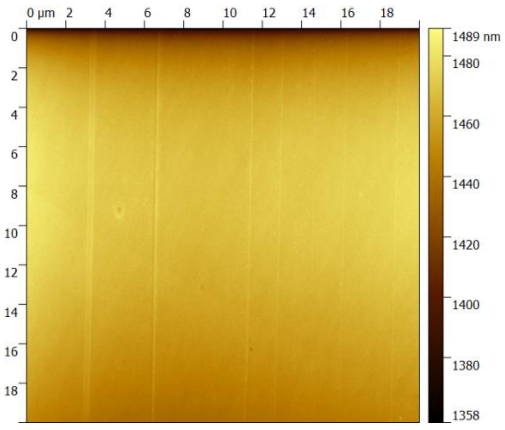

Figure B. 5 – Instec glass AFM analysis height image (2D)

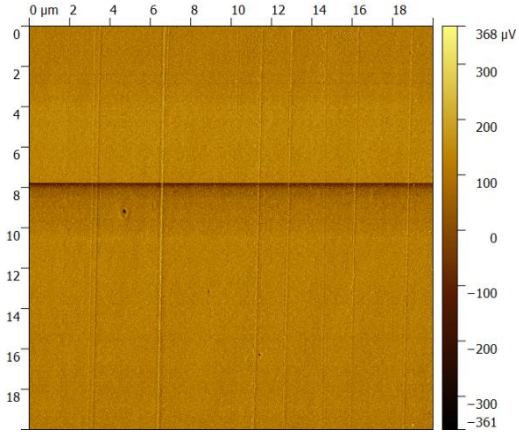

Figure B. 6- Instec glass AFM analysis phase image (2D)

Distance between stretch lines on 20µm x 20µm resolution : 3,1μm; 4,4 μm; 1,6 μm; 2,9 μm; 2,4 μm

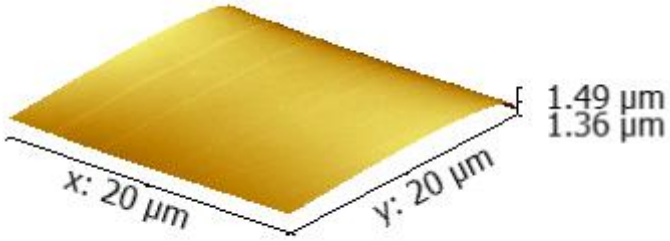

Figure B. 7- Instec glass AFM analysis height image (3D)

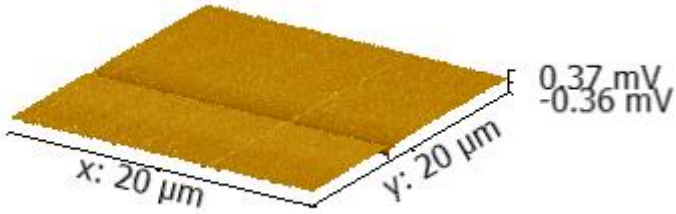

Figure B. 8 - Instec glass AFM analysis phase image (3D)

Instec glass covered with PDLC: 20µm x 20µm

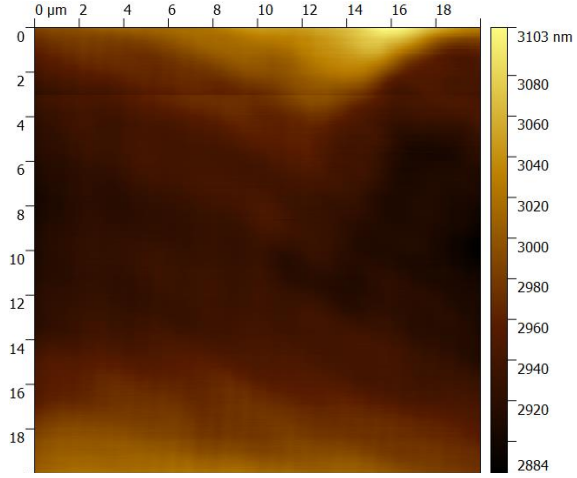

Figure B. 9– Intec glass covered with PDLC AFM analysis height image (2D)

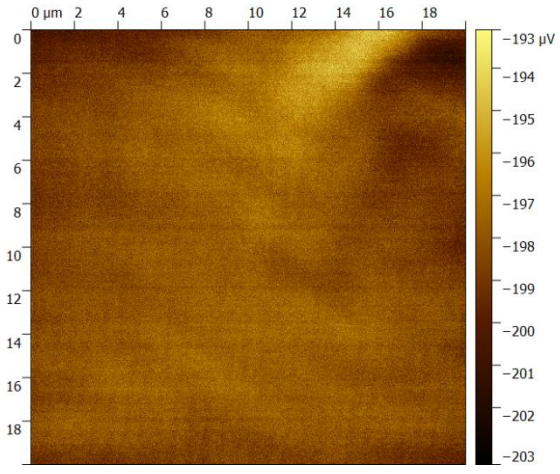

Figure B. 10 - Intec glass covered with PDLC AFM analysis phase image (2D)

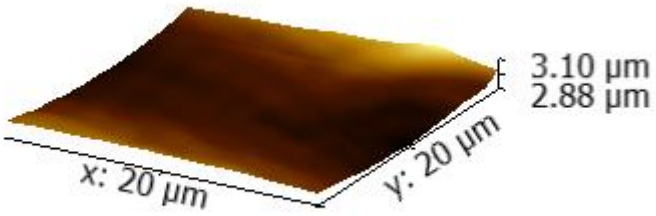

Figure B. 11 - Intec glass covered with PDLC AFM analysis height image (3D)

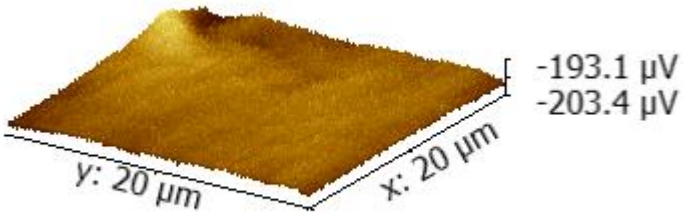

Figure B. 12 – Instec glass covered with PDLC phase image (3D)

C

Appendix C – SEM images

ITO glass

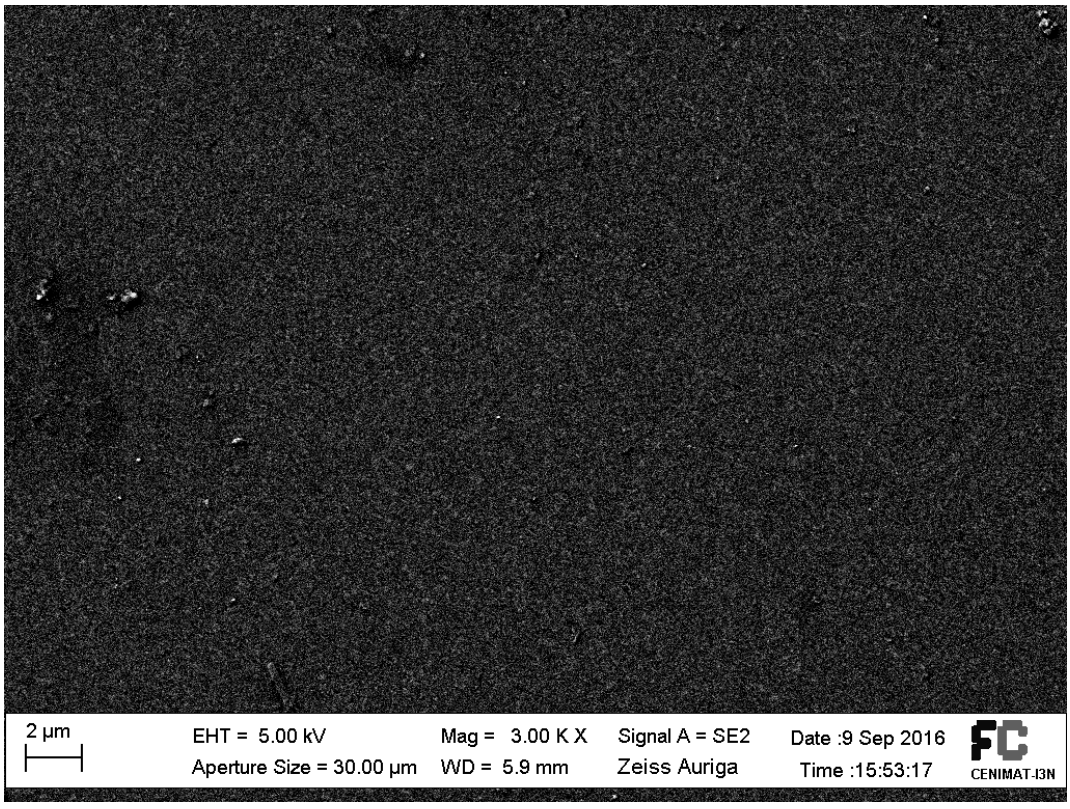

Figure C. 1 - SEM analysis for ITO covered glass (Mag=3.00K X)

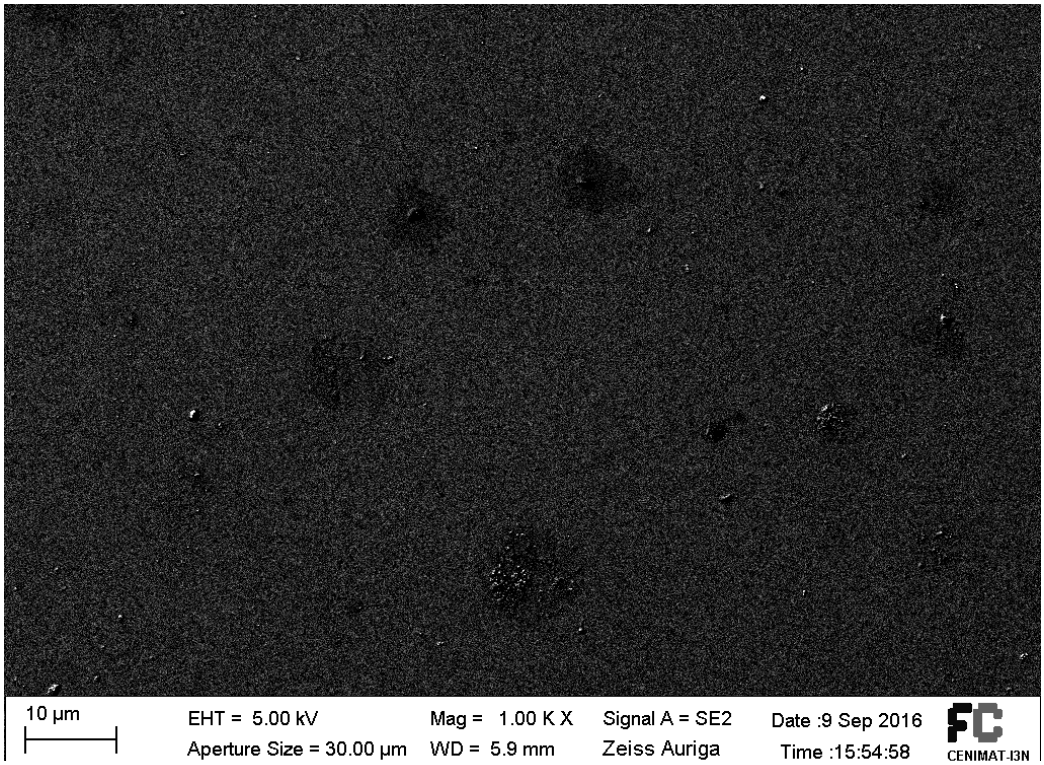

Figure C. 2 - SEM analysis for ITO covered glass (Mag=1.00K X)

Instec Glass

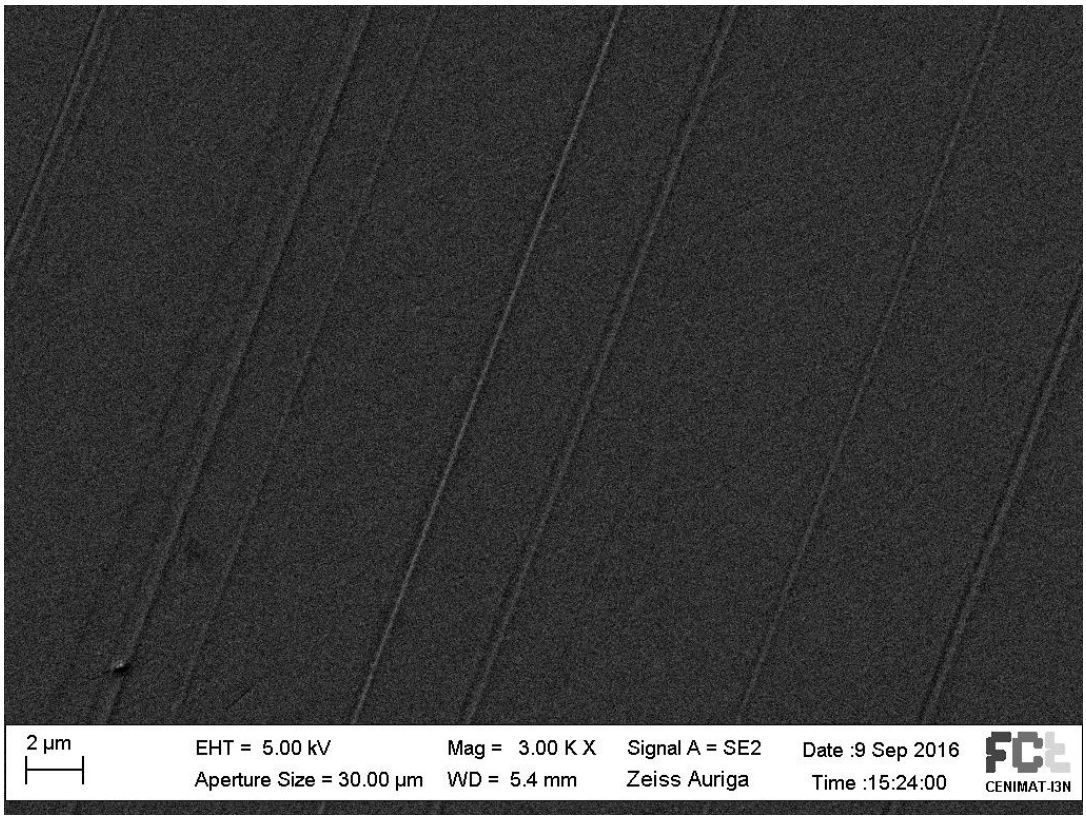

Figure C. 3 - SEM analysis for Instec glass (Mag=3.00K X)

Distance between stretch lines of figure C.3: 6,6μm; 6,0 μm; 3,8 μm and 2,0 μm

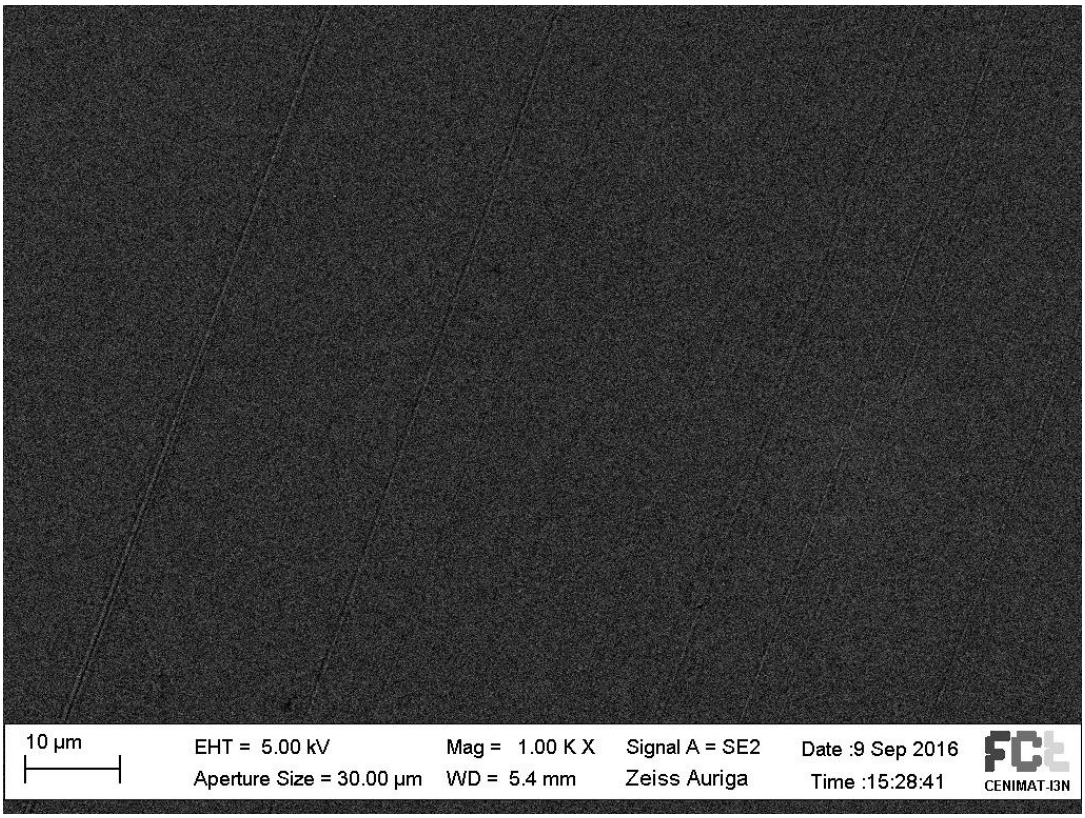

Figure C. 4 - SEM analysis for Instec glass (Mag=1.00K X)

Distance between stretch lines of figure C.4: between values of 3.75µm and 23.5µm

ITO glass covered with PDLC

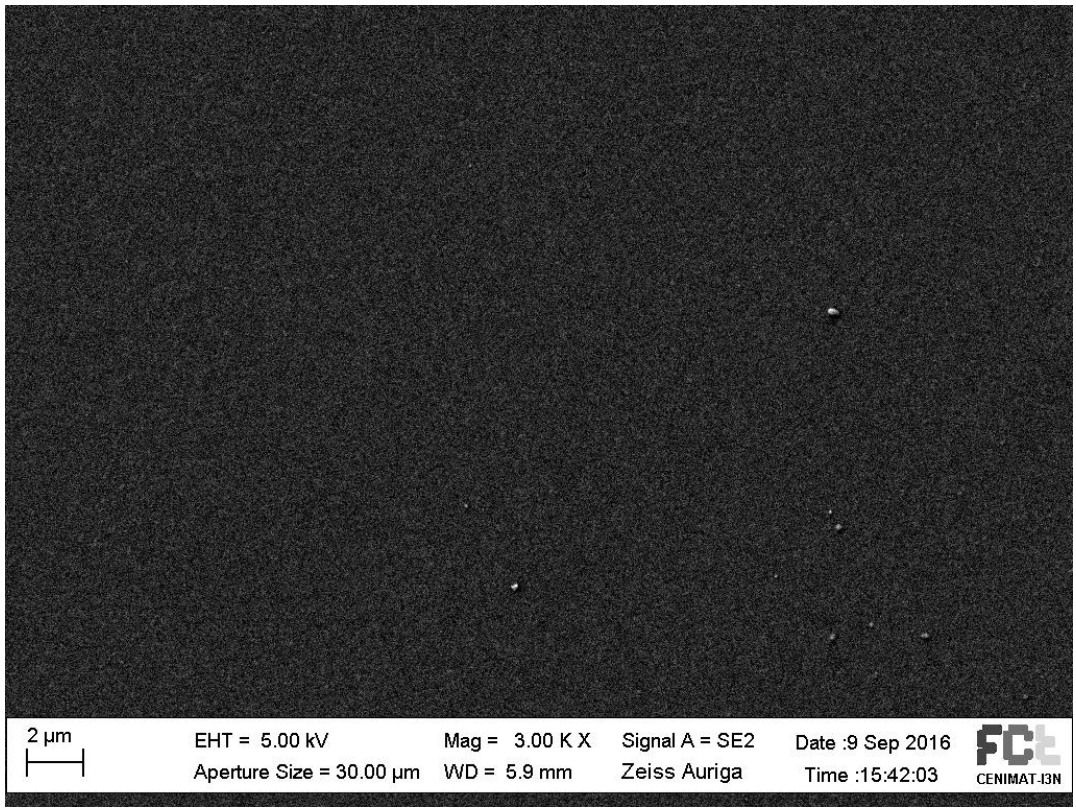

Figure C. 5- SEM analysis for ITO glass covered with PDLC (Mag=3.00K X)

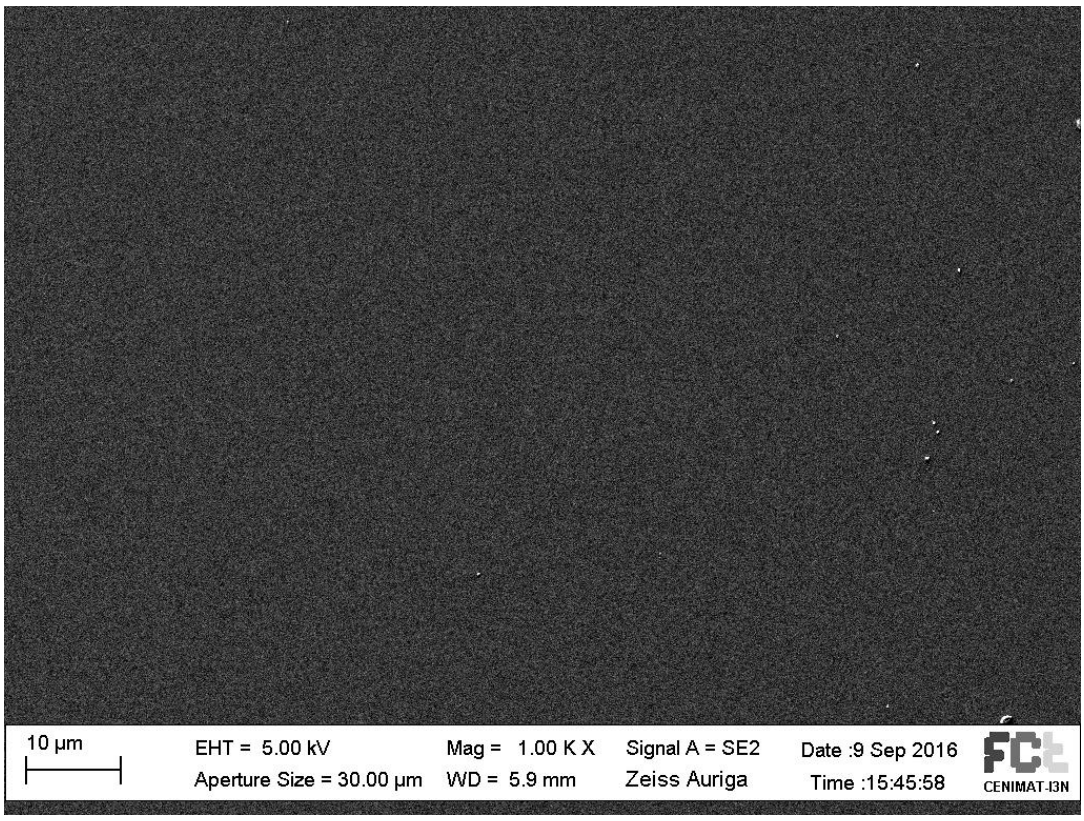

Figure C. 6- SEM analysis for ITO glass covered with PDLC (Mag=1.00K X)

Instec glass covered with PDLC

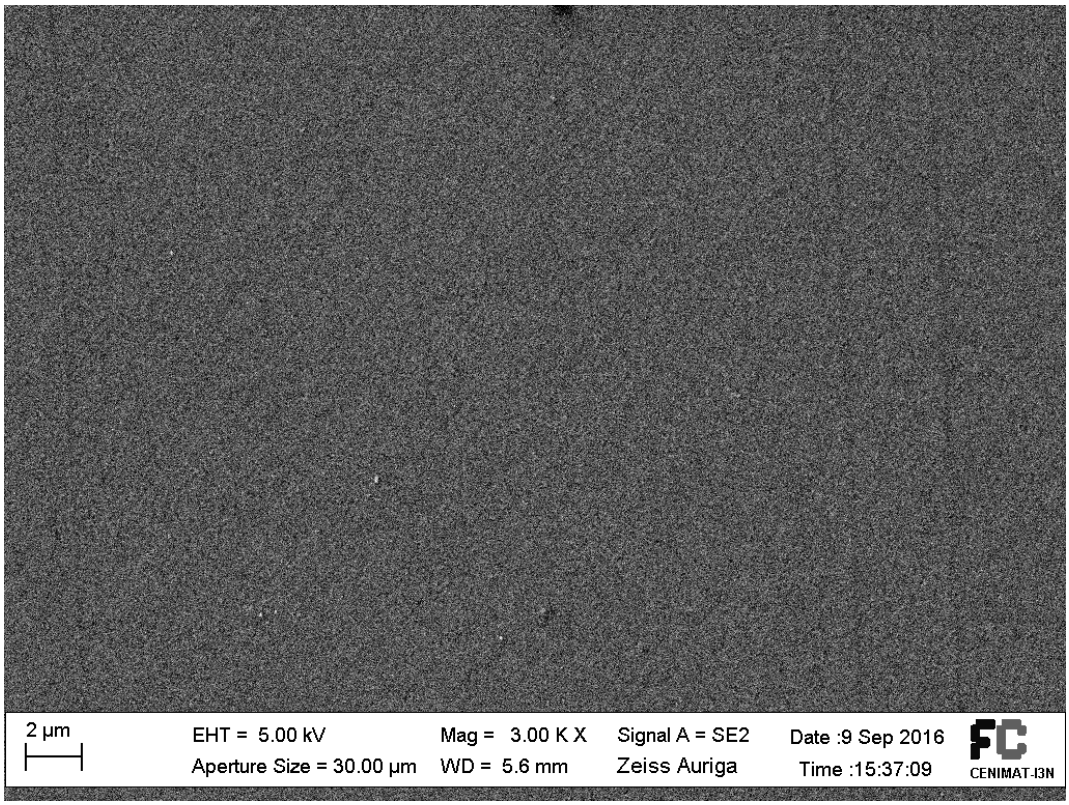

Figure C. 7- SEM analysis for Instec glass covered with PDLC (Mag=3.00K X)

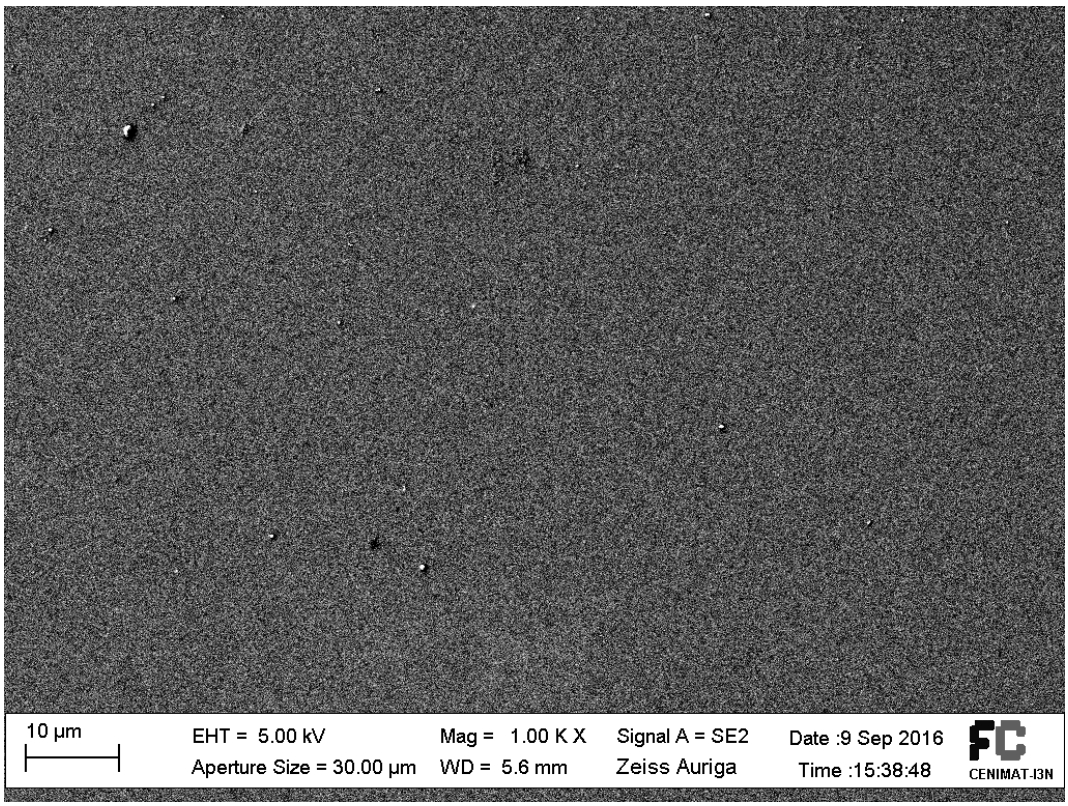

Figure C. 8- SEM analysis for Instec glass covered with PDLC (Mag=1.00K X)